



AFIT / GAE / ENY / 92D-14

AD-A258 841

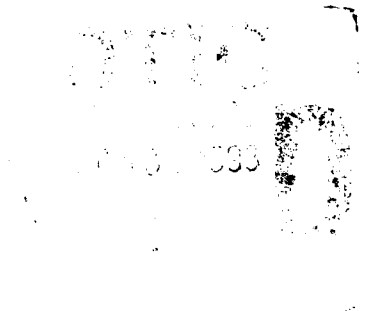


IMPROVEMENTS TO LQG/LTR METHODOLOGY
FOR PLANTS WITH
LIGHTLY DAMPED OR LOW FREQUENCY POLES

THESIS

An-Chi. Ju, Maj, Taiwan, R.O.C

AFIT / GAE / ENY / 92D-14



93-00051

Approved for public release; distribution unlimited

93 1 04 108

IMPROVEMENTS TO LQG/LTR METHODOLOGY FOR PLANTS WITH
LIGHTLY DAMPED OR LOW FREQUENCY POLES

THESIS

Presented to the Faculty of the School of Engineering
of the Air Force Institution of Technology

Air University

In partial Fulfillment of the
Requirements for the Degree of
Master of Science

by

An-Chi. Ju, B.S.

Major, Taiwan, R.O.C

December 1992

Accession For	
NTIS CRA&I	<input checked="checked" type="checkbox"/>
DTIC TAB	<input type="checkbox"/>
Unannounced	<input type="checkbox"/>
Justification	
By	
Distribution /	
Availability Codes	
Dist	Avail and/or Special
A-1	

Approved for public release; distribution unlimited

Acknowledgements

I would like to use this corner of my thesis to express my deepest thanks to my wife Hung-Yuan. She gave up her good job at home, came here — USA, and shared all the difficulty I faced during this one and a half years. I would also like to thank Dr. D.Brett. Ridgely for his nonstop help on academics, research and completing this thesis. All the friends I met in AFIT, who helped me, worked with me, I would also like to say thanks to them.

Table of Contents

	Page
List of Figures.....	vi
List of Tables.....	viii
List of Symbols.....	ix
Abstract.....	xiii
I. Introduction	1
1.1 Problem Statement.....	3
1.2 Background.....	6
1.3 Organization.....	8
II. Theory	9
2.1 Background.....	9
2.2 LQG/LTR.....	12
2.2.1 Singular Value.....	14
2.2.2 Performance and Stability Robustness Requirements.....	15
2.2.2.1 Tracking Performance.....	16
2.2.2.2 Disturbance Rejection.....	17
2.2.2.3 Noise Rejection.....	17
2.2.2.4 Bode Phase Delay Limitation.....	18
2.2.2.5 Stability Robustness.....	18
2.2.3 Good Loop Shape and Specification.....	20
2.2.4 Linear Quadratic Gaussian.....	22
2.2.4.1 Linear Quadratic Regulator	22
2.2.4.2 Kalman Filter.....	25
2.2.4.3 Linear Quadratic Gaussian Compensator	27
2.2.4.4 Loop Transfer Recovery.....	28
2.3 Static Output Feedback.....	31
2.3.1 Eigenvector Assignability	33
2.3.2 Partial Assignment of Desired Eigenvector.....	34
2.3.3 Static Output Feedback Gain (K_s) Calculation.....	35

2.4 Robust Eigenstructure Assignment.....	37
2.4.1 Eigenstructure Assignment.....	37
2.4.2 Eigenstructure Assignment with LQR Robustness	41
III. A-4 Aircrat System Design and Analysis.....	44
3.1 Model Description.....	44
3.2 LQG/LTR Methodology Overview.....	44
3.3 SISO System Design and Result Analysis.....	48
3.3.1 Plant.....	48
3.3.2 Nominal Plant LQG/LTR Design	49
3.3.3 Static Output Feedback.....	52
3.3.3.1 Output Selection.....	53
3.3.3.2 Pole Assignment.....	54
3.3.3.3 LQG/LTR Compensator Design.....	54
3.3.4 Robust Eigenstructure Assignment.....	57
3.3.4.1 LQG/LTR Compensator Design.....	60
3.3.5 Results Comparison.....	62
3.3.6 Robustness with Perturbed Plant	70
3.4 MIMO System Design and Result Analysis	74
3.4.1 Plant.....	74
3.4.2 MIMO Loop Shaping Technique	75
3.4.3 Nominal Plant LQG/LTR Compensator Design.....	77
3.4.4 Static Output Feedback and LQG/LTR Compensator Design.....	78
3.4.5 Robust Eigenstructure Assignment, LQG/LTR Design.....	80
3.4.6 Results Comparison.....	83
3.4.7 Robustness with Perturbed Plant	90
3.5 summary	93
IV X-29 Aircraft Longitudinal MIMO Model Design.....	94
4.1 Plant.....	94
4.2 Nominal Plant LQG/LTR Compensator Design.....	96
4.3 Static Output Feedback and LQG/LTR Compensator Design.....	98
4.4 Results Comparison.....	100
4.5 Summary	107
V. Conclusions and Recommendations.....	108

Appendix A : Plant State Space Models	112
Appendix B : Static Output Feedback Eigenstructure Assignment	113
Bibliography.....	115
Vita	118

List of Figures

Figure

page

1. LQG Compensator and Plant Model.....	4
2. Linear System Compensator and Plant Block Diagram	9
3. Output Multiplicative Uncertainty.....	11
4. Example of Good Loop Shape and Barriers.....	21
5. Simplified Block Diagram of Closed Loop LQR.....	23
6. SISO Nominal Plant TFL and LTR Singular Value Curves.....	50
7. SISO Nominal Plant Closed Loop Pitch Angle Step Input Response.....	52
8. LQG/LTR Compensator and Plant Block Diagram	55
9. SISO SOF Design TFL and LTR Singular Value Curves	56
10. SISO REA Design TFL and LTR Singular Value Curves.....	61
11. SISO Pitch Angle Step Input Response of Nominal, SOF, REA Designs.....	63
12. SISO $\sigma[T]$ Curves of Nominal, SOF, REA Designs.....	64
13. SISO θ Step Input with Noise Response of Nominal, SOF, REA Designs...	66
14. SISO Sensitivity σ Curves of Nominal, SOF, REA Designs.....	67
15. SISO Disturbance Response of Nominal, SOF, REA Designs	68
16. SISO Nyquist Plots of Nominal, SOF, REA Designs	69
17. SISO Perturbed Sensitivity σ Curves of Nominal, SOF, REA Designs	72
18. Perturbed Complementary Sensitivity σ Curves of Three Designs.....	73
19. MIMO Nominal Design TFL and LTR Singular Value Curves.....	77
20. MIMO SOF Design TFL and LTR Singular Value Curves.....	79
21. MIMO REA Design TFL and LTR Singular Value Curves	82
22. MIMO ϕ Step Input Response of Nominal, SOF, REA Designs.....	85

23. MIMO Sensitivity σ Curves of Nominal, SOF, REA Designs.....	86
24. MIMO $\sigma[T]$ Curves of Nominal, SOF, REA Designs.....	87
25. MIMO ϕ Input with Noise Response of Nominal, SOF, REA Designs	88
26. MIMO ϕ Step Input with Disturbance Response of Three Designs.....	89
27. MIMO Perturbed Sensitivity σ Curves of Nominal, SOF, REA Designs....	91
28. MIMO Perturbed Complementary Sensitivity σ Curves of Three Designs...	92
29. X-29 Nominal Design TFL Singular Value Curves.....	96
30. X-29 Nominal Design Reshaped TFL and LTR Singular Value Curves.....	97
31. X-29 SOF Design TFL and LTR Singular Value Curves	99
32. X-29 θ Step Input Response of Nominal, SOF Designs	101
33. X-29 Complementary Sensitivity σ Curves of Nominal, SOF Designs.....	102
34. X-29 θ Step Input with Noise Response of Nominal, SOF Designs.....	104
35. X-29 Sensitivity σ Curves of Nominal, SOF, REA Designs.....	105
36. X-29 θ Step Input with Disturbance Response of Nominal, SOF Designs..	106

List of Tables

Table	Page
1. SISO Open Loop Plant Eigenvalues, Eigenvectors and Zeros.....	49
2. SISO Nominal Design Compensator and Closed Loop System Poles	51
3. SISO SOF Design Compensator and Closed Loop System Poles	56
4. SISO Closed Loop Kalman Filter Poles of Nominal, SOF, REA Designs.....	60
5. SISO REA Design Compensator and Closed Loop System Poles.....	61
6. SISO Perturbed Plant Closed Loop System Poles.....	71
7. MIMO Open Loop Plant Eigenvalues, Eigenvectors and Zeros	74
8. MIMO Nominal Design Compensator and Closed Loop System Poles.....	78
9. MIMO SOF Design Compensator and Closed Loop System Poles.....	80
10. MIMO REA Design Compensator and Closed Loop System Poles	82
11. MIMO System Independent Gain and Phase Margins	84
12. MIMO Perturbed Plant Closed Loop System Poles.....	90
13. X-29 Open Loop Plant Eigenvalues, Eigenvectors and Zeros.....	95
14. X-29 Nominal Design Compensator and Closed Loop System Poles	98
15. X-29 SOF Design Compensator and Closed Loop System Poles	100
16. X-29 System Independent Gain and Phase Margins.....	103

List of Symbols

α	minimum singular value of return difference matrix
β	sideslip angle
δ_a	aileron deflection
δ_{ac}	aileron command
δ_r	rudder command
δ_{rc}	rudder command
θ	pitch angle
θ_i	eigenvector difference minimization parameter
λ_a	achievable eigenvalue
Λ_a	diagonal matrix of achievable eigenvalue
λ_d	desired eigenvalue
Λ_d	diagonal matrix of desired eigenvalue
ρ	constant for weight control when multiply unity matrix
ϕ	bank angle
Φ	characteristic matrix which is equal to $[sI - A]^{-1}$
$\bar{\sigma}$	maximum singular value
$\underline{\sigma}$	minimum singular value
A	state matrix
A_0	nominal state matrix
B	control matrix
B_0	nominal control matrix
C	output matrix
C_0	nominal output matrix

E	plant multilicative uncertainty matrix
$f_{\lambda i}$	weighting for i th eigenvalue
F_e	eigenvalue weighting matrix of input of program
F_v	eigenvector weighting matrix of input of program
F_{vi}	weighting for i th eigenvector
G	plant matrix
H	symmetric matrix for weight state deviation
I	identity matrix
i	imaginary number = square root of negetive one
J	LQR performance index
\bar{J}	REA algorithm performance index
$j\omega$	frequency domain index
k	SISO feedback gain
K	MIMO feedback gain matrix or compensator
K_c	LQR gain matrix
K_f	Kalman filter gain matrix
K_s	static output feedback gain matrix
L	bounded multilicative uncertainty
LQG	linear quadratic Gaussian
LQR	linear quadratic regulator
LTR	loop transfer recovery
M	symmetric matrix for weight the control, used to build R
MIMO	multiple input multiple output
p	roll rate
P	Riccati equation solution matrix
P_i	Liebst eigenvector weighting matrix
q	pitch rate

Q_c	LQR state weighing matrix
Q_f	Kalman filter state weighting matrix
r	yaw rate
R_c	LQR control weighting matrix
R_f	Kalman filter control weighting matrix
REA	robust eigenstructure assignment
Rcode	code of R matrix used for REA program
S	Laplace domain symbol
SISO	single input single output
S_u	control scaling matrix
S_x	state scaling matrix
S_y	output scaling matrix
T	similarity transformation matrix
T_i	transformation matrix for static output feedback
TF_{cl}	SISO closed loop transfer function
tol	convergence tolerance for REA algorithm
u	control vector or forward velocity
V	left modal matrix
v_a	achievable eigenvector
V_a	achievable eigenvector matrix
v_d	desired eigenvector
V_d	desired eigenvector matrix
v_i	i th eigenvector
W	right modal matrix
x	state vector
y	output vector

- z state deviation vector
- Z vector used for calculate output feedback gain

Abstract

The Linear Quadratic Gaussian / Loop Transfer Recovery (LQG/LTR) methodology has been widely applied to control system design, particularly in Multiple Input Multiple Output (MIMO) systems. One can construct a target loop transfer function by designing a Kalman filter to meet the performance and stability requirements, then recover the stability robustness of Kalman filter by tuning a Linear Quadratic Regulator (LQR). By duality, one may design the LQR first, then recover with Kalman filter. The outcome of this design is that the designed compensator will often invert the plant's dynamics. This plant inversion may be undesirable if the plant has lightly damped poles or moderate frequency unstable poles and non-minimum phase zeros. This thesis use Static Output Feedback (SOF) method to reassign the open loop plant poles. The SOF method uses partial output feedback to form an inner loop; with the inner loop closed the poles can be assigned to a better location. Alternatively the Robust Eigenstructure Assignment (REA) algorithm was used to reassign the closed loop Kalman filter poles and preserve the system robustness, then design the LQR to recover the Kalman filter loop shape. Results show that the SOF method can improve system performance and stability, especially for MIMO system design. The REA method is more flexible for eigenstructure assignment and SISO system LQG/LTR design, but not as flexible for MIMO system LQG/LTR design, where frequency domain loop transfer function shaping is required.

IMPROVEMENTS TO LQG/LTR METHODOLOGY FOR PLANT WITH LIGHTLY DAMPED OR LOW FREQUENCY POLES

I Introduction

A decade ago, aircraft flight control system design used single channel feedback control to achieve desired closed loop properties. The approaches were simple: measure the output (response), amplify or attenuate the signal by using gain adjustment, then feed it back to achieve desired system response. Design tools, like root locus, Bode and time response plots were widely applied in aircraft Single Input Single Output (SISO) design, which satisfactorily handled single channel system command and response relations. However, aircraft design goals have become very complex in recent years with more maneuverable, accurate and safe flight control systems in demand. For this reason, more controls like flaprons, canards and thrust vectoring were added. Thus, more states or responses can be controlled. The resulting flight control system is not SISO but Multiple Input Multiple Output (MIMO). MIMO design using SISO techniques is inefficient and tedious and sometimes coupled dynamics are excited thus making SISO design tools totally useless. In the late 70's, MIMO design methodologies like Linear Quadratic Regulator (LQR), Kalman Bucy filter, Linear Quadratic Gaussian (LQG) or Linear Quadratic Gaussian with Loop Transfer Recovery (LQG/LTR) and eigenstructure assignment were developed, allowing control engineers to use these methodologies to achieve better performance and stability.

The LQG/LTR design methodology uses a full state Linear Quadratic Regulator (LQR) to satisfy the performance and stability robustness specifications,

then recovers the stability robustness by tuning the Kalman filter. In a dual this procedure, the Kalman filter can be designed and then recovered by tuning the LQR. This method is an improvement of Linear Quadratic Gaussian (LQG) which recovers the stability margins. The LQG/LTR methodology has been used to design several successful control systems for aircraft engines, submarines and unmanned aircraft [3, 17, 19]. The well-described step-by-step procedures and available softwares, makes LQG/LTR a convenient tool for control system design. But LQG/LTR has some limitations on achievable performance. For instance, if the plant has a right-half-plane zero (non-minimum phase zero), LQG/LTR won't recover the designed transfer function at the zero's frequency. If the non-minimum phase zero is within the system bandwidth, the system performance will be degraded. Another major problem with LQG/LTR is that the compensator will tend to invert the plant and replace it with desired dynamics. Uncertainty in lightly damped poles in the plant (like lightly damped short period mode or Dutch roll mode), causes incomplete pole-zero cancellation and can lead to a closed loop system with a lightly damped pole. This thesis is a study on improving the LQG/LTR methodology for plant with lightly damped poles, so that the undesired low damping time response of LQG/LTR can be prevented.

As stated before, output feedback can improve system performance and stability. States feedback gives the designer the capability to modify every mode of the open loop plant; however, this is not practical when the states are not easy to measure or cost too much to measure. Thus, output feedback is a simpler and more affordable approach. When the compensator has no dynamics, this method can be named Static Output Feedback (SOF) or Gain Output Feedback. It use output feedback with a constant gain to reassign the system closed loop poles. When the dimension of the output is greater than the dimension of control, the number of poles

that can be assigned is the same as the dimension of the output. By moving the plant's lightly damped poles with Static Output Feedback method, the undesired plant inversion of LQG/LTR can be prevented.

Eigenstructure assignment is a design technique to achieve desired eigenvalues and eigenvectors. It has great flexibility in determining system performance, response shape and stability. Combining eigenstructure assignment with LQR or Kalman filter design can achieve good system performance and retain the robustness of the optimal controller. This method is named Robust Eigenstructure Assignment (REA). In the LQG/LTR design process, this method can be used to assign the LQR or Kalman filter closed loop poles to desired locations, then by the separation principle of LQG, the LQG/LTR closed loop system will have no undesired poles.

The two methods above will be studied to determine the effectiveness of how they may improve LQG/LTR closed loop system characteristics to avoid undesired plant inversion.

1.1 Problem Statement

Consider a linear time-invariant model with n dimension of states, m dimension of controls and r dimension of outputs. It has dynamics in state space form

$$\dot{x}(t) = A x(t) + B u(t) \quad (1)$$

$$y(t) = C x(t) \quad (2)$$

The transfer function matrix of the design model, often a square matrix, is given in Laplace domain as

$$G(s) = C \Phi(s) B \quad (3)$$

where

$$\Phi(s) = (sI - A)^{-1} \quad (4)$$

We shall assume that $[A, B]$ is stabilizable, i.e., all unstable modes of Eq (1) are controllable, and $[A, C]$ is detectable, i.e., all unstable modes in Eq (1), (2) are observable. Then the LQG or LQG/LTR compensator can be obtained, with the full LQG compensator and plant model as in Figure 1.

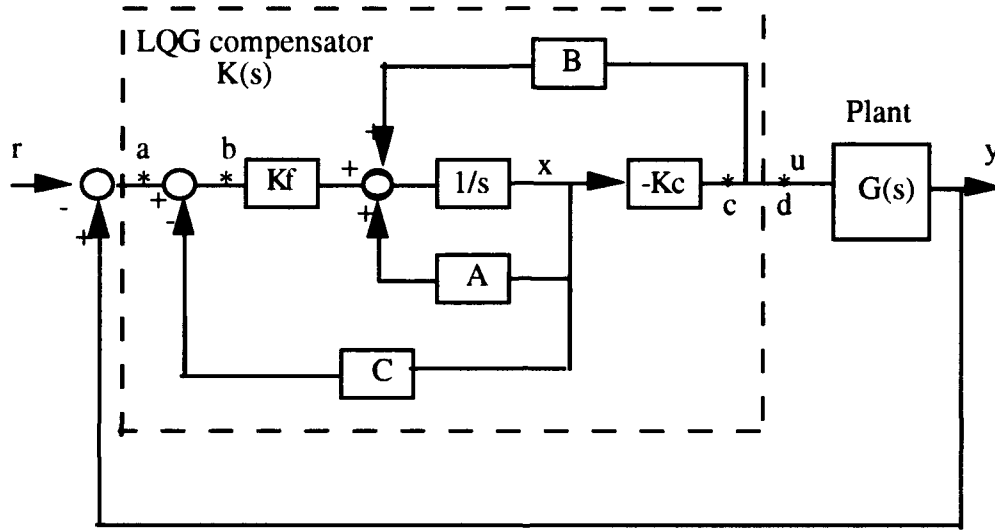


Figure 1 LQG Compensator and Plant Model

Following the LQG/LTR two step design procedures described by Ridgely [20: 9-1 ~ 9-15] and Athans [3:1289-1296], break the loop at the plant output (point a) and design the Kalman filter first by choosing a fictitious disturbance matrix Γ and noise intensity μ , to approximate the loop transfer function,

$$T_{KF} = C\Phi K_f \cong \frac{1}{\sqrt{\mu}} \sigma_i[C\Phi\Gamma] \quad (5)$$

where K_f is Kalman filter gain matrix, σ_i is singular value. Next design LQ Regulator

with weighting matrices

$$Q_c = H^T H + q^2 C^T V C \quad (6)$$

$$R_c = \rho I \quad (7)$$

where H is a weighting matrix on state deviation. $H^T H$ is symmetric, positive semidefinite, and normally chosen to be a unity matrix. ρ is the weighting on controls. By selecting q , a scalar, with increasingly larger values, as $q^2 \rightarrow \infty$, the LQ Regulator will gradually recover the target loop shape of the Kalman filter T_{KF} , so that

$$G(s)K(s) \equiv C\Phi B[(C\Phi B)^{-1}C\Phi K_d] = G(s)K_{LQG/LTR}(s) \quad (8)$$

The LQG/LTR compensator design will normally invert the plant's dynamics and replace it with the compensator's dynamics. The compensator will have zeros close to the plant open loop poles and when the open loop plant has lightly damped poles, like a pair of low damping Dutch roll poles, the compensator will put its zeros close to the poles. If the measurement of pole location involves any degree of uncertainty, then the closed loop system may not have exact pole-zero cancellation, resulting in lightly damped closed loop poles. This is an undesired design result of LQG/LTR.

1.2 Background

The LQG/LTR design procedure proposed by Doyle and Stein [5: 4 -16] has been proven to be a simple and effective design methodology for scalar and multivariable systems. The LQG/LTR design procedure offers loop transfer function shaping techniques for design in the frequency domain with the properties of an optimal full state LQR or Kalman filter, then frequency-wise recovery to the desired loop shape at either the plant input or output. LQG/LTR thus obtains good

performance and stability robustness. When the plant has non-minimum phase zeros, full recovery of the designed transfer function is not possible; the final loop shape does not have desired shape and system performance and stability are affected. This non-minimum phase zero problem has been studied by researcher like Stein and Athans [2] and Zhang and Freudenberg [23]. A suggested method is to select sensitivity and complementary sensitivity weightings to achieve H_2 type optimization, by factorization to a minimum phase plant with non-minimum phase constraints. When the open loop plant has lightly damped poles, the effect of plant inversion and uncertainty in the plant dynamics is to cause the closed loop system to have undesired low damping, resulting in poor time domain characteristics. This shortcoming of undesired inversion of lightly damped plant poles in LQG/LTR design hasn't been studied or corrected by any known researcher.

Static Output Feedback (SOF) or Gain Output Feedback is a method of feeding back the measurable output with a constant gain to assign desired eigenvalues (and eigenvectors). It is a more practical and feasible method than full state feedback. Moreover, this method modifies the system response and mode shape without increasing the dimension of the closed loop system. Several papers on the theory have shown the assignability of the eigenvalues and eigenvectors using constant output feedback [5, 14, 22]. Andry and Shapiro showed an algorithm to calculate the compensator constant gain matrix to achieve eigenvalue and eigenvector assignment [1]. Those studies showed that with a system as in Eq(1) and (2), $\max[m, r]$ number of eigenvalues can be assigned, and $\max[m, r]$ eigenvectors can be assigned with $\min[m, r]$ elements of the eigenvectors arbitrarily chosen. By using Static Output Feedback to assign the pole locations of the open loop plant before the LQG/LTR design, undesired plant inversion should be avoided.

Combined eigenstructure assignment and linear quadratic optimal controller

design is a method which utilizes the flexibility of eigenstructure assignment and the robust property of LQR or Kalman filter to design a closed loop system with both good time domain characteristics and robustness. This method was first introduced by minimizing a cost function that provides a tradeoff between desired and achievable eigenvalues and eigenvectors. Harvey and Stein [10] developed a method that uses the asymptotic properties of LQR to place eigenvalues and uses a linear projection to determine the achievable eigenvectors. Robinson [22] developed an algorithm using MATLAB software to provide eigenvalue placement using the LQR. Huckabone [11] wrote a Fortran program to assign the closed loop eigenstructure as close to desired as possible within the constraints of the LQR stability margins. In this thesis, Huckabone's Fortran program was used to find the achievable closed loop eigenvalues for Kalman filter design, and the returned parameters were used for LQG/LTR design. By using this method, not only were the frequency domain properties of loop transfer function shaped, but the eigenstructure of the closed loop system was specified.

1.3 Organization

This thesis is organized as follows:

Chapter II: Development of the theories for LQG/LTR, Static Output Feedback, and Robust Eigenstructure Assignment. Definition of performance and stability robustness.

Chapter III: A-4 aircraft SISO and MIMO system designs, using nominal, Static Output Feedback, and Robust Eigenstructure Assignment methodologies. Display all the design results and do a detailed analysis. The results from three designs are then compared with each other.

Chapter IV: X-29 experimental aircraft MIMO system design and analysis, using only nominal and Static Output Feedback methodologies, compare the results of these two design.

Chapter V: Summarized the design results and analysis, then suggest study directions for further research.

Appendix A: Design model state space A and B matrices.

Appendix B: MATLAB M-Files for the Static Output Feedback designs.

II Theory

2.1 Background

The purpose of control system design is to aid the product or process — the mechanism, the robot, the chemical plant, the aircraft or whatever — to do its job. Feedback theory has been developed to achieve the higher level of this goal; feedback design can be used to stabilize an otherwise unstable system, reduce the error in command following due to plant disturbance, and reduce the sensitivity of a closed loop transfer function to variations in system parameters. For a system with the feedback loop given in Figure 2

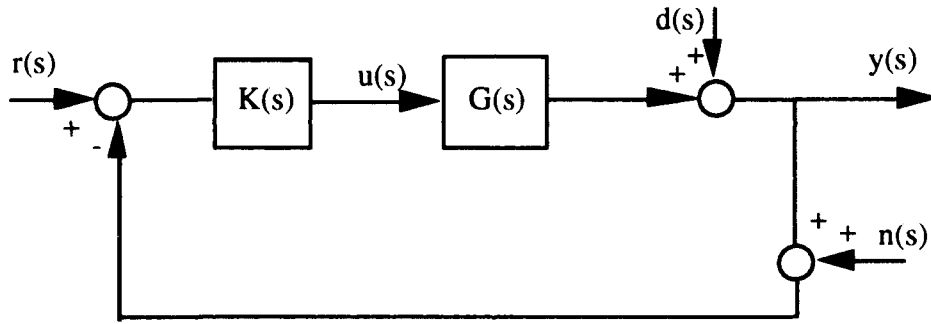


Figure 2 Linear System Compensator and Plant Block Diagram

the control design problem is to specify the dynamic compensator $K(s)$, for the plant G described by

$$\dot{\mathbf{x}}(s) = \mathbf{A} \mathbf{x}(s) + \mathbf{B} \mathbf{u}(s) \quad (9)$$

$$\mathbf{y}(s) = \mathbf{C} \mathbf{x}(s) \quad (10)$$

with n being the state dimension, m the control dimension, and r the output

dimension . The compensator has r inputs (the tracking error or state deviation signal) and m outputs (the input to the plant), is assumed to be linear, time-invariant, and should meet specification related to:

- (a) Nominal stability
- (b) Nominal performance
- (c) Stability robustness to modeling error

The most critical specification is the need to be stable and maintain this stability when encountering plant parameter variations.

LQR is a method for designing a compensator to stabilize a system and keep the plant in equilibrium. As long as the plant is stabilizable and detectable, the LQR compensator always results in a guaranteed stable closed loop system [24]. The gain and phase margins exhibited by Linear Quadratic design based on full state access are given by

$$- 6 \text{ db} < \text{Gain Margin} < \infty$$

$$- 60 \text{ deg} < \text{Phase Margin} < 60 \text{ deg}.$$

However, access to all the states is not always possible, so an observer is often required to estimate the states which are not accessible. The estimated state is then compared with the measured output and gained so as to converge the error between actual and estimated state with the effects of noise minimized. This is the Kalman filter. The LQG compensator is a combination of the Kalman filter and LQ Regulator. A well known consequence of the observer based compensator is the loss of guaranteed stability margins [7]. Doyle and Stein [6] developed an LQG design procedure that recovers the desired robustness properties of LQR. This procedure later came to be known as LQG/LTR. LQG/LTR is an integrated procedure in the sense that it uses both frequency and time domain concepts to achieve the

performance and robustness requirements. It is accomplished by tuning the state and control weighting matrices in the quadratic cost function

$$J = \int_0^{\infty} (x^T Q x + u^T R u) dt \quad (11)$$

to recover the LQ design. Q and R are weighting matrices for LQR or Kalman filter, depending on whether the system loop is broken at plant input or output, respectively. Either approach is valid and the choice is driven by the nature of the plant and the location of the uncertainty in the system.

Uncertainty in the plant dynamics and measurements may be modeled as either injected into the input of the plant, or appearing as an additive disturbance at the plant outputs. Input uncertainty can arise from unknown environmental forces acting on the system; for instance, the nonlinearity of an actuator or flexibility in the control system mechanism. Such a system would yield highly predictable outputs when the inputs are accurately known, but would still display some uncertain outputs as the result of uncertain inputs. Output uncertainty for aircraft, like aeroelastic effects of the structure when the aircraft flies through the air; sensor measurement noise, etc., affects system outputs. For this thesis we deal with output uncertainty only. The uncertainty involved in this study is limited to unstructured, multiplicative uncertainty as shown in Figure 3

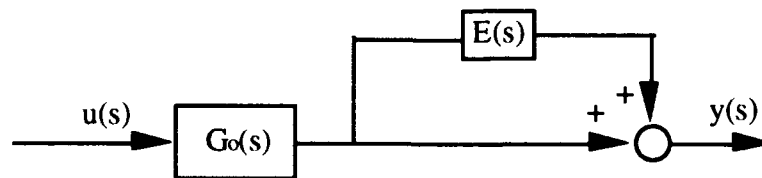


Figure 3 Output Multiplicative Uncertainty

Thus

$$G(s) = [I + E(s)] G_o(s) \quad (12)$$

where $G(s)$ is the true plant transfer function and $G_o(s)$ is the nominal plant transfer function. We will design the Kalman filter with recovery through tuning the LQ Regulator in LQG/LTR design. Ridgely and Banda's Technical Report [20] and Athans's tutorial [2, 3] have excellent presentation of the detailed procedures about designing an LQG/LTR compensator. Although LQG/LTR is shown to produce a controller which provides good performance and stability, there still exist some shortcomings. When the plant has non-minimum phase zeros they hamper the fully recovery of stability robustness at frequencies near the zero; when the plant has lightly damped pole, they cause closed loop system to have a resonant response; when the plant has moderately high frequency unstable poles the system bandwidth rises. In anticipation of unstable and lightly damped poles, the techniques of Static Output Feedback and Robust Eigenstructure Assignment can be used to improve pole location prior to application of LQG/LTR. The following theory development will describe LQG/LTR design and the pole assignment techniques.

2.2. *LQG/LTR*

The LQG/LTR methodology seeks to design the compensator $K(s)$ so that stability robustness and performance specifications are met. LQG/LTR is applicable to both SISO and MIMO design, but is inherently a multivariable design method. By this we mean that LQG/LTR method does not reduce the MIMO design problem into a sequence of SISO design problems, instead, it solves the MIMO design problem directly. The steps and philosophy are independent of the number of states, controls

or output variables. When applying LQG/LTR method to SISO and MIMO systems, several factors should be noted:

- (a) Matrix multiplication is not commutable in the MIMO case, so the open loop transfer function of breaking the loop at plant input, which is KG , is different from the open loop transfer function of breaking the loop at plant output, which is GK . Thus, in MIMO design, system performance and stability robustness need to be considered at both plant input and output.
- (b) For SISO system design we use classical Bode magnitude and phase angle plots to evaluate system performance. In MIMO systems the transfer functions are a matrix of transfer functions, so the magnitude of the transfer function matrix is best expressed by a norm of the matrix — the singular values of the transfer function. These can be plotted frequency-wise, with the maximum and minimum singular value curves containing the frequency domain information.
- (c) Measuring gain and phase margins by analyzing the Nyquist plot is used for SISO systems. Although MIMO system gain and phase margins may also be derived by the same concepts as Nyquist plot, it is much more complicated. Rather, margins are often defined as Independent Gain and Phase margins, which are calculated by using the return difference, sensitivity or complementary sensitivity of the transfer function. These calculations will be discussed later in this section.

Generally, LQG/LTR procedures for a MIMO system is more complex than for a SISO system. This theory development section will only discuss MIMO system LQG/LTR design.

2.2.1. *Singular Values.* In the previous section we briefly mentioned that the determination of the magnitude of a SISO transfer function and a MIMO transfer function is different. For the SISO problem it is relatively easy; in a MIMO problem, the transfer function is a matrix of transfer functions. The size of a MIMO transfer function matrix is found by defining the norm of the matrix. The singular value is one of the norms used for determining the size of a matrix. Singular values are denoted by σ , and are defined by

$$\sigma_i(A) = \sqrt{\lambda_i(A A^*)} = \sqrt{\lambda_i(A^* A)} \quad (13)$$

where $i = 1, 2, \dots, \min[\text{rows in } A, \text{columns in } A]$, A is a matrix of complex numbers, A^* denotes the complex conjugate transpose of A , and λ_i is the i th eigenvalue. The notation describing the maximum and minimum singular values is $\bar{\sigma}$ and $\underline{\sigma}$ respectively. The most common vector norm, the Euclidean norm, is defined by

$$\|x\|_2 = \sqrt{\langle x, x \rangle} = \sqrt{x^T x} \quad (14)$$

The Euclidean norm of a vector is used in defining the spectral norm of a matrix, as given by

$$\|A\|_2 = \sup \frac{\|A x\|_2}{\|x\|_2} \quad (15)$$

where $x \neq 0$. The supremum is often difficult to calculate directly, so the following is useful

$$\begin{aligned}
\|A\|_2 &= \max \{ \sqrt{\lambda_i (A^* A)} \} \\
&= \max \{ \sqrt{\lambda_i (A A^*)} \} \\
&= \bar{\sigma} (A)
\end{aligned} \tag{16}$$

where $i = 1, 2, \dots, \min [\text{rows in } A, \text{columns in } A]$. Another useful identity involving singular values is

$$\|A^{-1}\|_2 = \frac{1}{\underline{\sigma} (A)} \tag{17}$$

Some of the singular values properties useful for deriving performance and stability robustness criteria can be found in Ridgely's Technical Report [20: 2-9~2-13].

2.2.2. Performance and Stability Robustness Requirement Consider the system in Figure 2. We can derive the input and output relationships

$$e = r - n - y \tag{18}$$

$$y = d + GK e \tag{19}$$

where e is the error between reference input and output. Substitute Eq (18) into Eq (19)

$$y = d + GK r - GK n - GK y \tag{20}$$

or

$$[I + GK] y = d + GK [r - n] \tag{21}$$

then

$$y = [I + GK]^{-1} GK [r - n] + [I + GK]^{-1} d \tag{22}$$

or

$$y = [I + GK]^{-1} GK r - [I + GK]^{-1} GK n + [I + GK]^{-1} d \quad (23)$$

The relation of command, disturbance and noise to output can be observed from Eq (23).

We define

GK	loop transfer function
$I + GK$	return difference transfer function
$[I + GK]^{-1}$	sensitivity, denoted as S
$[I + GK]^{-1} GK$	complementary sensitivity or closed loop transfer function, denoted as T

2.2.2.1 Tracking Performance Output following of the reference signal is usually a system requirement. This reference signal is normally confined to some frequency band. For an aircraft, pilot input frequency normally is low and we assume the noise to be negligible at this frequency, by linearity, ignored for now. Then Eq (23) gives

$$y = [I + GK]^{-1} GK r \quad (24)$$

For good command tracking, we need

$$[I + GK]^{-1} GK \cong I \quad (25)$$

When $GK \gg I$, we have

$$T = [I + GK]^{-1} GK \cong [GK]^{-1} GK = I \quad (26)$$

or from Eq (24) and with the equality of

$$T = I - S \quad (27)$$

we get the relationship of

$$y = [I - S] r \quad (28)$$

Thus, for good command tracking, we need S to be small. We know that

$$S = [I + GK]^{-1} \quad (29)$$

This means we have to have the singular values of the open loop transfer function GK large for small sensitivity. To say a MIMO transfer function matrix has "small" magnitude is equivalent to the maximum singular value is small, and "large" magnitude is equivalent to the minimum singular value is large. Therefore, from Eq (26) and (29), we can conclude that for good command tracking we need to have $\sigma [GK]$ large and thus low sensitivity at all frequencies where we want good command following.

2.2.2.2 Disturbance Rejection From Eq (23), assuming the command signal and noise to be zero, we get the following relationship:

$$y = - [I + GK]^{-1} d \quad (30)$$

or

$$y = - S d \quad (31)$$

The above two equations show that good disturbance rejection requires sensitivity (S) small, and this requires GK large. That is, $\sigma [GK]$ needs to be large at frequencies where we have disturbances.

2.2.2.3 *Noise Rejection.* From Eq (23), assuming the command signal and disturbance are zero, we have

$$y = [I + GK]^{-1} GK n \quad (32)$$

or

$$y = [I - S] n \quad (33)$$

For good noise rejection we need have $[I + GK]^{-1} GK$ small, which means that T should be small at all frequencies where we expect measurement noise. By applying the matrix inversion lemma and some algebra, we obtain:

$$\begin{aligned} \bar{\sigma} [I + GK]^{-1} GK &= \bar{\sigma} [(I + (GK)^{-1})^{-1}] \\ &= \frac{1}{\underline{\sigma} (I + (GK)^{-1})} \end{aligned} \quad (34)$$

Thus by Eq(32), for good noise rejection, we want $\underline{\sigma} [I + (GK)^{-1}]$ large or $\underline{\sigma} (GK)^{-1}$ large. This is the same as $\bar{\sigma} [GK]$ small, and by Eq (32) or Eq (33) we also can directly tell that for good noise rejection, we need the singular values of complementary sensitivity to be small or sensitivity equal to unity.

2.2.2.4 *Bode Phase Delay Limitation.* Doyle [6] shows that the steepness of the singular value curve near crossover frequency has a large effect on stability and stability robustness. Steepness greater than - 20 db/decade means the existence of excess effective poles at the crossover frequency. Therefore, the singular value curve should cross the zero db line with a slope less than or equal to - 20 db/decade.

2.2.2.5 *Stability Robustness.* In a classical SISO problem, tradition dictates that gain margin (gm) and phase margin (pm) characterize tolerable uncertainty. These margins are suitable for output multiplicative uncertainty in the following form:

$$g(s) + \delta g(s) \approx (1 + E) g(s) \quad (35)$$

where E is an arbitrary real scalar with $\text{abs}(E) \leq \text{gm} \ln(10) / 20$ for pure gain uncertainty. Alternatively, E is an arbitrary imaginary scalar with $\text{abs}(E) \leq \text{pm} / 57.3$ for pure phase uncertainty. This characterization can be generalized to the MIMO problem as

$$G(s) + \delta G(s) = [I + E(s)] G(s) \quad (36)$$

Let $L(s)$ be an arbitrary positive function with

$$\sigma [E(j\omega)] \leq L(\omega) \quad (37)$$

$L(\omega)$ covers simultaneous gain, phase and direction errors which are unknown but bounded in size. The bound $L(\omega)$ indicates the maximum normalized magnitude which the model error can attain; it is typically small at low frequency but invariably rises toward unity and well above unity as frequency increases. It has been shown in Ridgely's Technical Report [20] that stability is maintained in the presence of all possible uncertainty characterized by Eq (37), if and only if the complementary sensitivity (closed loop) transfer function satisfies

$$\overline{\sigma} [T (j\omega)] \leq \frac{1}{L (\omega)} \quad (38)$$

This condition leads to " keep $T (j\omega)$ small wherever $L (\omega)$ is large". This also can be interpreted as restricting closed loop bandwidth to the frequency range over which the plant model is valid.

2.2.3. Desired Loop Shape and Specifications In the previous section we developed the requirement for good performance and stability robustness, good command tracking, noise and disturbance rejection, and robustness. Sometimes both sensitivity (S) and complementary sensitivity (T) need to be small, but since

$$S (s) + T (s) = I \quad (39)$$

S and T cannot both simultaneously be small . Rather, we must trade off the size of one function against the size of the other, in accordance with the relative importance of command tracking , noise, disturbance rejection and model uncertainty at each frequency.

Normally, the output of the system dynamics can be assumed to be dominated by unmodeled dynamics and noises at high frequency, while the disturbances and commands are assumed to lie in relatively low frequency. Command following and disturbance rejection normally require $\sigma (GK) > 20 \text{ db}$ at frequencies less than 0.1 rad/ sec . It is also required that all output variables have zero steady state error to constant reference inputs, thus dictating integral augmentation. This means the low frequency loop shape must have a minimum of 20 dB at 0.1 rad/sec

frequency, increasing at 20 db/decade backwards in frequency from 0.1 rad/sec. This low frequency requirement should also cover the low frequency uncertainty. Uncertainty normally varies with frequency; it is small and approximately constant at low frequency, then at a certain frequency it starts to grow without bound. For this thesis, the uncertainty is constant at low frequency. At some point it start to increase at 20 db/decade, so as to cross the zero dB line at 20 rad/sec. This defines $L(\omega)$, which from the small gain theorem the loop shape must be above its reciprocal. From the above, to satisfy performance and stability robustness requirement when shaping the loop transfer function, we can put "barriers" on the frequency plots. A desired loop shape should have an open loop transfer function singular value curve which stays outside of this "barriers". An example of a desired loop shape, performance and stability robustness requirement barriers is shown in Figure 4. The "barriers" in Figure 4 will be used for further design and analysis.

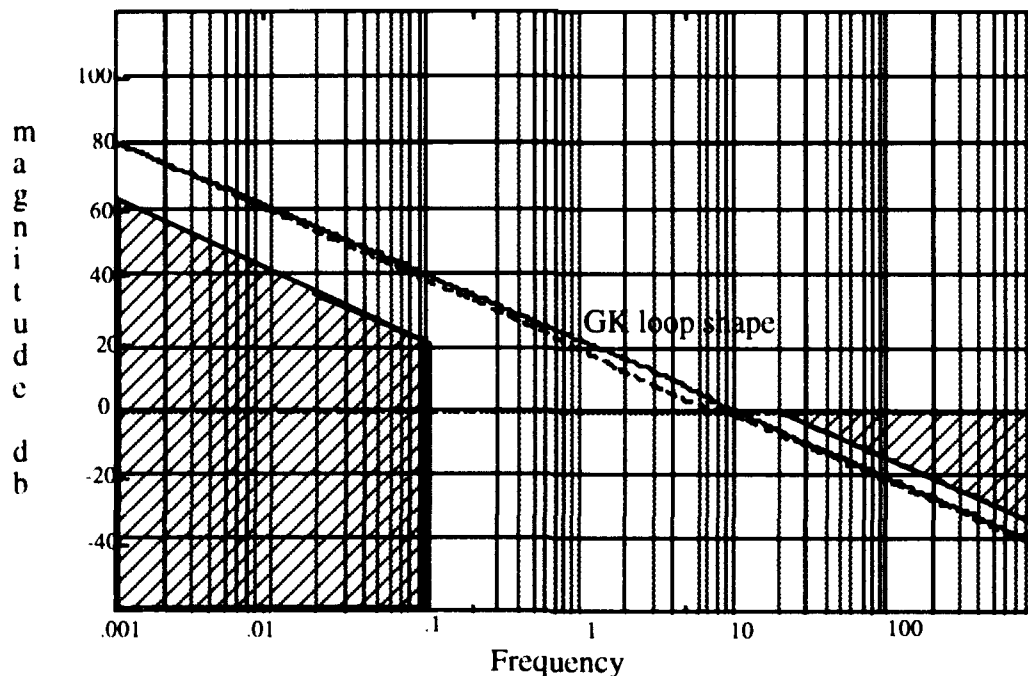


Figure 4 Example of Desired Loop Shape and Barriers

2.2.4 Linear Quadratic Gaussian.

2.2.4.1 Linear Quadratic Regulator. Consider a system as in Eq (1) and (2). The Linear Quadratic Regulator problem is to find the control signal which will minimize the deterministic cost function

$$J = \int_0^{\infty} [z^T(t) Q z(t) + u^T(t) R u(t)] dt \quad (40)$$

where $z = H x$ is some linear combination of the states which are important to system control, and Q and R are such that

$$Q = Q^T \geq 0, R = R^T > 0 \quad (41)$$

Then we can find a controller by letting the control signal u be a linear function of the state,

$$u = -K_c x \quad (42)$$

K_c is the optimal state feedback gain matrix, which is given by

$$K_c = R^{-1} B^T P \quad (43)$$

where P is the solution of algebraic Riccati equation

$$A^T P + P A - P B R_c^{-1} B^T P + Q_c = 0 \quad (44)$$

and P is symmetric, positive semidefinite. If $[A, B]$ is stabilizable and $[A, H]$ is detectable, then the closed loop regulator

$$\dot{x}(t) = (A - B K_c) x(t) \quad (45)$$

is asymptotically stable.

Now we will examine the stability robustness of the LQ Regulator. The simplified block diagram of the LQ Regulator with full state feedback is:

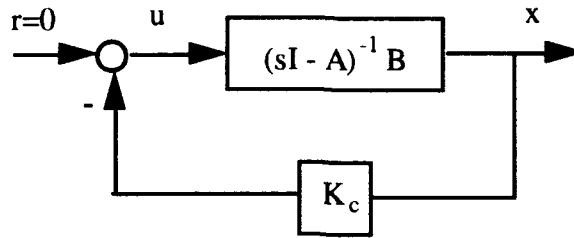


Figure 5 Simplified Block Diagram of Closed Loop LQR

The closed loop transfer function for a SISO system in Figure 5 is

$$TF_{cl} = \frac{(j\omega I - A)^{-1} B}{1 + K_c (j\omega I - A)^{-1} B} \quad (46)$$

The $1 + K_c (j\omega I - A)^{-1} B$ term is referred to as the return difference function.

Robustness for a SISO system is typically measured using gain and phase margins.

The gain margin is defined as the amount the gain K_c can be changed before the closed loop system becomes unstable. The system becomes unstable when the value of the return difference is zero. Phase margin is the amount of phase shift that can be tolerated before the closed loop system becomes unstable.

For a MIMO system, the return difference becomes the matrix $I + K_c (j\omega I - A)^{-1} B$. The definition of gain and phase margins for SISO systems cannot be applied to a MIMO system. Ridgely [20: chapter 3] gave the definitions of independent gain and phase margins, which are suitable for measuring the stability of MIMO system:

Independent Gain Margins (IGM) are limits within which the gains of all feedback loops may vary independently at the same time without destabilizing the system, while the phase angles remain at their nominal values.

Independent Phase Margins (IPM) are limits within which the phase angles of all loops may vary independently at the same time without destabilizing the system, while gains remain at their nominal values. [20: 3-73]

Ridgely also derived the equations for calculating IGM and IPM:

$$\frac{1}{1 + \alpha} < \text{IGM} < \frac{1}{1 - \alpha} \quad (47)$$

$$-2 \sin^{-1}\left(\frac{\alpha}{2}\right) < \text{IPM} < 2 \sin^{-1}\left(\frac{\alpha}{2}\right) \quad (48)$$

where α is the minimum singular value of the return difference matrix given by

$$\alpha = \inf \underline{\sigma} [I + K_c (j\omega I - A)^{-1} B] \quad (49)$$

and $\alpha \leq 1$. It should be noted that these equations for the MIMO stability margins are based on errors that are multiplicative in nature and they are conservative. The system may be able to accept more gain and phase change than the calculated IGM and IPM.

Ridgely also derived the Kalman Inequality [20: 7-1~ 7-3], which is

$$[I + R^{1/2} K_c (-j\omega I - A)^{-1} B R^{-1/2}]^T [I + R^{1/2} K_c (j\omega I - A)^{-1} B R^{-1/2}] \geq I \quad (50)$$

where R must be positive definite. When $R = \rho I$, where ρ is any scalar value, the

Kalman Inequality can be reduced to

$$[I + K_c (-j\omega I - A)^{-1} B]^T [I + K_c (-j\omega I - A)^{-1} B] \geq I \quad (51)$$

The above inequality is true, if and only if

$$\alpha = \underline{\sigma} [I + K_c (j\omega I - A)^{-1} B] \geq 1 \quad (52)$$

In the extreme case $\alpha = 1$, from Eq (47) and (48), the IGM and IPM for this limiting case are

$$-6 \text{ db} < \text{IGM} < \infty \quad (53)$$

$$-60 \text{ deg} < \text{IPM} < +60 \text{ deg} \quad (54)$$

Safonov and Athans [24] proved that any diagonal R matrix will result in the above guaranteed stability margins, as long as the perturbations in each channel occur independently of one another. The guaranteed stability margins are good for LQR designs when using the "design model", but not good for the real system which has unmodelled dynamics.

2.2.4.2 Kalman Filter. Given the linear time invariant system

$$\begin{aligned} \dot{x}(t) &= A x(t) + B u(t) + \Gamma \xi(t) \\ y(t) &= C x(t) + \eta(t) \end{aligned} \quad (55)$$

with $\xi(t)$ and $\eta(t)$ being zero mean, wide sense stationary, uncorrelated, white Gaussian noise with intensities

$$\begin{aligned} E [\xi(t) \xi^T(\tau)] &= Q_0 \delta (t - \tau) \\ E [\eta(t) \eta^T(\tau)] &= R_f \delta (t - \tau) \end{aligned} \quad (56)$$

where

$$Q_0 = Q_0^T \geq 0, R_f = R_f^T > 0 \quad (57)$$

a unique Kalman filter gain matrix exists which minimizes the expected value of $E [e^T(t) e(t)]$, where

$$e = x(t) - \hat{x}(t) \quad (58)$$

$x(t)$ is defined by

$$\dot{\hat{x}}(t) = A \hat{x}(t) + B u(t) + K_f [y(t) - C x(t)] \quad (59)$$

and

$$K_f = \Sigma C^T R_f^{-1} \quad (60)$$

where Σ is a symmetric, semidefinite constant matrix, which is the solution of the algebraic Riccati equation

$$A\Sigma + \Sigma A^T + Q_f - \Sigma C^T R_f^{-1} C \Sigma = 0 \quad (61)$$

Then the Kalman filter closed loop poles are given by the poles of the error dynamics

$$\dot{e}(t) = [A - K_f] e(t) + [\Gamma - K_f] \begin{bmatrix} \xi(t) \\ \eta(t) \end{bmatrix} \quad (62)$$

which are asymptotically stable if and only if $[A, C]$ is detectable and $[A, \Gamma]$ is stabilizable. The Kalman filter also possess the same guaranteed stability margins as LQ Regulator.

2.2.4.3 Linear Quadratic Gaussian Compensator. The Linear Quadratic Gaussian (LQG) compensator is simply the combination of the Kalman filter with the LQ Regulator. Under LQG assumptions, the optimal stochastic controller has the *certainty equivalence* property. Under the certainty equivalence property, each component can be designed independently, with no knowledge of the other. In other words, the LQ Regulator is designed deterministically, assuming complete and accurate knowledge of the state, while the Kalman filter is designed based only on the noises assumed in the system. Cascading the filter with the LQ Regulator yields the optimal stochastic controller. This combination of the two is guaranteed to be the optimal solution for the regulation problem when faced with linear combinations of states and noisy measurements.

We can now derive the state space representation of the complete system. The input to the plant, u , is given by

$$u = -K_c \hat{x} \quad (63)$$

Substituting Eq (63) into Eq (59) yields

$$\dot{\hat{x}}(t) = [A - B K_c - K_f C] \hat{x} + K_f y \quad (64)$$

Taking the Laplace transform of Eq (64)

$$\hat{x}(s) = [s I - A + B K_c + K_f C]^{-1} K_f y(s) \quad (65)$$

Finally, substituting Eq (65) back into the Laplace transform of Eq (63) gives the expression for the LQG compensator

$$u(s) = -K_c [s I - A + B K_c + K_f C]^{-1} K_f y(s) \quad (66)$$

2.2.4.4 Loop Transfer Recovery. Ridgely gave a counterexample in his Technical Report [20; 8-1 ~ 8-7], showing that the observer based LQG compensator will lose guaranteed stability margins of full state regulator. Doyle and Stein [7] also showed same robustness detriment when using an observer to estimate the states. The better the regulator and observer performance, the worse the stability robustness. Doyle and Stein developed a method to "tweak" the filter's components to recover LQ Regulator robustness [6]. This method is named Loop Transfer Recovery (LTR).

In the preceding sections, we described that the filter's job as estimating the states of the system optimally, but LTR requires modifications of the parameters associated with the stochastic nature of the plant. Since the design of the filter and regulator is now based on modified parameters, the goal of producing a controller meeting the specifications supercedes the preceding goal of producing optimal estimates and providing optimal control. The filter or regulator is detuned from design conditions in order to enhance robustness. The variables describing noises become

tuning parameters. With LTR, uncertainties are reflected by uncertainty bounds, which were discussed in previous section.

One parameter modification concerns the definition of the estimator Riccati equation

$$A \Sigma + \Sigma A^T + \Gamma \Gamma^T - \frac{1}{\mu} \Sigma C^T C \Sigma = 0 \quad (67)$$

This modification is the result of using $Q_f = I$ and $R_f = \mu I$ in Eq (61), where these definitions are sufficient to design the Kalman filter with desired loop shapes, followed by LTR tuning with an LQ Regulator. Now μ is a design parameter used to affect the loop shape of the filter.

We also alter the regulator's Riccati equation

$$A^T P + P A - P B R_c^{-1} B^T P + Q_c = 0 \quad (68)$$

where

$$Q_c = H^T H + q^2 C^T V C \quad (69)$$

and

$$R_c = \rho I \quad (70)$$

Substituting these into the regulator's cost index, Eq (40), we obtain

$$J = \int_0^\infty \left[x^T(t) (H^T H + q^2 C^T V C) x(t) + \frac{1}{\rho} u^T(t) u(t) \right] dt \quad (71)$$

These definitions include the designer chosen parameters, q , ρ , Γ , V , and μ . Previous development relies on these parameters to define the noise in the system and the weighting applied in the performance index. Here these values are chosen to achieve the goal of meeting the specifications as reflected by the "barriers" in the frequency domain. The amount of uncertainty in the system is included in the "barriers".

First, the designer selects μ and Γ such that the singular value plots meet the specifications in the lower frequencies. Ridgely [20: 9-8 ~ 9-15] shows the low frequency singular values of the Kalman filter approximate the singular values of the open loop filter as

$$\sigma_i [T_{KF}] \approx \frac{1}{\sqrt{\mu}} \sigma_i [T_{FOL}] \quad (72)$$

where

$$\begin{aligned} T_{FOL} &= C [sI - A]^{-1} \Gamma \\ T_{KF} &= C [sI - A]^{-1} K_f \end{aligned} \quad (73)$$

Therefore, μ acts as a gain to raise or lower the singular value plot of T_{KF} . The matrix Γ is chosen by the designer to affect the shape of the singular value curves. Different choices for this matrix can move the singular value curves closer together in different frequency bands.

Next, the designer uses the values of Γ and μ to solve the modified Riccati equation as given in Eq (68); this solution is then used to find the Kalman filter gain matrix

$$K_f = \frac{1}{\mu} \Sigma C^T \quad (74)$$

This procedure is iterated until the singular value curves meet the specifications.

The recovery of the loop shape is accomplished through the design of the LQ Regulator. The regulator is designed by solving the algebraic Riccati equation given in Eq (69), (70), with V , ρ , and H chosen by the designer. V is often set to identity in order to apply equal weight to each of the outputs. The parameter ρ is arbitrarily chosen, but must be positive, since R_c must be positive definite. In this thesis $\rho = 1$ is used. Eq (71) illustrates the effects of ρ and V on the problem. These parameters determine the weighting applied to control usage relative to the weighting on the deviations of the states from the nominal. Higher value for ρ lessen the importance of control usage in the cost function, but relative weighting is absorbed into the parameter q^2 allowing the arbitrary selection of ρ . Asymptotically, the controller will invert the plant as $q^2 \rightarrow \infty$, leaving the open loop transfer function identical to the filter transfer function.

2.3 Static Output Feedback

When control engineers found that sometimes it is not possible to have full state feedback to design the controller, they started to develop a procedure based on using only the measurable variables as feedback. Davison [5] showed that for the system given by Eq (1) and (2), if the system is controllable and if $\text{rank}[C] = r$, then a linear feedback control law of the form

$$u = F y \tag{75}$$

can always be found so that r eigenvalues of the closed loop system matrix ($A + BFC$) are arbitrarily close (but not necessary equal) to the r preassigned values.

Later, Davison found that if the system is controllable and observable and if $\text{rank}[B] = m$ and $\text{rank}[C] = r$, then $\max(m, r)$ eigenvalues are assignable almost arbitrarily.

Kimura [14] showed that if the system is controllable and observable and if $n \leq (r + m - 1)$, then an almost arbitrary set of distinct closed loop poles are assignable by output feedback. However, in practice $n \geq (r + m - 1)$ generally.

When considering the entire eigenstructure assignment using output feedback, Shapiro [1] stated that given the controllable and observable system in Eq (1) and (2), with the assumptions that the matrices B and C are of full rank, then $\max(m, r)$ closed loop eigenvalues can be assigned and $\max(m, r)$ eigenvectors (or reciprocal vectors by duality) can be partially assigned with $\min(m, r)$ entries in each vector arbitrarily chosen using gain output feedback, i.e., with a control law as Eq (75).

Andry and Shapiro [1] presented a techniques, by which $\max(m, r)$ number of the system's poles can be shifted, with the remaining poles drifting to unassigned positions. Furthermore, this method allows almost arbitrary assignment of portions of the system eigenvectors. By Andry's method, the output feedback problem is to find a constant gain matrix K_s , with dimension $m \times r$, which performs the reassignment of the poles through inner loop feedback. In other words, the plant's inputs become a combination of external input and gain-modified outputs. The state equation for the new system with K_s in place becomes

$$\dot{x} = A x + B [u + K_s y] \quad (76)$$

$$y = C x$$

Through output feedback, Eq (76) becomes

$$\begin{aligned} \dot{x} &= [A + B K_s C] x + B u \\ y &= C x \end{aligned} \quad (77)$$

2.3.1 Eigenvector assignability. In Andry's paper, procedures for finding the output feedback gain matrix K_S are stated. The procedures we will use are stated here. By the definition of the eigenvalue, eigenvector pair $(\lambda_i$ and $v_i)$

$$[A + B K_S C] v_i = \lambda_i v_i \quad (78)$$

or

$$v_i = [\lambda_i I - A]^{-1} B K_S C v_i \quad (79)$$

where the eigenvalues are assumed distinct, allowing the matrix inverse operation.

Eq (79) shows that v_i must lie in the subspace spanned by the columns of $[\lambda_i I - A]^{-1} B$, which is of dimension $\text{rank}(B)$. Hence, the eigenvectors must lie in a space with dimension equal to $\text{rank}(B)$.

Since the desired eigenvector will probably not lie precisely in the subspace mentioned above, a best possible choice (in the least square sense) is made. That is, an achievable eigenvector (v_i^a) is the result of a projection of the desired vector (v_i^d) onto the subspace spanned by the columns of $[\lambda_i I - A] B$. v_i^d is chosen so that designer can accomplish the specific response shape, such as coupling or decoupling modes of the system. The unassigned element can be left in the original form.

This projection of the desired eigenvector on the achievable subspace is calculated by first defining

$$L_i = [\lambda_i I - A] B \quad (80)$$

Since the allowable eigenvector must lie in the space spanned by the columns of L_i ,

$$v_i^a = L_i z_i \quad (81)$$

where z_i is an m dimensional vector. When using a projection method to minimize the least square error, z_i is calculated as

$$z_i = [L_i^T L_i]^{-1} L_i^T v_i^d \quad (82)$$

Substituting into Eq (81) yields

$$v_i^a = L_i [L_i^T L_i]^{-1} L_i^T v_i^d \quad (83)$$

2.3.2 Partial assignment of desired eigenvector. In many practical situations, complete assignment of eigenvectors is not required, but rather the designer is interested only in certain elements of the eigenvector. For this situation, assume the desired eigenvector v_i^d has following structure

$$v_i^d = \begin{bmatrix} v_{i1} \\ x \\ x \\ v_{ij} \\ x \\ v_{in} \end{bmatrix}$$

where v_{ij} are designer specified elements and x is unspecified elements. We define the reordering operator as $\{\cdot\}^{Ri}$ and reorder v_i^d as

$$\{v_i^d\}^{Ri} = \begin{bmatrix} l_i \\ d_i \end{bmatrix}$$

where l_i is a vector of specified elements of v_i^d and d_i is a vector of unspecified

elements. The rows of the matrix $(\lambda_i I - A)^{-1} B$ need to be reordered to conform with the reordered elements of v_i^d as

$$\{ (\lambda_i I - A)^{-1} B \}^{R_i} = \begin{bmatrix} L'_i \\ D_i \end{bmatrix}$$

Then we can proceed in precisely the same manner as in Eq (82), (83), with l_i replacing v_i^d and L'_i replacing L_i to obtain the projection of achievable eigenvector.

2.3.3 Static Output Feedback Gain (K_S) Calculation. After we get the desired eigenvectors (or their projection lies in the achievable subspace), we can start to calculate the gain matrix K_S . We begin by transforming the system such that the B matrix becomes

$$B' = \begin{bmatrix} [I_m] \\ \dots \\ [0] \end{bmatrix} \quad (84)$$

this transformation is accomplished by finding a matrix T, such that

$$x = T x' \quad (85)$$

The T matrix can be defined as

$$T = \begin{bmatrix} [B] & [P] \end{bmatrix} \quad (86)$$

where P is any matrix such that T is invertible. Now , using this matrix as a similarity transformation

$$\begin{aligned} A' &= T^{-1} A T \\ B' &= T^{-1} B \\ C' &= C T \end{aligned} \tag{87}$$

A desired eigenvector or its projection on the achievable subspace is also transformed as

$$v_i^{d'} = T^{-1} v_i^d \tag{88}$$

Subsequent development is performed under the assumption that the system has been transformed according to Eq (87) and (88).

Recalling the equation for the closed loop eigenvalues and eigenvectors

$$[\lambda_i I - A] v_i = B K_s C v_i \tag{89}$$

rewrite Eq (89) in partitioned form

$$\begin{bmatrix} [\lambda_i I_m - A_{11}] & [-A_{12}] \\ [-A_{21}] & [\lambda_i I_{n-m} - A] \end{bmatrix} \begin{bmatrix} [z_i] \\ [w_i] \end{bmatrix} = \begin{bmatrix} [I_m] \\ [0] \end{bmatrix} K_s C \begin{bmatrix} [z_i] \\ [w_i] \end{bmatrix} \tag{90}$$

Taking the top partition of Eq (90) and rearranging yields

$$\lambda_i z_i - [A_{11} z_i + A_{12} w_i] = K_s C v_i \tag{91}$$

Defining $A_1 = [A_{11} \ A_{12}]$, Eq (91) can be written as

$$[A_1 + K_S C] V = Z \quad (92)$$

where

$$\begin{aligned} V &= [v_1 \ v_2 \ \dots v_r] \\ Z &= [\lambda_1 z_1 \ \lambda_2 z_2 \ \dots \lambda_r z_r] \end{aligned} \quad (93)$$

In general, the V and Z matrices are complex. To alleviate the need for complex arithmetic we use the transformation presented by Moore [18], to transform V and Z to real matrices. Finally, K_S can be calculated from Eq (92)

$$K_S = [Z - A_1 V] [C V]^{-1} \quad (94)$$

The procedure of using Static Output Feedback method to assign eigenstructure is implemented in a MATLAB M-File which is described in Appendix B.

2.4 Robust Eigenstructure Assignment

2.4.1 Eigenstructure Assignment. Consider a linear, time invariant system described by Eq (1) and (2), with $\text{rank}(B) = m$, $\text{rank}(C) = r$, and the system is controllable and observable. Andry showed in his paper [1] that the state trajectory is described by

$$x(t) = \sum_{i=1}^n M^{-1} x_0 \exp(\lambda_i t) v_i \quad (95)$$

where λ_i is an eigenvalue, v_i is a corresponding eigenvector, M is the modal matrix which is a matrix composed of individual eigenvectors of the system and x_0 is the initial state. Every solution of Eq (95) represent a free response of the system, and it depends on three quantities:

- (1) Eigenvalue, which determines the decay or growth rate of the response.
- (2) Eigenvector, which determines the shape of the response.
- (3) Initial condition, which determines the degree to which each mode will

participate in the free response.

If we need to use feedback to alter the time characteristics and shape of the system transient response, both eigenvalue and eigenvector (i.e., the eigenstructure) must be reassigned.

The eigenstructure assignment problem for full state feedback can be stated as: given a self-conjugate set of scalar $[\lambda_i^d]$, $i = 1, 2, \dots, n$, and a corresponding self-conjugate set of n dimension vectors $[v_i^d]$, $i = 1, 2, \dots, n$, find a real $(m \times n)$ matrix K such that r of the eigenvalues of $[A + BK]$ are precisely those of the self-conjugate set $[\lambda_i^d]$ with corresponding eigenvectors the self-conjugate set $[v_i^d]$.

Moore [18] identified the freedom offered by state feedback to assign the eigenvalues and eigenvectors, when the eigenvalues are distinct. Moore also gave the procedure to find the gain matrix K , which yields prescribed eigenvalues and eigenvectors. We define

$$S_\lambda = \begin{bmatrix} [\lambda I - A] & [B] \end{bmatrix} \quad (96)$$

and a compatibly partitioned matrix

$$R_{\lambda} = \begin{bmatrix} N_{\lambda} \\ M_{\lambda} \end{bmatrix} \quad (97)$$

where the columns of R_{λ} form a basis for the null space of S_{λ} . For $\text{rank}(B) = m$, one can show that the columns of N_{λ} are linearly independent. With this background Moore [18] has the following theorem:

Let $[\lambda_i], i = 1, 2, \dots, n$, be a self-conjugate set of distinct complex numbers. There exists a real $(m \times n)$ matrix K such that $[A + B K] v_i = \lambda_i v_i, i = 1, 2, \dots, n$. if and only if for each i :

- (1) $[v_i], i = 1, 2, \dots, n$, are a linearly independent set in C^n , the space of complex n -vector.*
- (2) $v_i = v_j^T$ when $\lambda_i = \lambda_j^T$.*
- (3) $v_i \in \text{span} [N_{\lambda_i}]$.*

The eigenstructure assignment design technique to specify the eigenvalues and associated eigenvectors is to let

$$w_i = K v_i \quad (98)$$

so that

$$[\lambda_i I - A] v_i + B K v_i = 0 \quad (99)$$

can be written as

$$[\lambda_i I - A] v_i = B w_i \quad (100)$$

As already shown, all of the eigenvalues can be placed exactly, so as long as the

desired eigenvectors lie within the achievable subspace. The only unknowns in Eq (100) are the elements of each w_i . Eq (100) can be solved for the elements of the w_i . Once the elements of each w_i have been calculated, the gain matrix K can be determined by combining the set of n equations from Eq (98) into a single matrix equation. Define the matrices W and V as

$$W = [w_1, w_2, \dots, w_n] \quad (101)$$

$$V = [v_1, v_2, \dots, v_n] \quad (102)$$

The matrix V containing the right eigenvectors is often referred to as the modal matrix. Combining equations obtained from Eq (98) yields

$$W = K V \quad (103)$$

Since the eigenvectors are linearly independent, the V matrix is nonsingular and Eq (103) becomes

$$K = W V^{-1} \quad (104)$$

In practice, the desired eigenvectors are often not achievable, not lying within the subspace spanned by $[\lambda_i I - A]^{-1} B$. This means that a solution for K that will yield a closed loop system that has the desired eigenvectors is not possible. One method to get around this problem is to project the desired eigenvectors onto the achievable subspace, minimizing the difference between the desired and achievable vectors. Liebst and others [16] achieve this by introducing a quadratic cost function to be minimized subject to Eq (100) as

$$J = [v_i^a - v_i^d]^T P_i [v_i^a - v_i^d] \quad (105)$$

where P_i is a diagonal weighting matrix for the i th eigenvector. Then we can solve for W and K matrices that come close to providing the desired eigenstructure. The eigenstructure assignment method then provides a means to specifically place eigenvalues and optimally place eigenvectors for a control system.

2.4.2 Eigenstructure Assignment with LQR Robustness. From the theory discussed in section 2.2.4.1, we showed LQR possesses guaranteed stability margins. By using full state feedback with the control law:

$$u = -Kx \quad (106)$$

The closed loop system is:

$$\dot{x} = (A - BK)x \quad (107)$$

The gain matrix is

$$K = R^{-1} B^T P \quad (108)$$

so

$$\dot{x} = (A - BR^{-1}B^T P)x \quad (109)$$

The achievable closed loop eigenvalues can be found by

$$\det [\lambda_i I - (A - BR^{-1}B^T P)] = 0 \quad (110)$$

The achievable right eigenvectors can be found by solving the nullspace of

$$[\lambda_i I - (A - BR^{-1}B^T P)] v_i = 0 \quad (111)$$

Robinson [22] and Huckabone [11] used an algorithm to assign the eigenstructure by minimizing combined distance between the elements of desired and LQR achievable eigenstructure. They introduced a quadratic performance index \bar{J} , where

$$\bar{J} = \sum_{i=1}^n [f_{\lambda_i} (\lambda_{di} - \lambda_{ai})^2 + (v_{di} - \theta_i v_{ai})^T F_{vi} (v_{di} - \theta_i v_{ai})] \quad (112)$$

where

f_{λ_i} = weighting on the i th eigenvalue

λ_{di} = i th desired eigenvalue

λ_{ai} = i th achievable eigenvalue

v_{di} = i th desired eigenvector

v_{ai} = i th achievable eigenvector

F_{vi} = diagonal weighting matrix for the i th eigenvector

θ_i = real or complex constant that minimizes $(v_{di} - \theta_i v_{ai})$

Minimizing \bar{J} will minimize the combined distance between the elements of the desired and LQR achievable eigenstructure. The weightings f_{λ_i} and F_{vi} allow the designer to specify the relative importance of achieving individual elements of the eigenstructure. Assuming a weighting of zero for any desired element will leave the algorithm free to place that element to any necessary value. The algorithm searches for the minimum cost \bar{J} within the constraint of closed loop LQR described by Eq (110), (111).

Feedback gains are a function of P ; where P is the solution of the algebraic Riccati equation, which is a function of R and Q , Q need to be symmetric and positive semidefinite and we define $Q = H^T H$, where H is any $n \times n$ symmetric matrix. For

ensuring R is symmetric and positive definite, we define a symmetric matrix M such that $R = M^T M$. During the iteration, the algorithm will vary the elements of M and H to find the closest eigenstructure to the desired eigenstructure. Because M and H are symmetric, the number of elements need to be varied is limited to the upper triangular portion of each matrix. If R is restricted to p I or a diagonal matrix, the number of elements is reduced further. After finding the achievable eigenstructure closest to desired, the algorithm will return the finalized Q and R matrices.

III A - 4 Aircraft System Design and Results Analysis

3.1 Design Model Description

Since aircraft flight control system design using the LQG/LTR technique is emphasized in this thesis, two very different aircraft are studied. The first one is an A-4 aircraft with conventional stable static stability and control surfaces, i.e., horizontal tails for longitudinal control, ailerons and rudder for lateral and directional control. Two models of the A-4 aircraft are used. Longitudinal control of the pitch angle response is used as a SISO design model; design with this SISO model allows starting with a simpler problem. Lateral-directional control of the bank and sideslip angle responses is used as a MIMO model, so MIMO design can be evaluated. As addressed in the previous section, the LQG/LTR methodology has drawbacks when the design plant has right-half-plane (nonminimum phase) zeros, lightly damped poles or moderate frequency unstable poles. An A-4 aircraft flying at 15,000 feet, 0.6 Mach gives the typical low damping phugoid mode longitudinally in the SISO model and Dutch roll mode laterally in the MIMO model, so these A-4 models present the lightly damped poles problem of the LQG/LTR method. The detailed model characteristics will be described in following section of design process.

3.2 LQG/LTR Methodology Overview

For an aircraft, the plant input is control commands and plant output is aircraft responses. When designing control systems for aircraft, we are interested in having the responses track the commands, so we prefer to design the LQG/LTR compensator by breaking the loop at the plant output. By following the two step LQG/LTR compensator design procedure in Ridgely's Technical Report [20], we will design the loop transfer function shape or the target feedback loop (TFL) shape by

designing the Kalman filter first, then by tuning the LQ regulator state weighting matrix to recover target feedback loop shape. The steps are :

Step 1: Full state Kalman filter design.

Given the state space model as Eq (1) and (2), we treat Γ and μ as completely tunable parameters rather than fixed noise intensities. The loop transfer function of the filter is given by

$$T_{KF} = C\Phi K_f \quad (113)$$

where

$$\Phi = [sI - A]^{-1} \quad (114)$$

Using the Kalman equality corresponding to the filter, we have the relation

$$[I + T_{KF}] [I + T_{KF}]^* = I + \frac{1}{\mu} [C\Phi\Gamma] [C\Phi\Gamma]^* \quad (115)$$

therefore

$$\sigma_i [I + T_{KF}] = \sqrt{1 + \frac{1}{\mu} \sigma_i^2 [C\Phi\Gamma]} \geq 1 \quad (116)$$

and at low frequency, where $\sigma_i[T_{KF}] \gg 1$, this can be simplified to

$$\sigma_i [T_{KF}] \cong \frac{1}{\sqrt{\mu}} \sigma_i [C\Phi\Gamma] \quad (117)$$

Again, many choices of Γ and μ may be made without solving Riccati equations in order to meet the performance specifications. The same guaranteed margins hold for the Kalman filter as for the LQ Regulator, so that crossover properties are very good. Finally, as $\mu \rightarrow 0$

$$\sqrt{\mu} K_f \rightarrow W \Gamma \quad (118)$$

where W is any orthonormal matrix. This implies

$$\omega_{c_{\max}} = \bar{\sigma}[C \ \Gamma] / \sqrt{\mu} \quad (119)$$

where $\omega_{c_{\max}}$ is the maximum crossover frequency.

We wish to design an LQG/LTR feedback system which has the property that it has zero state error to arbitrary constant (step) commands and disturbances. This specification implies that we must have an integrator in each channel of the open loop system. Also, we would like to have all loop singular values close together at both low and high frequencies; this requirement often leads to designs in which all crossover frequencies are approximately the same, so that the MIMO system has about the same speed of response in all directions.

Since we are using the LTR method, all the desirable attributes of the design must be reflected in T_{KF} (or TFL). To meet the zero steady state error specifications, we must first correctly define the design plant model, so that it contains the necessary integrators. This can be accomplished by adding one integrator in each control channel of our plant. Mathematically, we define the vector $u(t)$ by

$$\dot{u}_0(t) = u(t) \quad (120)$$

or

$$u_0(s) = (1/s) u(s) \quad (121)$$

where u_0 is the nominal control vector. The design plant model is then defined by the augmented dynamics and it is now an $(n+m)$ dimensional system. In the state space

model, the A , B and C matrices are now

$$A = \begin{bmatrix} A_o & B_o \\ 0 & 0 \end{bmatrix}, B = \begin{bmatrix} 0 \\ I \end{bmatrix}, C = [C_o] \quad (122)$$

where A_o , B_o , C_o are the original system matrices.

Now we shall choose the design matrix Γ to cause the TFL singular values to be identical at both low and high frequencies. First decompose Γ as follows

$$\Gamma = \begin{bmatrix} \Gamma_L \\ \Gamma_h \end{bmatrix} \quad (123)$$

We shall use the $n \times m$ matrix Γ_L to influence the low frequency behavior of the singular values, and the $m \times m$ matrix Γ_h to influence the high frequency behavior of the singular values. Ridgely showed that Γ_L and Γ_h can be chosen as

$$\Gamma_L = -[C_o A_o^{-1} B_o]^{-1} \quad (124)$$

$$\Gamma_h = C_o^T [C_o C_o^T]^{-1} \quad (125)$$

so that

$$\lim_{\omega \rightarrow \infty} \sigma_i(C \Phi(j\omega) \Gamma) = (1/\omega) \quad (126)$$

Now, the singular value curves have the same integral action and are close to each other.

Step 2 : Full state loop transfer recovery using the regulator

Design the LQ Regulator with weighting matrices

$$Q_c = H^T H + q^2 C^T V C \quad (127)$$

$$R_c = \rho I \quad (128)$$

where q is a scalar taking on increasingly larger values and V is an arbitrary, symmetric positive definite matrix. As $q^2 \rightarrow \infty$

$$\frac{K_c}{q} \rightarrow WC \quad (129)$$

and

$$G(S)K(S) \rightarrow C\Phi B[(C\Phi B)^{-1}C\Phi K_f] = C\Phi K_f \quad (130)$$

which is the Kalman filter loop T_{KF} we just designed. Notice this recovery inverts the plant.

3.3 SISO System Design and Results Analysis

3.3.1 Plant . The SISO system state space A , B matrices are shown in Appendix A. The states, control and output are

$$x = \begin{bmatrix} \text{airspeed (v) - ft/sec} \\ \text{AOA } (\alpha) - \text{deg} \\ \text{pitch rate (q) - deg/sec} \\ \text{pitch angle } (\theta) - \text{deg} \\ \text{elevator} \\ \text{deflection } (\delta_e) - \text{deg} \end{bmatrix}, \quad u = [\text{elevator command } (\delta_{ec})], \quad y = [\text{pitch angle}]$$

The open loop plant eigenvalues, eigenvectors and zeros are given in Table 1. The plant is stable, minimum phase, the short period mode is not well damped ($\zeta_{ph} = 0.3$), and the phugoid mode has very low frequency (0.0891 rad/sec) and low damping ($\zeta_{ph} = 0.0631$). The low damping poles will be shifted by using the static output feedback and robust eigenstructure assignment methods, so that the LQG/LTR closed loop system won't have dominant slow poles.

Table 1 SISO Open Loop Plant Eigenvalues, Eigenvectors and Zeros

mode	short period	phugoid	actuator
eigenvalue	-1.19±3.5i	-.0056±.0628i	-20
eigenvector	.036±.023i .232±.126i .374±.851i .189±.167i 0	-.992±.053i .0024±.0001i -.007±.0006i .0187±.11i 0	-.0011 .0338 .7112 -.0356 .7013
zeros	-.7306, -.0121		

3.3.2 *Nominal Plant LQG/LTR Compensator Design* . By following the two step procedure stated above, we design the target feedback loop shape first. For satisfying the zero steady state error performance requirement (which is normal for an fighter type aircraft like A-4), a single integrator is augmented into the plant. Since this is a SISO case, the system just has one singular value curve (Bode magnitude plot). Choosing the Γ matrix, it is not necessary to consider the maximum and minimum singular value curves matching problem, so while choosing Γ and μ an approximation of

$$C\Phi K_f \cong \frac{1}{\sqrt{\mu}} \sigma_i[C\Phi\Gamma] \quad (131)$$

to meet the performance and robustness specification is the primary consideration in shaping the target loop. As long as the target loop shape stays outside the " barriers ", Γ can be arbitrarily chosen. The parameter μ is chosen to satisfy the system bandwidth requirement. For this SISO design, the low and high frequency singular

value curves matching equations are still used to calculate Γ , so that integral action can be assured. $\mu = .01$ is chosen to have the crossover frequency around 9 rad/sec. In tuning the Regulator to recover the Kalman filter process, Q_c is chosen as

$$Q_c = H^T H = C^T C \quad (132)$$

because the measured variable is also the variable we want to control. ρ is chosen to be unity. $q=300$ is selected to give a reasonable trade off between optimality and robustness recovery.

The Target Feedback Loop (TFL) and LTR singular value curves are shown in Figure 6. The LTR curve has -20 db/decade more roll-off than the TFL curve, as expected. Both curves meet performance and robustness specifications. The large hump is caused by low phugoid damping.

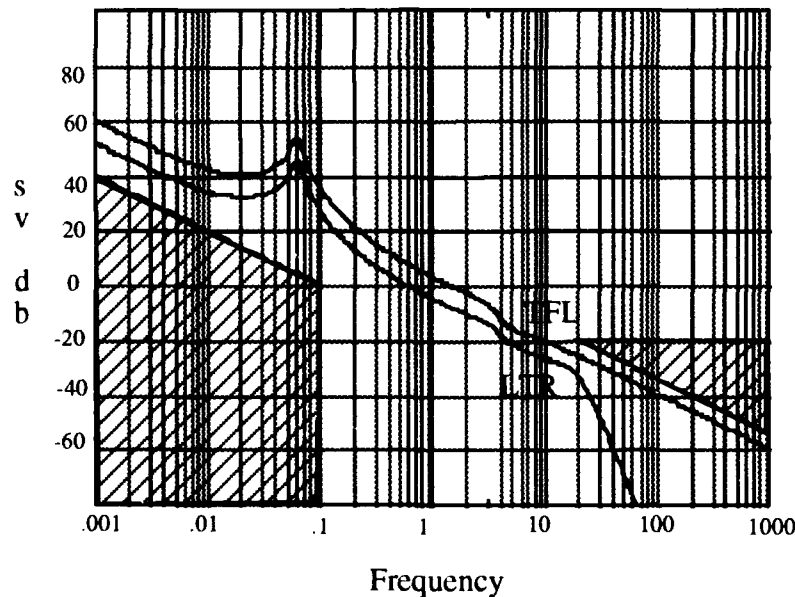


Figure 6 SISO Nominal Plant TFL and LTR Singular Value Curves

Table 2 shows the poles and zeros of the LQG/LTR compensator and closed loop system. It shows the compensator approximately inverts the plant, putting two zeros on real axis close to the phugoid complex poles, causing the closed loop system phugoid mode to disappear. The compensator has two poles which go to the plant transmission zeros as expected. Because part of compensator and closed loop plant dynamics are high frequency, they won't dominate the system response. In the following analysis, high frequency poles will not be listed.

Table 2 Nominal SISO LQG/LTR Compensator and Closed Loop Poles and Zeros

	poles	zeros
compensator	-25.47±9.85 i -6.74±19.9 i -.7603 -.01209	-20 -1.38±3.93 i -.227 -.0121
closed loop system	-.88±4.11i -.2378 -.7603 -.0121	

When angle of attack is chosen as the output, the system becomes angle of attack to elevator response. The transmission zeros become one at high frequency and two complex zeros close to the phugoid poles. With this configuration, the LQG/LTR compensator will closely invert the plant. Thus when plant has transmission zero on the real axis and close to system pole, the compensator may not invert the plant closely.

The closed loop system response to a pitch angle step input is shown in figure 7. The oscillatory response due to the nominal short period mode is not well damped. The response shows good tracking performance. The phugoid mode cannot be observed.

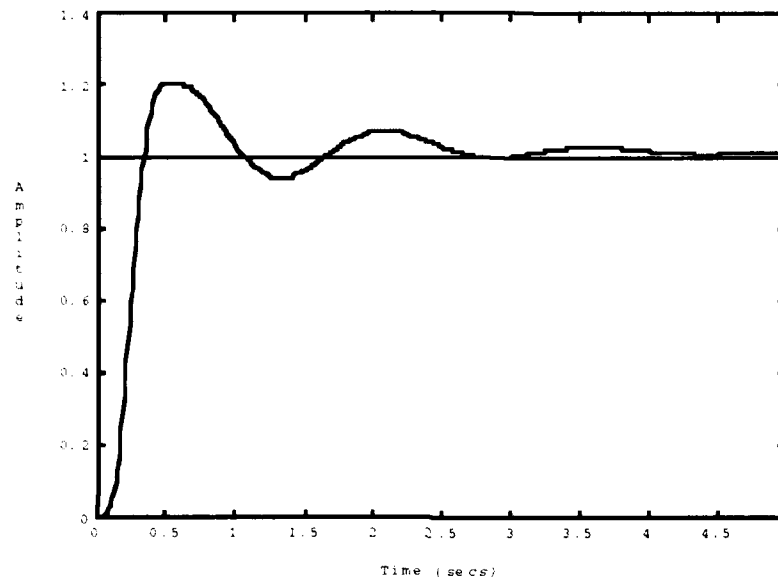


Figure 7 SISO Nominal Plant Closed Loop Pitch Angle Step Response

3.3.3 Static Output Feedback In classical aircraft SISO system feedback design, using single output feedback inner loop with proportional and integral gains, the closed loop poles can be assigned to all positions along the root locus. But a system has its inherent limitations on closed loop pole assignment; moving some poles to better location can result in moving the remaining poles to a degraded location. For instance, feedback pitch angle or airspeed can move phugoid poles to a higher damping location, but will sacrifice short period damping; feedback pitch rate or AOA rate can move short period poles to increased damping location, but will not affect phugoid too much. Thus, SISO feedback design technique has a major limitation — pole assignment is limited to the system root locus, and arbitrary closed loop pole

assignment is not possible. For MIMO systems, the root locus technique is not a practical tool for feedback design. Hence static output feedback will be used to reassign system poles.

3.3.3.1 Output Selection. In the feedback gain matrix equation

$$F = (Z - A_1 V) (C V)^{-1} \quad (133)$$

for assigning complex pair poles like phugoid or short period, the V matrix has two columns. In order to have CV invertible, we need to have two outputs. Since improving the plant's phugoid mode is a main concern of this design, airspeed and pitch angle feedback makes the phugoid poles more assignable. Other combinations do not give more assignability on phugoid poles. Output feedback can exactly assign plant poles, but the unassigned poles will drift randomly. Selecting some combination of two other variables as feedbacks, like pitch rate and pitch angle, the unassigned poles will drift to unstable. Basically, the output feedback affects the pole assignability following the classical feedback rules and depends on how the feedback variable changes the closed loop dynamics equation. One way to select the output is to look at the corresponding normalized eigenvector of the desired eigenvalue; if any element of the eigenvector has relatively larger magnitude, it is more effective to changing that mode when feeding it back. For example, the airspeed and pitch angle elements of the phugoid eigenvector are large compared to other elements, therefore, are good candidates for feedback.

3.3.3.2 Pole Assignment . We will use airspeed and pitch angle output to increased phugoid damping, keep constant phugoid frequency, and leave the other three poles unassigned. While the phugoid assigned is to a better damping location , the short period damping also increases. If the phugoid frequency is increased with phugoid damping higher than 0.3, the short period poles will come to the origin. Generally, improving one mode will sacrifice the other. Since we cannot improve both phugoid and short period modes, and choosing phugoid poles faster than normal (slower than .01 rad/sec) will cause the phugoid to affect pitch response, it was decided to improve phugoid damping and not change the phugoid frequency. When assigning phugoid poles to $-.0534 \pm .0468 i$, the closed loop poles and static gain F are:

closed loop poles : $-.0534 \pm .0468i$, $-1.022 \pm 3.749i$, -20.1

static gain F : $-.0006$, $.0925$

The phugoid poles can be assigned exactly to the desired location, but to keep the unassigned poles stable, the assignable region of the phugoid is limited.

3.3.3.3 LQG/LTR Compensator Design. We now augment the SOF inner closed loop plant with a single integrator to control steady state error, then design a target feedback loop and recover the loop transfer function. We obtain the LQG/LTR compensator which stabilizes the SOF inner loop plant. The combined compensator, integrator and SOF plant block diagram is given in Figure 8.

3.3.3.2 Pole Assignment . We will use airspeed and pitch angle output to increased phugoid damping, keep constant phugoid frequency, and leave the other three poles unassigned. While the phugoid assigned is to a better damping location , the short period damping also increases. If the phugoid frequency is increased with phugoid damping higher than 0.3, the short period poles will come to the origin. Generally, improving one mode will sacrifice the other. Since we cannot improve both phugoid and short period modes, and choosing phugoid poles faster than normal (slower than .01 rad/sec) will cause the phugoid to affect pitch response, it was decided to improve phugoid damping and not change the phugoid frequency. When assigning phugoid poles to $-.0534 \pm .0468 i$, the closed loop poles and static gain F are:

closed loop poles : $-.0534 \pm .0468i$, $-1.022 \pm 3.749i$, -20.1

static gain F : $-.0006$, $.0925$

The phugoid poles can be assigned exactly to the desired location, but to keep the unassigned poles stable, the assignable region of the phugoid is limited.

3.3.3.3 LQG/LTR Compensator Design. We now augment the SOF inner closed loop plant with a single integrator to control steady state error, then design a target feedback loop and recover the loop transfer function. We obtain the LQG/LTR compensator which stabilizes the SOF inner loop plant. The combined compensator, integrator and SOF plant block diagram is given in Figure 8.

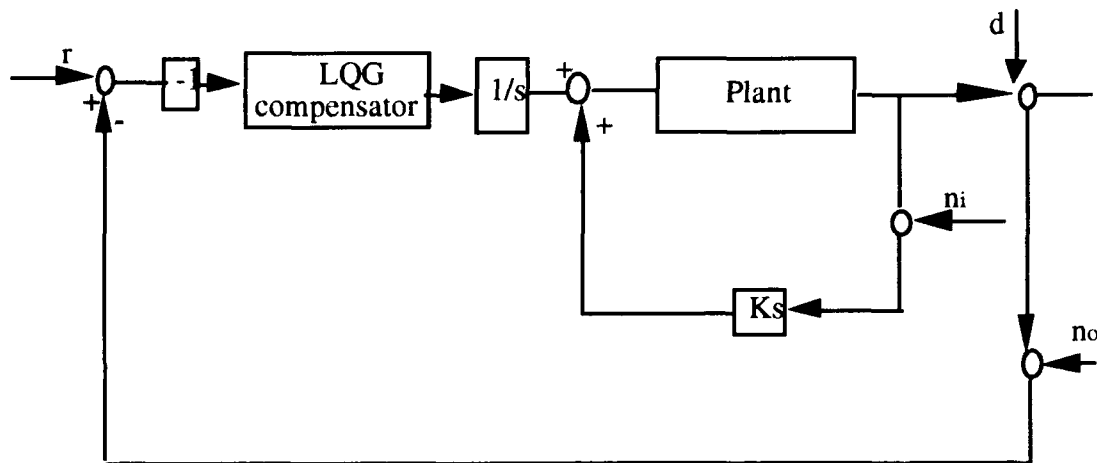


Figure 8 LQG/LTR Compensator and Plant Block Diagram

The system in Figure 8 includes d , which are the disturbances injected at the output of the plant, n_i which is noise in the inner static output feedback loop, and n_o which is the noise in the outer feedback loop measurements. This block diagram will be used for all the model design analysis.

While tuning the LQ Regulator to recover the loop transfer function, the same q and μ as the nominal design are chosen, so that we can compare the system performance and stability robustness on the same baseline. The target feedback loop and LTR singular value curves are shown in Figure 9. The loop shape is very close to the nominal plant designed shape, except the low damping phugoid peak does not exist. System bandwidth is about the same as the nominal design.

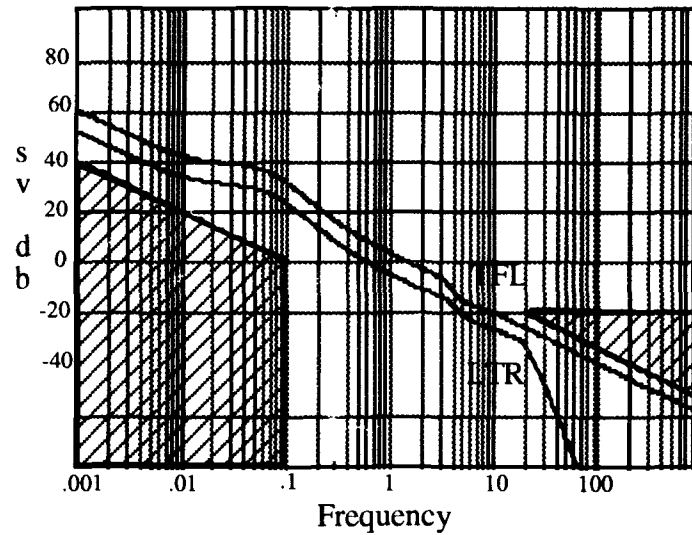


Figure 9 SISO SOF Plant TFL and LTR Singular Value Curves

The compensator and closed loop system poles and zeros are showed in Table 3. Notice that the compensator also does not closely invert the plant. The phugoid mode became well damped, and short period damping is reduced compared with the nominal design.

Table 3 SISO SOF Plant Compensator and Closed Loop System Poles and Zeros

	poles	zeros
compensator	$-25.5 \pm 9.86i$ $-6.72 \pm 18.96i$ $-.7306$ $-.012$	-20.1 $-1.33 \pm 4.16i$ $-.288$ $-.0121$
closed loop system	$-.80 \pm 4.36 i$ $-.3$ $-.7603$ $-.0121$	

3.3.4 *Robust Eigenstructure Assignment.* We use the duality of the Kalman filter with the LQ Regulator for Huckabone's [11 : 78 - 103] Fortran program. The inputs and outputs of the program are

$$[Q, R, P, \Lambda_a, V_a, \theta, \bar{J}] = \text{LQREA} (A, B, \Lambda_d, F_e, V_d, F_v, \text{tol}, \text{Rcode})$$

The user must provide the following inputs by defining them in MATLAB

- A and B matrices
- Λ_d , diagonal matrix containing the desired eigenvalues
- F_e , diagonal matrix containing the weightings for each eigenvalue
- V_d , the desired modal matrix
- F_v , a matrix containing the eigenvector weightings, columns of F_v corresponding to columns of V_d
- tol, convergence tolerance
- Rcode, code specify type of R matrix used. Rcode = 1 is a diagonal matrix

Available outputs from the program are

- Q, LQR state weighting matrix
- R, LQR control weighting matrix
- P, unique positive semidefinite solution to the algebraic Riccati equation
- Λ_a , diagonal matrix containing the achievable closed loop eigenvalues
- θ , diagonal matrix containing the eigenvector difference minimization parameter
- \bar{J} , the final value of the performance index

Input the plant with integrator augmented and transpose the A,C matrices. When we input the transposed A matrix (A^T), the eigenvalues of A^T matrix are the same as A

matrix, but eigenvectors are different, the eigenvector of A^T becomes the left eigenvector. It can be derived that the left eigenvectors modal matrix (W) and right eigenvectors (V) modal matrix have the relationship of $W = [V^{-1}]^T$, that is the rows of the inverse right eigenvector matrix are the columns of the left eigenvector matrix. We then can use above relationship to assign the desired eigenstructure of the closed loop Kalman filter.

For this SISO design, we assign

$$F_e = \begin{bmatrix} 1 \\ 1 \\ 1 \\ 1 \\ 1 \\ 1 \\ 1 \end{bmatrix}, \quad \Lambda_d = \text{diag} \begin{bmatrix} -4.0 \pm 1.5 i \\ -2.5 \pm 2.7 i \\ -20 \\ -.0121 \end{bmatrix}$$

The desired eigenvalues are assigned to delete the phugoid mode by moving it to higher frequency and damping. Short period eigenvalues are assigned to have better damping and frequency also. The actuator pole is assigned to its original location, so that actuator performance can be maintained. The desired eigenvalues are equally weighted. Because we are not designing a flight control system to give unconventional flying qualities, reshaping the eigenvector to have decoupled response is not the design goal. To shorten the calculating time, eigenvectors are not assigned and the eigenvector weighting matrix is chosen as zeros. Tolerance is selected to be one and a diagonal control matrix is selected. The returned achievable eigenvalues are:

$$\Lambda_a = \text{diag} \begin{bmatrix} -3.594 \pm 1.347 i \\ -2.413 \pm 2.255 i \\ -20.23 \\ -.0121 \end{bmatrix}$$

The cost function index is $\bar{J} = .8382$; it has acceptable approximation to the desired eigenvalues. Increased damping and higher frequency eigenvalues assignment was tried with desired eigenvalues like

$$\Lambda_d = \text{diag} \begin{bmatrix} -4.0 \pm 3.0 i \\ -3.2 \pm 3.4 i \\ -20 \\ -.0121 \end{bmatrix}$$

The REA program returned achievable eigenvalues were:

$$\Lambda_a = \text{diag} \begin{bmatrix} -3.8 \pm 2.47 i \\ -3.03 \pm 2.78 i \\ -19.99 \\ -.0121 \end{bmatrix}$$

The achievable eigenvalues are not close to desired eigenvalues and the cost function index is $\bar{J} = 1.45$. Assigning less damping and slower frequency, the achievable eigenvalues are much closer to desired, and the cost function can be reduce to $\bar{J} = 0.000054$. Thus, there is a certain region close to original eigenvalues where the Kalman filter can achieve the desired.

Table 4 lists the eigenvalues of the closed loop Kalman filter of original open loop plant, static output feedback closed inner loop plant and robust eigenstructure assignment. We know that the closed loop Kalman filter poles will be part of the system closed loop poles. Table 4 shows robust eigenstructure assignment has better assignability than static output feedback method in this SISO problem. The computing time for running the LQREA program is on average 3 minutes; the short computing time is due to low order of this SISO system, and unassigned eigenvectors.

Table 4 SISO Nominal, SOF, REA Designs Closed loop Kalman Filter Poles

design	nominal	SOF	REA
Kalman filter closed loop poles	-19.89 -10.86 -.883±4.1 i -.2378 -.0121	-19.98 -10.7 -.8±4.36 i -.3 -.0121	-20.23 -2.41±2.25 i -3.59±1.34 i -.0121

3.3.4.1 *LQG/LTR Compensator Design* . The LQREA returned a Kalman filter state weighting matrix Q_f which is symmetric, positive semidefinite, and control weighting matrix R_f , which is a diagonal matrix and positive definite. A^T, C^T, Q_f and R_f are used to solve the algebraic equation

$$AP + PA^T - PC^T R_f^{-1} CP + H^T QH = 0 \quad (134)$$

then

$$K_f^T = R_f^{-1} C P \quad \text{or} \quad K_f = (R_f^{-1} C P)^T \quad (135)$$

The $C\Phi K_f$ singular value curve is shown in Figure 10. The loop shape satisfies the specifications. By using this robust eigenstructure assignment algorithm, and using the returned state and control weighting matrices to calculate Kalman filter gain matrix, we cannot fine tuning the $C\Phi K_f$ loop shape, except changing the μ value in

$$R_f = \mu I \quad (136)$$

so the crossover frequency can be changed. By choosing $q = 300$, the LTR singular value curve is also shown in Figure 10; the recovered loop shape met the specifications. The LQG/LTR compensator and closed loop system poles and zeros are in Table 5. The closed loop short period and phugoid modes are much improved.

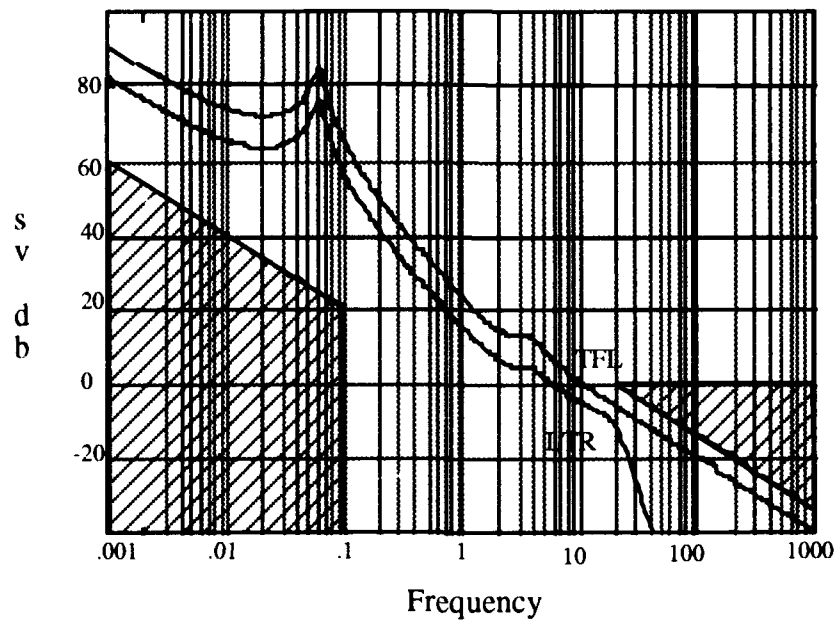


Figure 10 REA design $C\Phi K_f$ and LTR singular value curves

Table 5 SISO REA design compensator and closed loop poles and zeros

	poles	zeros
compensator	$-25.59 \pm 10.16i$ $-6.45 \pm 19.42i$ $-.7306$ $-.012$	-19.98 $-1.24 \pm 2.97i$ -1.19 $-.0121$
closed loop system	$-3.59 \pm 1.34i$ $-2.41 \pm 2.26i$ $-.7603$ $-.0121$	

3.3.5 Results Comparison. By comparing the closed loop poles of the nominal plant design, SOF and REA method designs in Tables 2, 3 and 5, we see that using the SOF method, the phugoid poles cannot be assigned arbitrarily, resulting in the closed loop poles differing somewhat from nominal. With the REA method the phugoid poles can be moved to a further left location, resulting in a closed loop system with good short period damping. The pitch angle step input responses are given in Figure 11. The REA method has improved the short period damping and tracking performance is good for all methods.

The complementary sensitivity T singular value indicates system robustness, as stated in the "small gain theory": for a robust system

$$\bar{\sigma}[T] = \bar{\sigma}[GK(I + GK)^{-1}] \leq \frac{1}{\sigma[L(\omega)]} \quad (138)$$

The lower the maximum singular value of the complementary sensitivity and crossover frequency, the more robust the closed loop system. All three complementary sensitivity singular value curves are shown in Figure 12. The REA curve has higher crossover frequency, since we didn't change returned the R_f matrix. If we adjust R_f to have same crossover frequency as the nominal and SOF designs, then $\sigma[T]$ of the REA design will have a lower value at high frequency, and will be more robust. The lower the $\sigma[T]$ at high frequency the better the high frequency noise rejection capability. Figure 13 shows the responses of step pitch angle input with noise injected into the feedback path. The SOF design response has noise injected both at inner and outer feedback path.

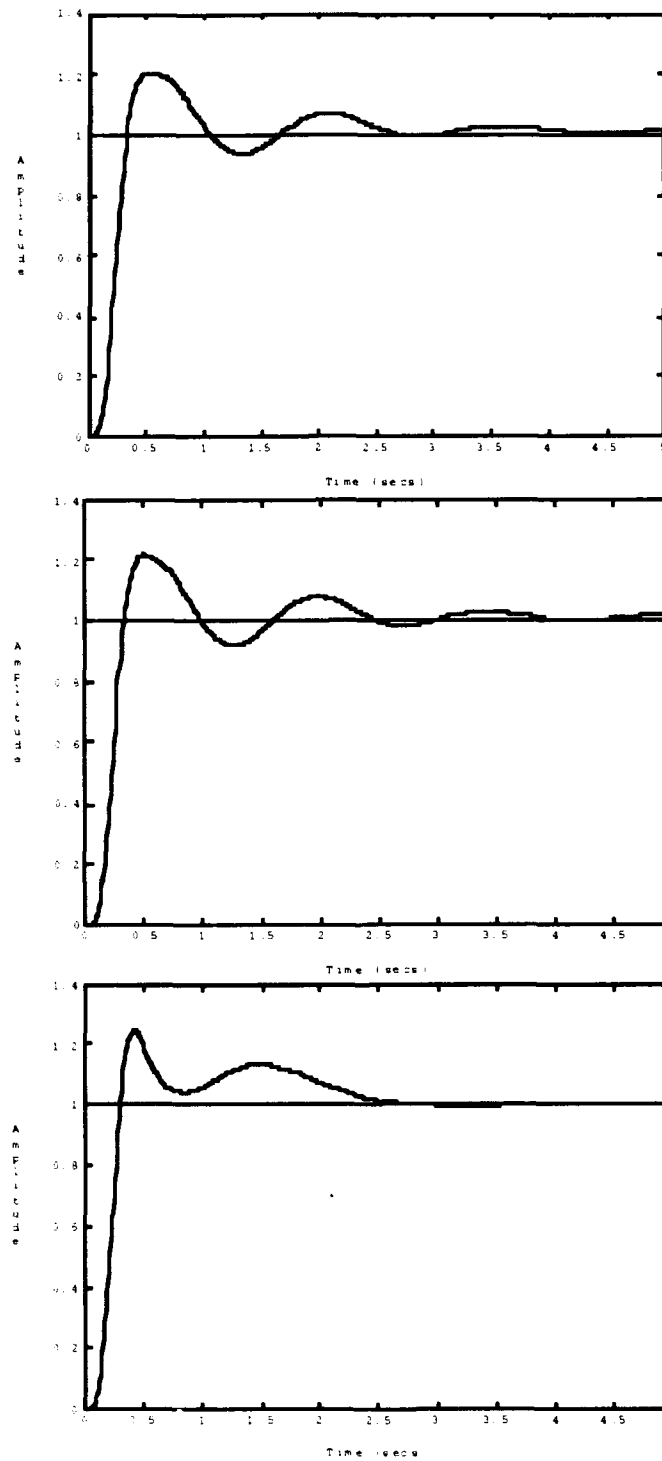


Figure 11 SISO θ step input response of nominal, SOF, REA design (top down)

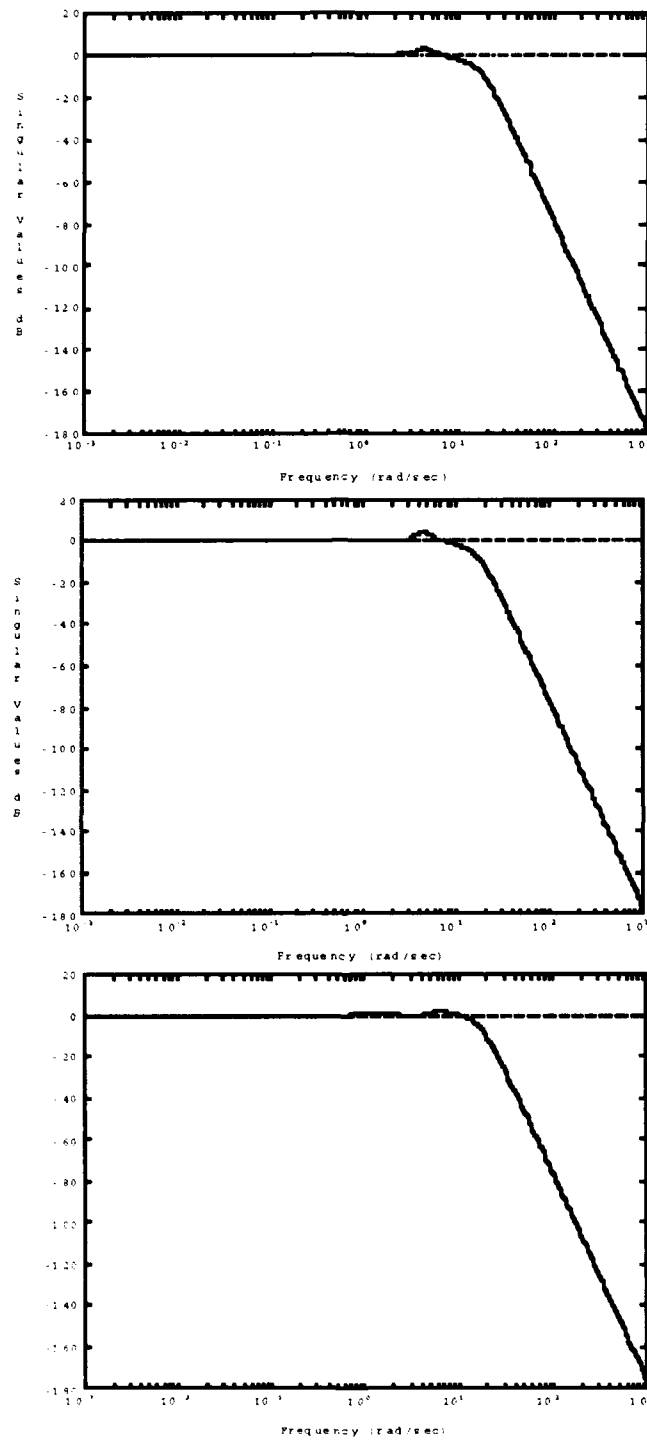


Figure12 $\sigma[T]$ Curves of Nominal, SOF, REA designs (top down)

In the inner loop the static gain vector is $[-.0006, .0925]$, so inner loop noise will be attenuated. Time responses show no difference between nominal and SOF designs. The REA design should have better noise rejection capability, if we adjust the crossover frequency to lower σ [T].

The sensitivity curves of all the closed loop system are shown in Figure 14. All curves show mismatch of low frequency poles and zeros. The SOF method has slightly lower sensitivity than nominal at low frequency. The REA method gave lowest sensitivity at low frequency, and this should be reflected in the disturbance rejecting capability. The A-4 gust transfer function is used in the simulation model, and the closed loop system is excited with white Gaussian noise, cascaded with a $0.1 / (s+1)$ lag filter to clear the high frequency signal. The pitch angle step input with disturbance responses of all the designs are shown in Figure 15.

The best way to analyze stability margins of a SISO system is by looking at the Nyquist plot of the open loop system. Two points on the plot give gain and phase margins. The closest point of the open loop transfer function gk to the $(-1, 0)$ point on the plot gives the gain margin. The point where gk intersects with a unit circle centered at origin indicates the phase margin. Nyquist plots of all three designs are shown in Figure 16. The SOF method doesn't improve the stability margin, and the REA method has slightly better phase margins, but reducing gain margin. Because we didn't choose a high q value for completely recovering stability robustness, the gain and phase margins shown here are not as good as the guaranteed gain and phase margins of a full state Kalman filter.

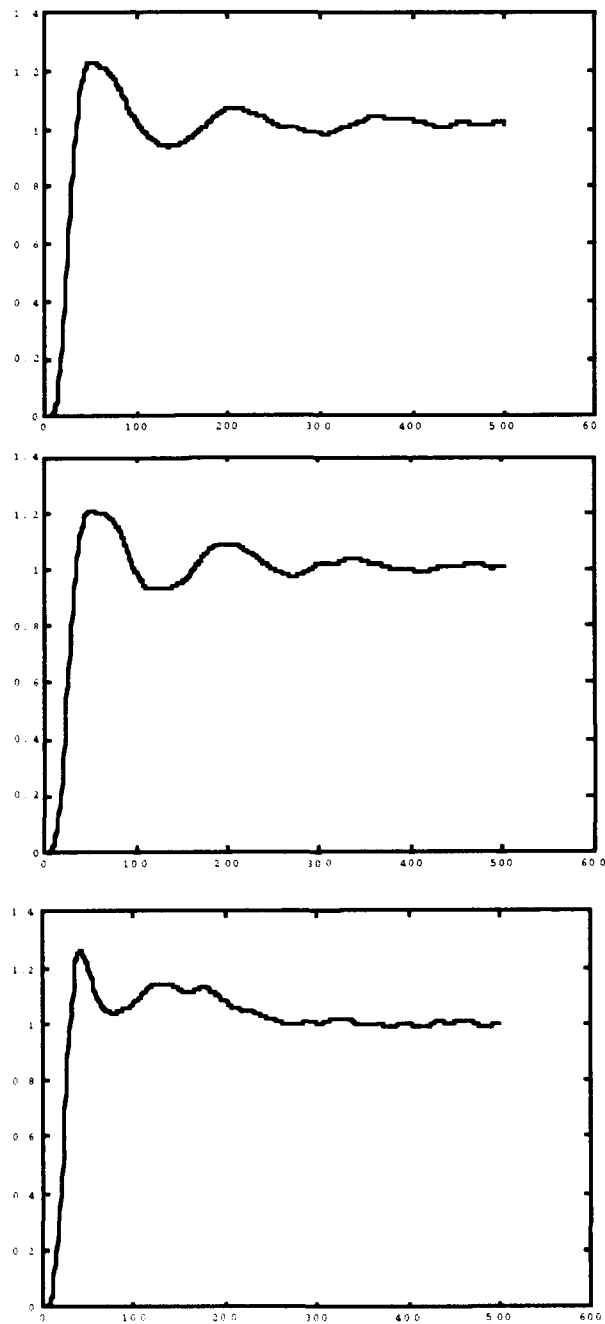


Figure 13 SISO Step Input with Noise Response of Nominal, SOF, REA Designs
(x coordinate is SIMULINK time unit, 100 \approx 1sec)

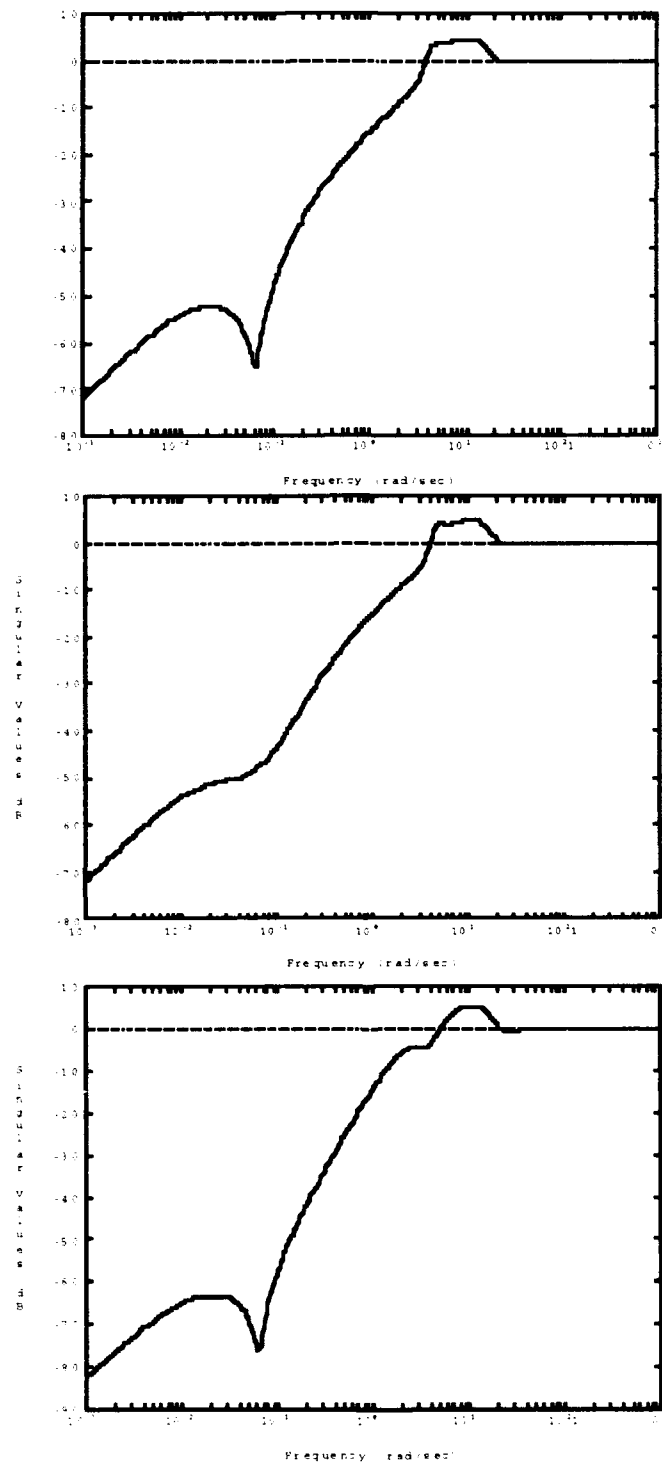


Figure 14 SISO Sensitivity σ curves of nominal, SOF, REA designs (top down)

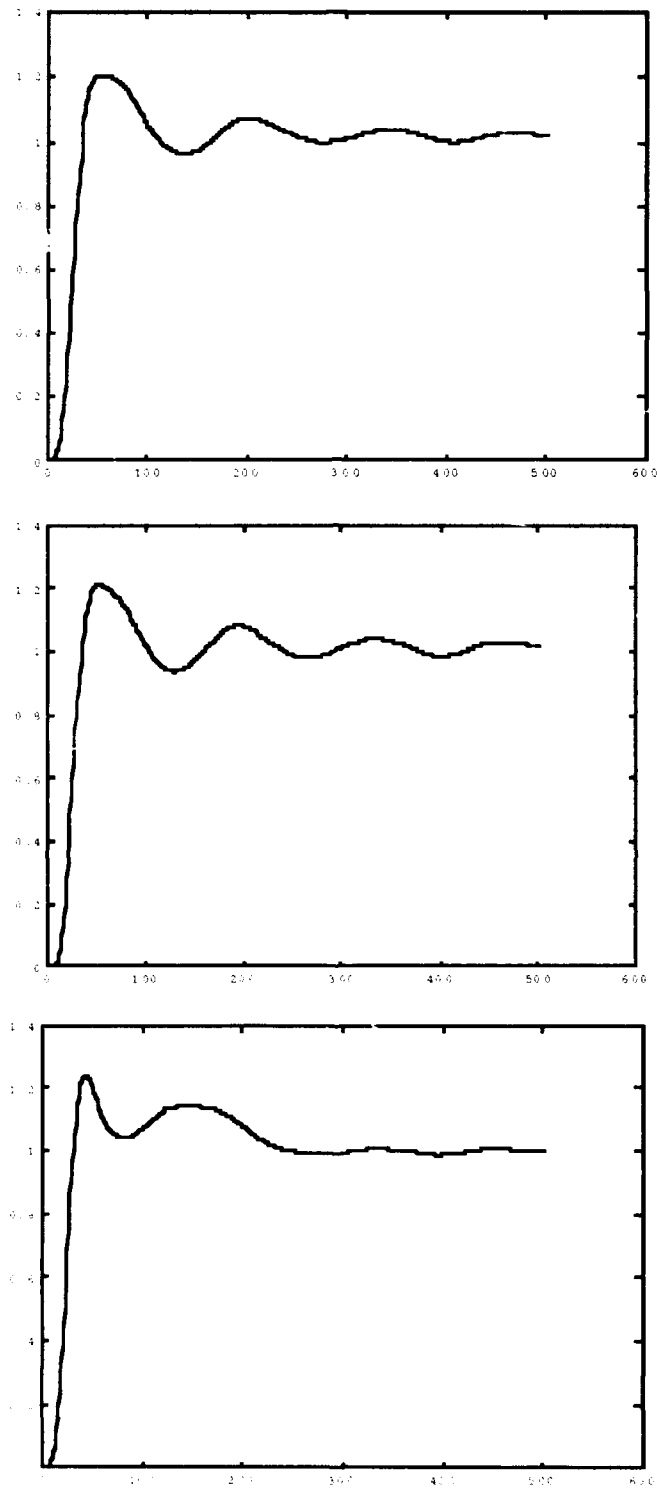


Figure 15 SISO Disturbance Response of Nominal, SOF, REA Designs

(x coordinate is SIMULINK time unit, 100 \approx 1sec)

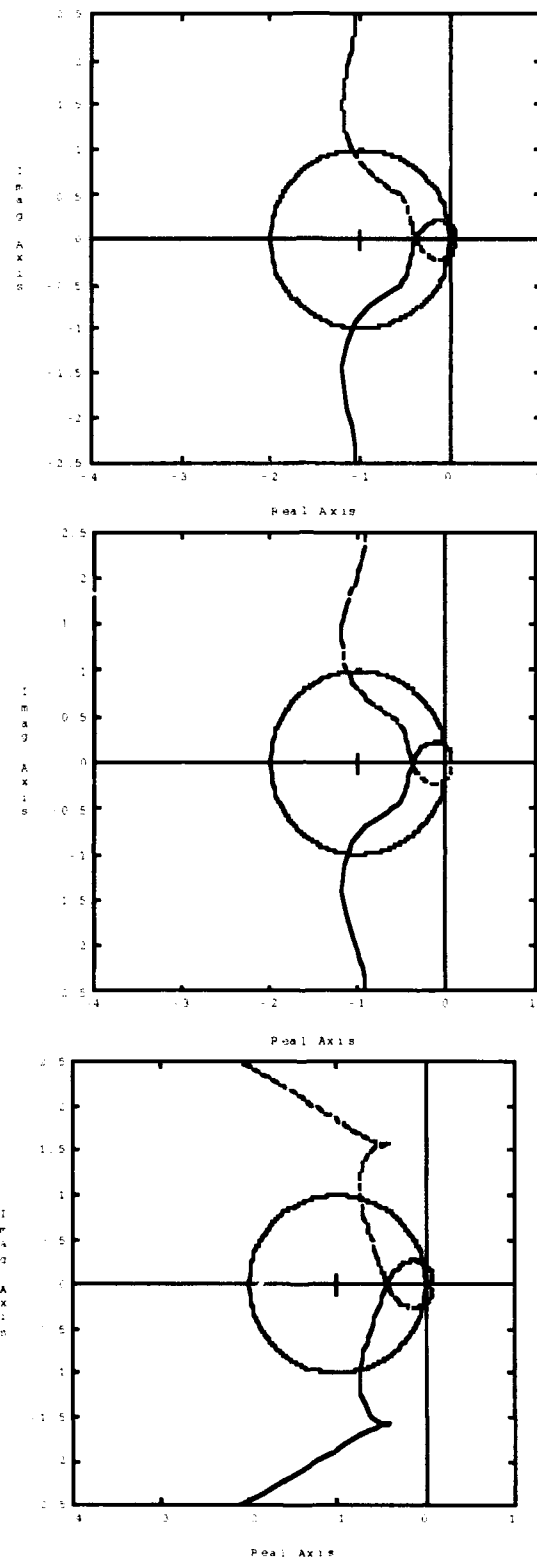


Figure 16 SISO Nyquist plot of nominal, SOF, REA designs

3.3.6 Robustness with Perturbed Plant. For an aircraft like the A-4, which is a subsonic fighter aircraft, the altitude / airspeed operational envelope is still considerably broad. Different flight conditions from the nominal, like different Mach, altitude or angle of attack cause the plant characteristics to differ from the nominal plant. Other factors like measurement error, structure flexibility, etc., can perturb the nominal plant. Flight control design is based on a certain nominal design model; when the plant is perturbed, the controller designed for the nominal plant may not be effective in stabilizing the perturbed plant. Suppose the actual and nominal plant has following relationship

$$G_a = (1 + \epsilon) G_o \quad (139)$$

where G_a and G_o are the actual and nominal plant, respectively. The actual plant poles may also be affected, thus suppose the following relationship on pole location holds:

$$(Re + Im)_a = (1 + \epsilon) (Re + Im)_o \quad (140)$$

where Re and Im are the real and imaginary parts of the plant pole. If, given the worst case, only the real part varies by decreasing the real value, i.e, ϵ is negative, the damping will decrease from nominal system. Suppose there is a - 5% perturbation of the phugoid mode from nominal condition, ($\epsilon = -.05$). Using the same static gain from the SOF method and the same LQG/LTR compensators from all the designs, the perturbed system is formed. The closed loop poles are showed in Table 6. All the closed loop system are still stable and in the SOF design the system damping even improved. Figure 17 and Figure 18 show the sensitivity and complementary sensitivity of perturbed closed loop system. The SOF sensitivity is increased, but

should be good for tracking and disturbance rejection. The complementary sensitivities have no apparent change.

Table 6 Perturbed Closed Loop Poles of Nominal, SOF, REA Designs

design	nominal	SOF	REA
closed loop pole	-.0053	-.0053	-.0118
	-.0121	-.0121	-.012
	-.2366	-.2991	-.7601
	-.7679	-.7679	-2.41±2.256 i
	-.883±4.11 i	-.805±4.36 i	-3.598±1.34 i

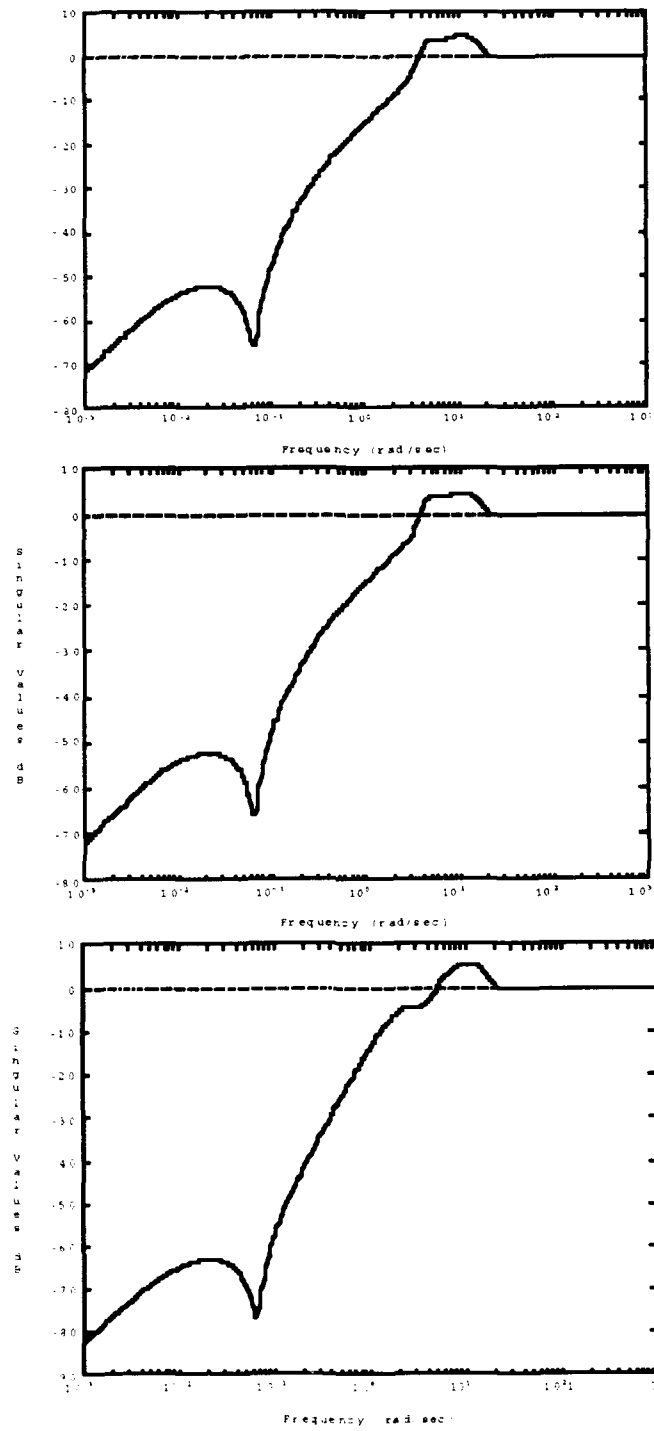


Figure 17 Perturbed Plant Sensitivity σ Curves of Nominal, SOF, REA Design

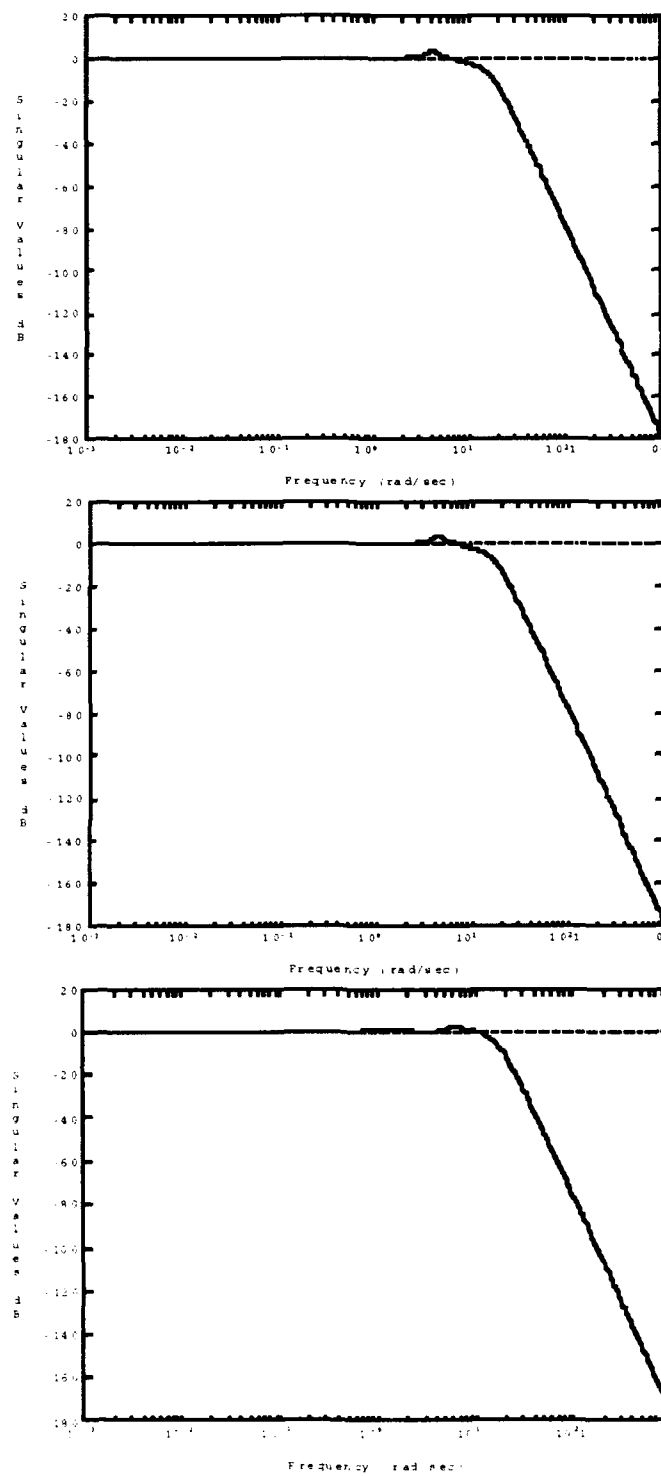


Figure 18 Perturbed $\sigma[T]$ Curves of Nominal, SOF, REA Designs

3.4 MIMO System Design and Results Analysis

3.4.1 *Plant.* The state space form of the MIMO plant with actuators is given in Appendix A. The states, controls and outputs are:

$$x = \begin{bmatrix} \text{sideslip angle } (\beta) - \text{deg} \\ \text{roll rate } (p) - \text{deg/sec} \\ \text{bank angle } (\phi) - \text{deg} \\ \text{yaw rate } (r) - \text{deg/sec} \\ \text{aileron deflection } (\delta_a) \\ \quad - \text{deg} \\ \text{rudder deflection } (\delta_r) \\ \quad - \text{deg} \end{bmatrix}, \quad u = \begin{bmatrix} \text{aileron command } (\delta_{ac}) \\ \quad - \text{deg} \\ \text{rudder command } (\delta_{rc}) \\ \quad - \text{deg} \end{bmatrix}, \quad y = \begin{bmatrix} \text{sideslip angle} \\ \text{bank angle} \end{bmatrix}$$

Table 7 MIMO open loop plant eigenvalues, eigenvectors and zero

mode	dutch roll	roll	spiral	actuator	actuator
eigenvalue	$-.386 \pm 4.322i$	-1.53	-.0058	-20	-20
eigenvector	$-.087 \pm .066 i$ $-.239 \pm .819 i$ $-.183 \pm .072 i$ $.262 \pm .39 i$ 0 0	-.0003 .8368 -.5467 -.0278 0 0	.0015 -.0058 .9988 .0496 0 0	-.0009 -.9976 .0499 -.0185 .0433 0	.028 -.7838 .0392 .6146 0 .0749
zero	-207.3				

The open loop eigenvalues, eigenvectors and zeros are given in Table 7. The plant has a lightly damped Dutch roll mode ($\zeta_{DR} = .0891$), which must be moved to a better damped location to avoid poor LQG/LTR plant inversion results. To eliminate steady state step response error, integrators are augmented in the two control

channels. The two inputs and outputs have the same units, and have about the same magnitude, so scaling is not necessary for this MIMO model.

3.4.2 MIMO Loop Shaping Technique. In a MIMO system, the number of singular value curves is determined by $\min[m, r]$, where m and r are the dimension of control and output, respectively. For this two input two output problem, we will have two curves, the maximum ($\bar{\sigma}$) and minimum ($\underline{\sigma}$) singular value curves. Widely separated $\bar{\sigma}$ and $\underline{\sigma}$ curves means a change in input direction will result in different shape and magnitude of the output, thus the system characteristics will be hard to predict. One of the steps in shaping the target feedback loop (TFL) in a MIMO problem is to use the loop shaping techniques to match $\bar{\sigma}$ and $\underline{\sigma}$ curves as close as possible at low, high and crossover frequency, so that system performance and stability can be consistent with inputs in different directions. Low / high frequency matching techniques by selecting the Γ matrix were described in Section 3.2. Another method used for loop shape matching at a certain selected frequency is by forming:

$$C [(j\omega) I - A]^{-1} \Gamma_c = I \quad (141)$$

where $j\omega$ is selected frequency. $\Gamma_c = \Gamma M$, where M is a so-called matching matrix, and Γ is the original Γ matrix. Then

$$M = \{ C [(j\omega) I - A]^{-1} \Gamma \}^{-1} \quad (142)$$

The M matrix will be complex, and will be approximated by its real part. The new matrix $\Gamma_c = \Gamma M$ should give good matching of the $\bar{\sigma}$ and $\underline{\sigma}$ curves at the selected frequency [19: 70].

Sometimes in MIMO systems the outputs and inputs have different units or large differences in magnitude. For instance, in the engine control problem, one output is Rotations Per Minute (RPM) and normally has large magnitude. The other output may be nozzle or compressor vane angle, where the unit is degrees and has small magnitude. The $\bar{\sigma}$ and $\underline{\sigma}$ curves will be widely separated, and prescribed loop shape matching techniques will not make them close enough to each other. To solve this problem, rescale the units or magnitude of state space matrices before applying LQG/LTR. To scale the system, given the state space model:

$$\dot{x}(t) = A x(t) + B u(t) \quad (143)$$

$$y(t) = C x(t) \quad (144)$$

the scaled variables $x'(t)$, $u'(t)$, $y'(t)$ are related to $x(t)$, $u(t)$, $y(t)$ as:

$$\begin{aligned} x'(t) &= S_x x(t) \\ u'(t) &= S_u u(t) \\ y'(t) &= S_y y(t) \end{aligned} \quad (145)$$

where S_x , S_u , S_y are diagonal and invertible matrices. Substitute Eq (145) into Eq (143) and (144). The scaled state space model is

$$\dot{x}'(t) = S_x A S_x^{-1} x'(t) + S_x B S_u^{-1} u'(t) \quad (146)$$

$$y'(t) = S_y C S_x^{-1} x'(t) \quad (147)$$

For the A-4 aircraft, the MIMO lateral and directional control model we used, the two input and output units and magnitudes are equivalent to each other, thus scaling is not necessary.

3.4.3 Nominal plant LQG/LTR Compensator Design. The MIMO system TFL singular value curves were shaped by using the low and high frequency matching technique with $\mu = .01$ as shown in Figure 19. Choosing $q = 300$ and control weighting matrix R as an identity matrix, the LTR singular value curves are also shown in Figure 19. The LTR did not fully recover the target loop shape, because of the compromising between optimality, robustness, and bandwidth consideration. Both curves meet the specifications. At the Dutch roll frequency, a mismatch of the plant poles and compensator zeros is obvious.

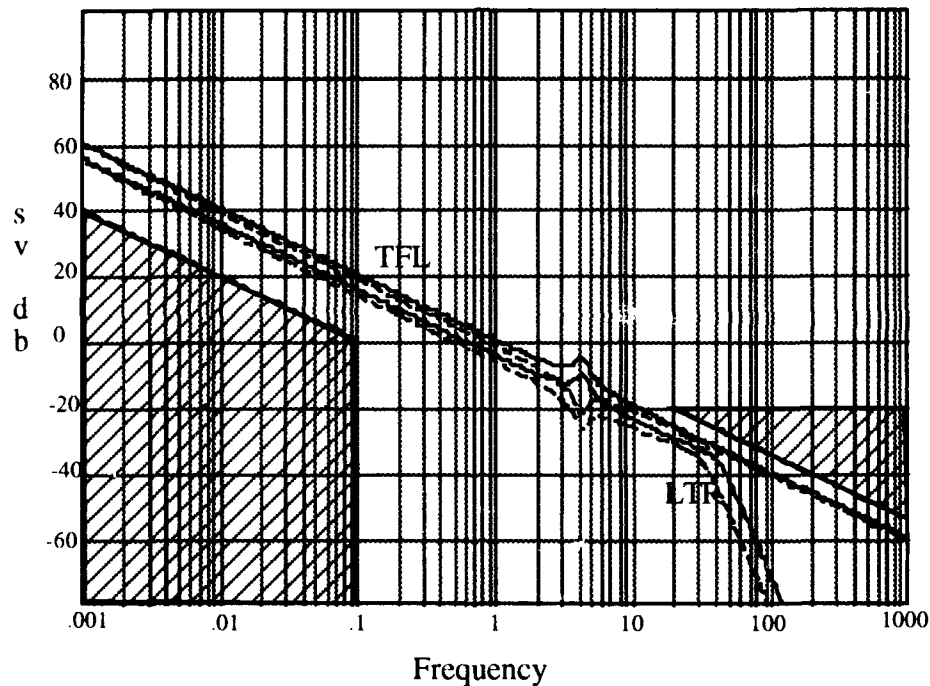


Figure 19 MIMO Nominal Plant TFL and LTR Singular Value Curves

The LQG/LTR compensator and closed loop system poles are listed in Table 8. The compensator's zeros closely invert the plant's poles. The open loop plant transmission zero is at -207.3 rad/sec, so the plant inversion is only on low frequency dynamics. Because the q value is not selected large enough, the compensator's pole

did not go to plant zero. The closed loop system does have a lightly damped Dutch roll mode.

Table 8 Nominal Plant Compensator and Closed Loop System Poles and Zeros

	poles	zeros
compensator	$-14.17 \pm 40.86 i$ $-11.3 \pm 30.84 i$ $-35.79 \pm 14.91 i$ $-49.29 \pm 20.69 i$	$-.327 \pm 4.28 i$ -1.4635 $-.0062$ -20.06 -20
closed loop system	$-.374 \pm 4.22 i$ $-.0062$ -1.4432 $-10.24 \pm 8.37 i$ -19.74 -19.99	

3.4.4 Static Output Feedback and LQG/LTR Compensator Design. The complex, low damping Dutch roll poles need to be moved to a better damping location. Two outputs are required to move the Dutch roll complex pair poles. Bank angle and yaw rate outputs are selected to assign the Dutch roll mode to a better damping location; choosing other outputs always causes an unstable spiral or roll mode. While successfully assigning Dutch roll poles, the two actuator poles wandered randomly, and one went to around 10 rad/sec. To avoid degraded actuator affects on system performance, another two outputs, aileron and rudder deflection are fed back to fix the actuator modes. Like the SISO problem, there is a certain gain selection or certain region in the complex plane where the Dutch roll poles can be assigned without the unassigned poles drifting to undesired location. The SOF inner closed loop reassigned poles are $[-3.433 \pm 2.655i, -.0135, -3.11, -20.98, -21.58]$, and the Dutch roll mode has good damping ($\zeta_{DR} = 0.79$). The roll and spiral modes are improved also. The static

feedback gain matrix F is

$$F = \begin{bmatrix} .0016 & -.0314 & -.0646 & .2448 \\ -.0121 & .0481 & .0323 & -.4211 \end{bmatrix}$$

Standard LQG/LTR procedures and loop shape matching techniques are applied to the SOF design with $q=300$, $\mu = .01$. The TFL and LTR singular value curves are shown in Figure 20. Both curves clear the performance and robustness "barriers". The mismatched pole-zero peak of low damping Dutch roll mode disappeared. The compensator and closed loop system poles and zeros are listed in Table 9. The compensator still inverts the plant, but because the inner loop plant was better conditioned, a low damping Dutch roll mode does not exist in the closed loop system. The SOF method for this MIMO design demonstrated that undesired plant inversion can be prevented.

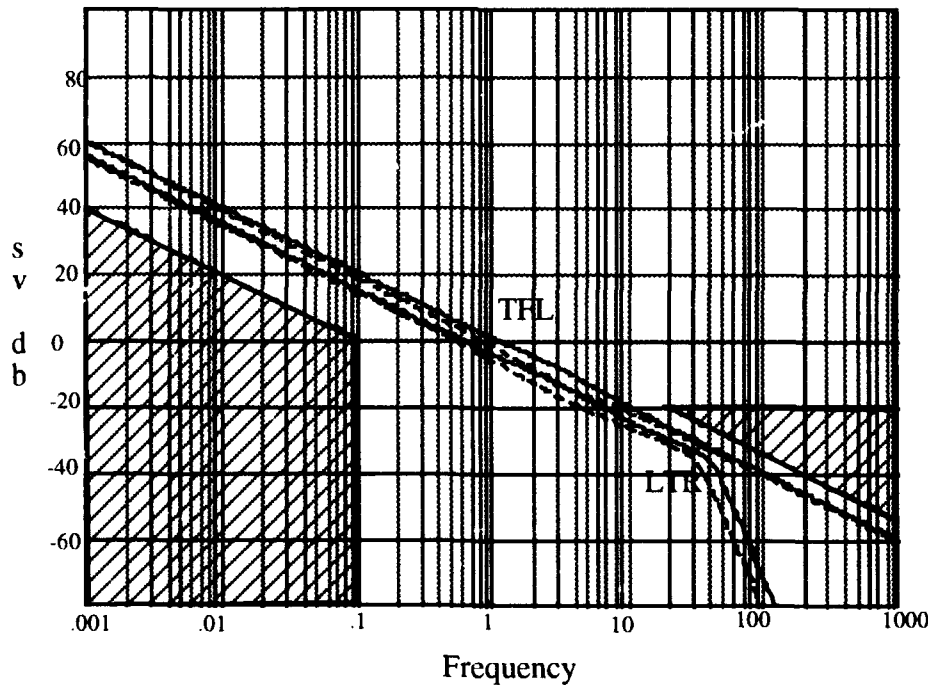


Figure 20 MIMO SOF Design TFL and LTR Singular Value Curves

Table 9 MIMO SOF Design Compensator and Closed Loop System Poles and Zeros

	poles	zeros
compensator	-14.29±40.51 i -11.5±30.64 i -36.27±14.88 i -45.98±20.37 i	-3.504±3.246 i -2.664 -.0139 -21.09 -21
closed loop system	-.0193 -2.497 -3.01±3.352 i -10.18 -11.37	

3.4.5 Robust Eigenstructure Assignment and LQG/LTR Compensator Design.

Because SOF method has good LQG/LTR design results, the desired poles for eigenstructure assignment are chosen to be the same as the SOF design closed loop poles (see Table 9). By this choice, the results of these two method can then be compared with each other. The MIMO open loop plant with integrators augmented into each control channel was used. The desired eigenvalues were weighted equally with one, with no weighting on the eigenvectors. The LQREA program returned the Kalman filter achievable eigenvalues as

$$\Lambda_a = \text{diag} \begin{bmatrix} -3.028 \pm 3.346i \\ -2.511 \\ -.042 \\ -10.24 \\ -11.23 \\ -21.08 \\ -21.12 \end{bmatrix}$$

the cost function index was $\bar{J} = .0028$ and the achievable eigenvalues are very close to desired. The calculating time for this MIMO problem is approximately 30 minutes.

The Q_f and R_f from the LQREA program were used to obtain the target Kalman filter $C\Phi K_f$ loop transfer function. The singular value curves are shown in Figure 21. The $\underline{\sigma}$ curve has very low value at low frequency and the specifications are not met at low frequency. This undesired $\underline{\sigma}$ curve loop shape can not be improved with the prescribed method. Because of the low $\underline{\sigma}$ curve, μ cannot be selected to a higher value to decrease the bandwidth. This is a drawback when using the Robust Eigenstructure Assignment algorithm with LQG/LTR compensator design. By using the REA method, we lost the best nature of LQG/LTR methodology — target loop transfer function shaping — which gives designer the capability to construct the required system performance and stability characteristics according to specifications. In order not to violate the high frequency "barrier", $q=300$ was chosen and the Kalman filter loop shape was not fully recovered. The LTR singular value curves of the REA design are also shown in Figure 21. It has same loop shape as the Kalman filter singular value curves.

The LQG/LTR compensator and closed loop system poles and zeros are shown in Table 10. The compensator doesn't invert the plant dynamics and it has the dynamics required to assign closed loop poles as desired.

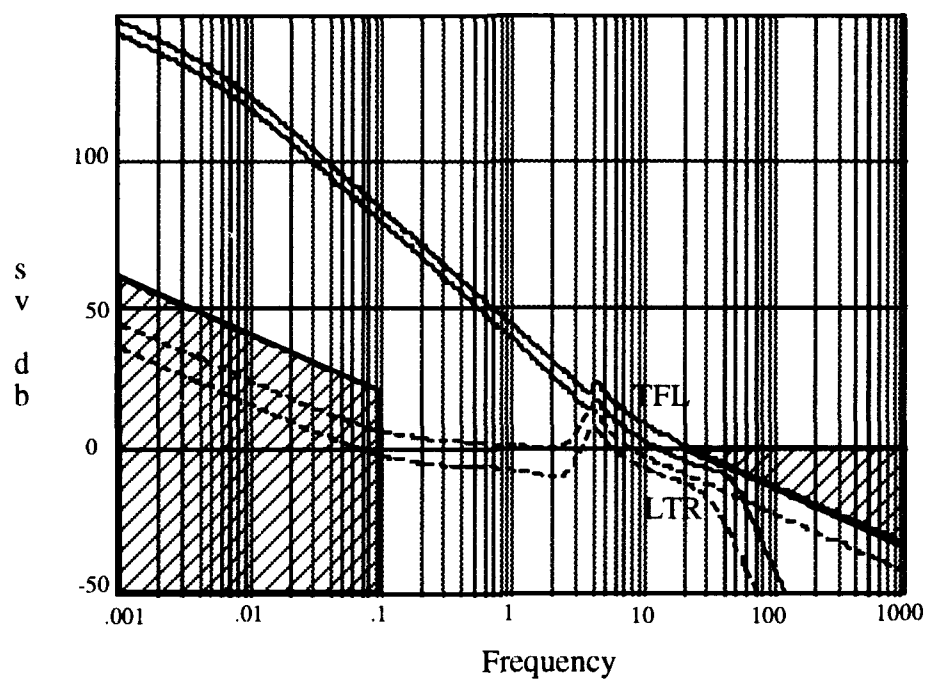


Figure 21 MIMO REA Design $C\Phi K_f$ and LTR Singular Value Curves

Table 10 MIMO REA Design Compensator and Closed Loop Poles and Zeros

	poles	zeros
compensator	$-13.45 \pm 45.49 i$ $-11.73 \pm 29.00 i$ $-53.51 \pm 24.68 i$ $-33.88 \pm 13.42 i$	-6.3944 $-3.23 \pm .87 i$ $-20.85 \pm .14 i$ $-.0628$
closed loop system	$-.045$ -1.926 $-6.36 \pm 3.85 i$ $-11.01 \pm 1.88 i$	

3.4.6 Results Comparison . By looking at the LQG/LTR closed loop poles in Table 8, 9, and 10, we see that SOF and REA design have the same assignability on eigenvalues. REA has a larger assignable region in complex plane than SOF method. From a time domain or transient response point of view, the REA method may be better than the SOF method.

Bank angle step input responses from the three designs are shown in Figure 22. The SOF design's response has improved Dutch roll damping. The REA method has large overshoot due to the closed loop bandwidth and cannot be reduced without sacrificing sensitivity. All three designs give good tracking on bank angle input and keep sideslip angle closed to zero. Sideslip step input does not have much practical meaning from an aircraft flying quality point of view, and is not given. The poor loop shape of LQG/LTR open loop transfer function GK in REA design isn't reflected here in the step input response, since the input direction doesn't excite the shape of σ curve depicted.

Sensitivity singular value curves are shown in Figure 23. The SOF design doesn't have the low damping peak at Dutch roll frequency that the nominal design has. The REA design has poor sensitivity at low frequency.

The complementary sensitivity (T) singular value curves, shown in Figure 24, display the same trend as the sensitivity. The resonant peak of low damping Dutch roll mode does not exist in the SOF design. The REA design has higher closed loop bandwidth, causing higher $\bar{\sigma}[T]$ at high frequency and may result in poor noise rejection. The bank angle step input with noise response are shown in Figure 25; the nominal and SOF designs reject noise very well. The REA design has poor noise rejection capability as predicted by complementary sensitivity. The step input with disturbances in sideslip angle and roll rate responses are shown in Figure 26; all response have good disturbance rejection. The REA design doesn't show poor

response, and may be due to the input direction not exciting the shape of the σ curve.

The independent gain and phase margins for each design are listed in Table 11. The SOF design has the best independent gain and phase margins. The REA design has lower gain and margins.

Table 11 MIMO Independent Gain and Phase Margins

design	nominal	SOF	REA
independent gain margin (db)	[- 8.04, 4.1]	[-23.42, 5.72]	[-6.38, 3.64]
independent phase margin (deg)	± 35.14	± 55.59	± 30.15

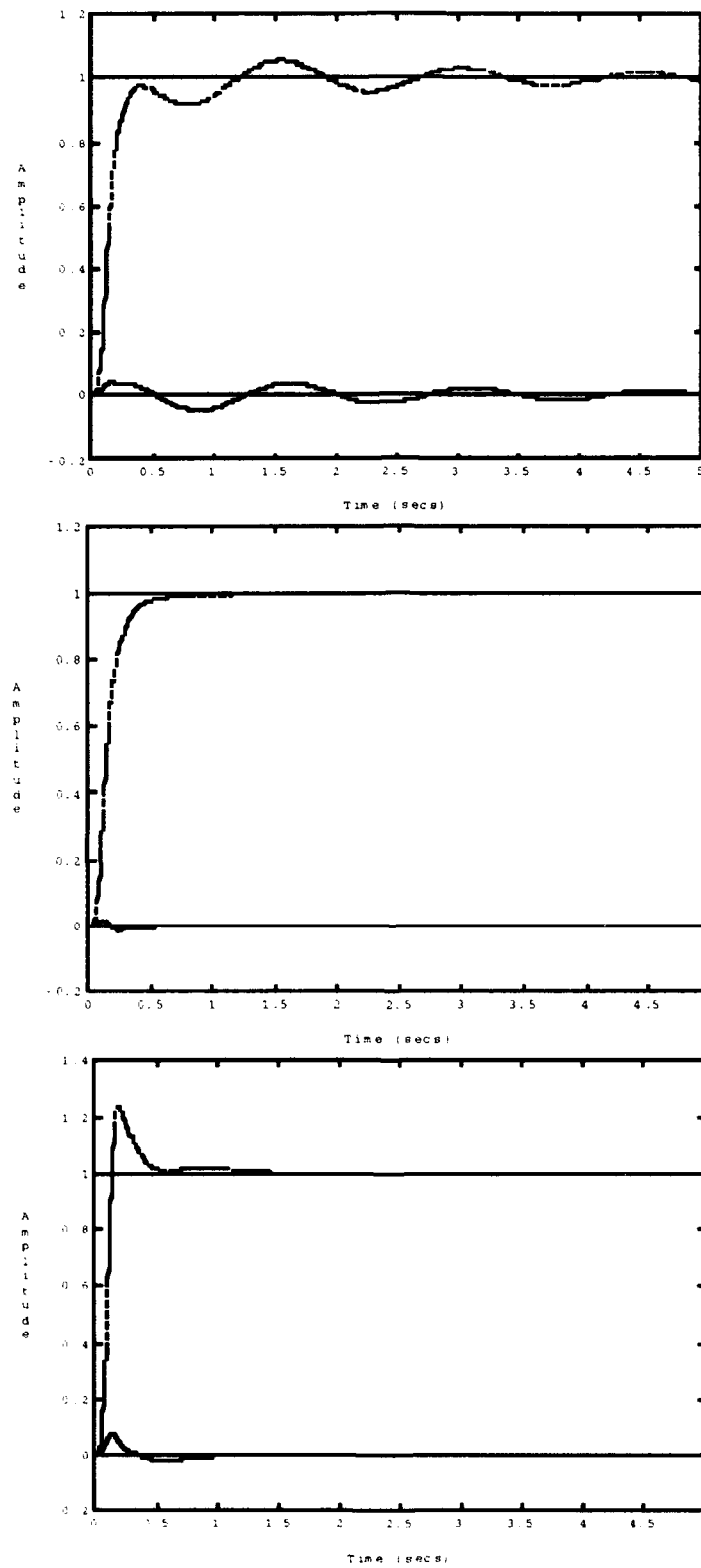


Figure 22 MIMO system ϕ Step Input Response of Nominal, SOF, REA designs

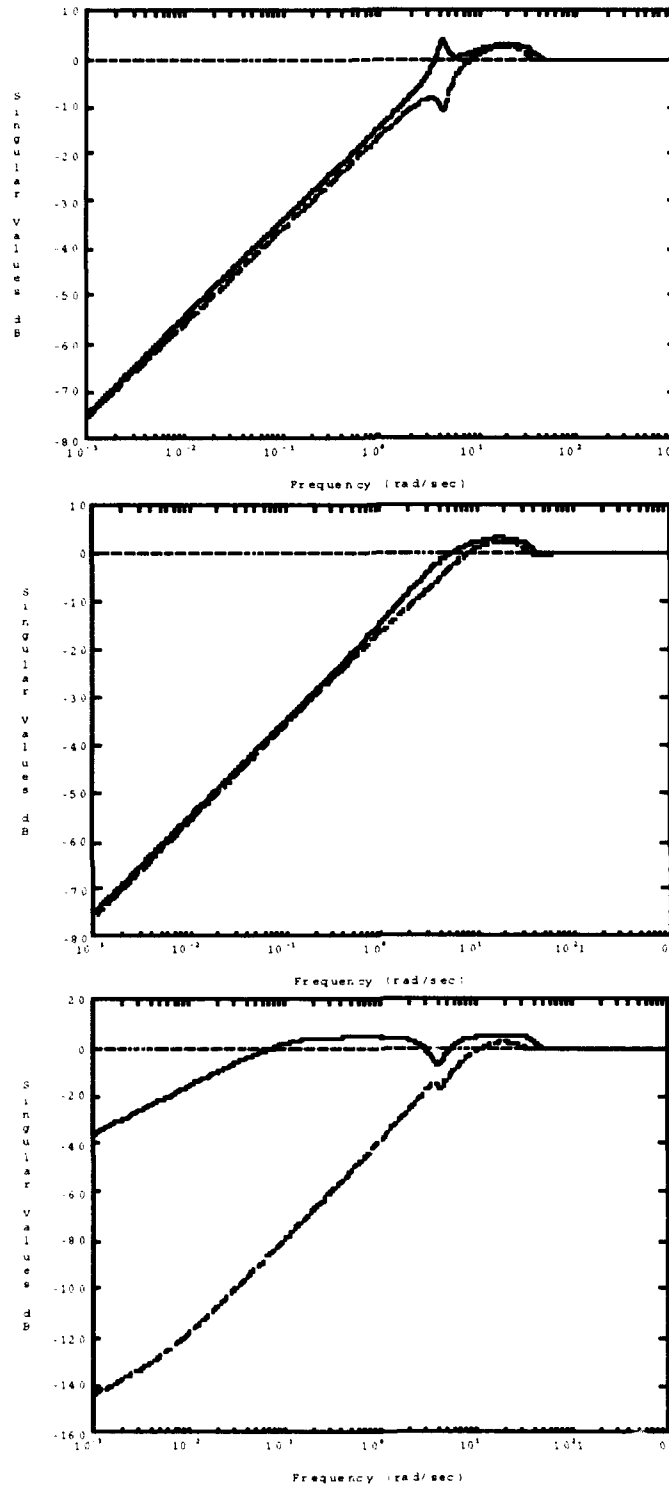


Figure 23 MIMO Sensitivity Curves of Nominal, SOF, REA Designs

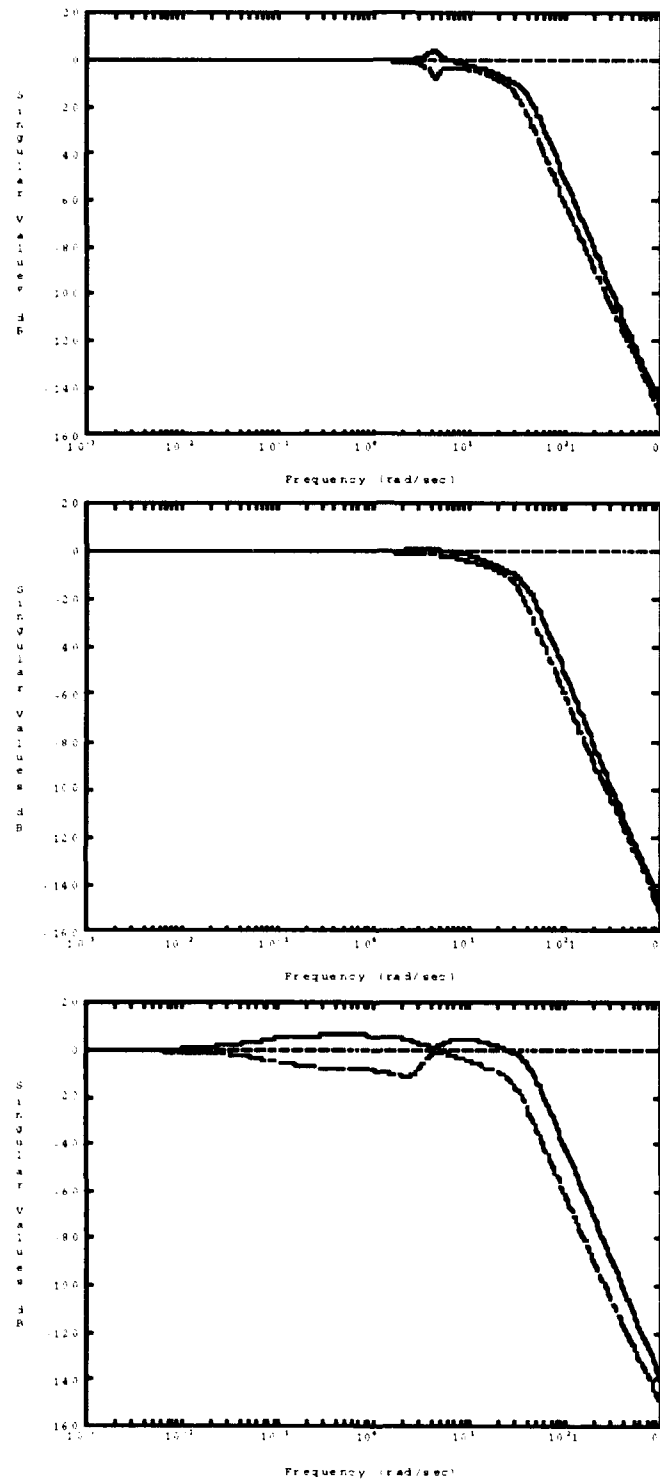


Figure 24 MIMO $\sigma[T]$ Curves of Nominal, SOF, REA Design

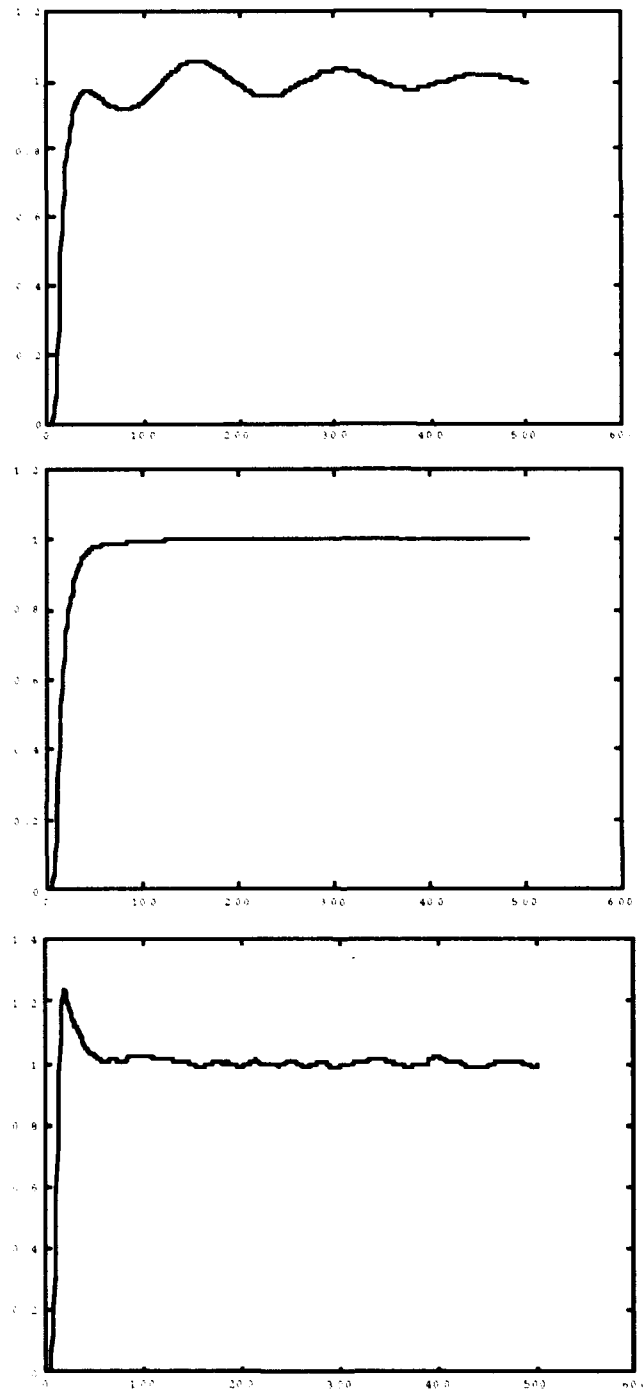


Figure 25 MIMO Step Input with Noise Responses of Nominal, SOF, REA Design
(x coordinate is SIMULINK time unit, 100 \approx 1sec)

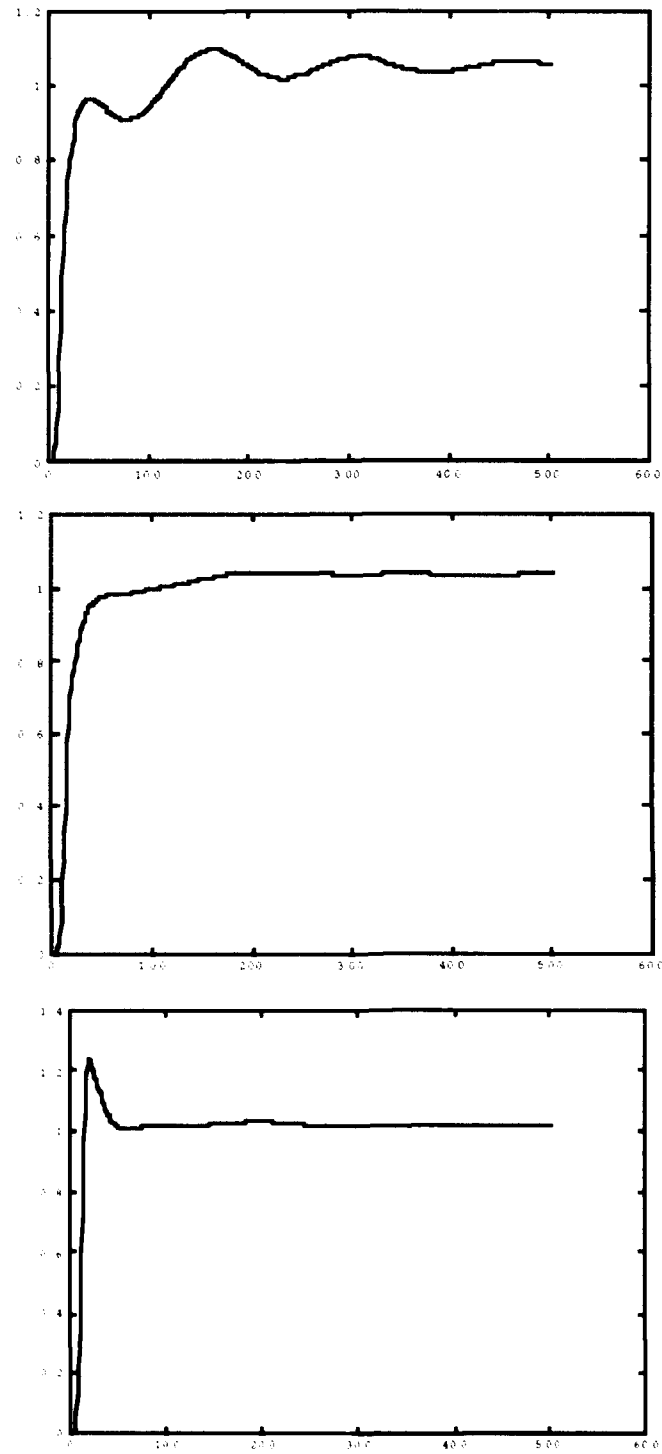


Figure 26 ϕ Step Input with Disturbance Respose of Nominal, SOF, REA Design
(x coordinate is SIMULINK time unit, 100 \approx 1sec)

3.4.7 *Robustness with Perturbed Plant* . The same perturbation as in the SISO plant is added to MIMO plant, using the same LQG/LTR compensators obtained from the unperturbed plant design, and the same static gain matrix in SOF design. The closed loop poles for the three perturbed systems are in Table 12. In all three designs, dutch roll damping is reduced. Using the SOF and REA method the poles are still well-damped and don't result in undesired plant inversion.

Table 12 MIMO perturbed plant closed loop poles

design	nominal	SOF	REA
closed loop pole	-.0062 -1.44 $-.369 \pm 4.235 i$ $-10.22 \pm .828 i$	-.0139 -.4895 $-3.02 \pm 3.375 i$ -10.1843 -11.3118	-.1108 -2.513 $-3.028 \pm 3.35 i$ -10.23 -11.23

The sensitivity singular value curves are given in Figure 27. The SOF design $\bar{\sigma}$ curve was increased and $\underline{\sigma}$ curve was reduced. The nominal and REA design are the same as the unperturbed system. The complementary sensitivity curves are in Figure 28 and showed that all designs have about the same shape as the unperturbed plant.

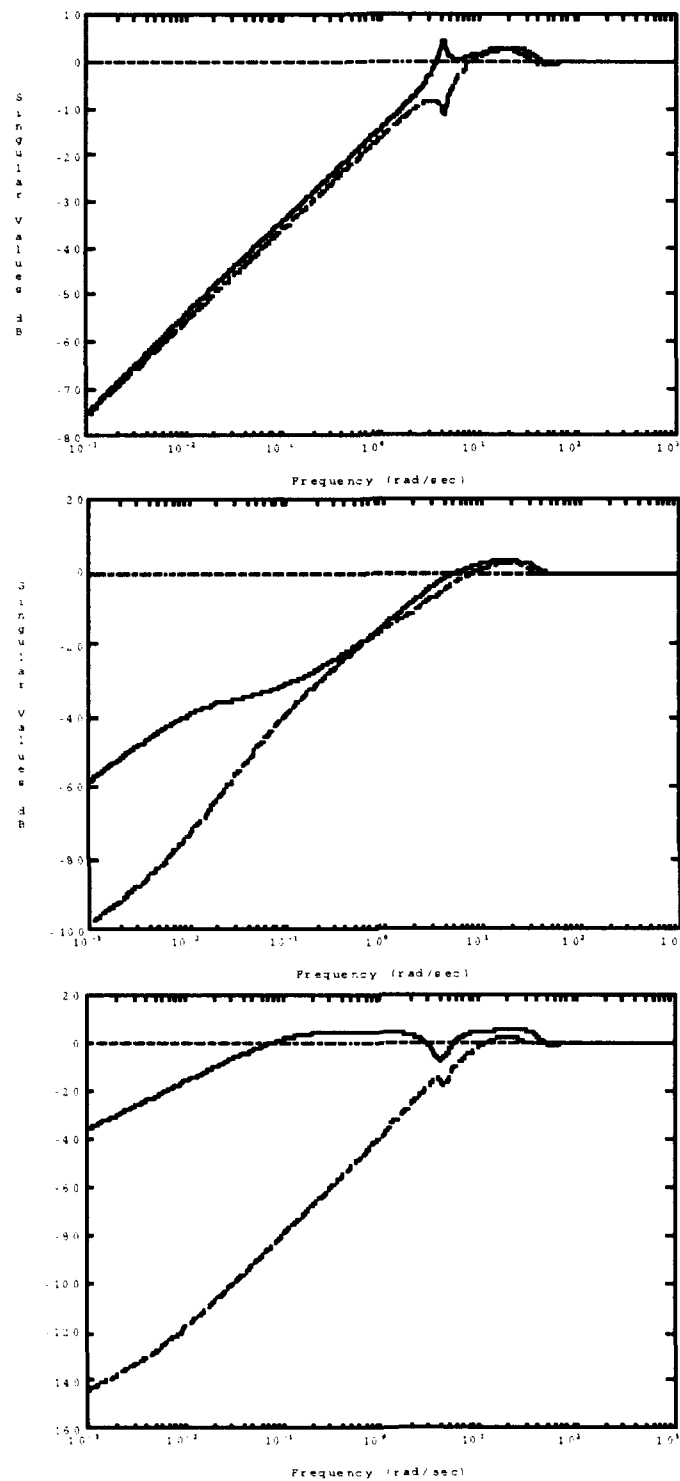


Figure 27 MIMO Perturbed Sensitivity Curves of Nominal, SOF, REA Designs

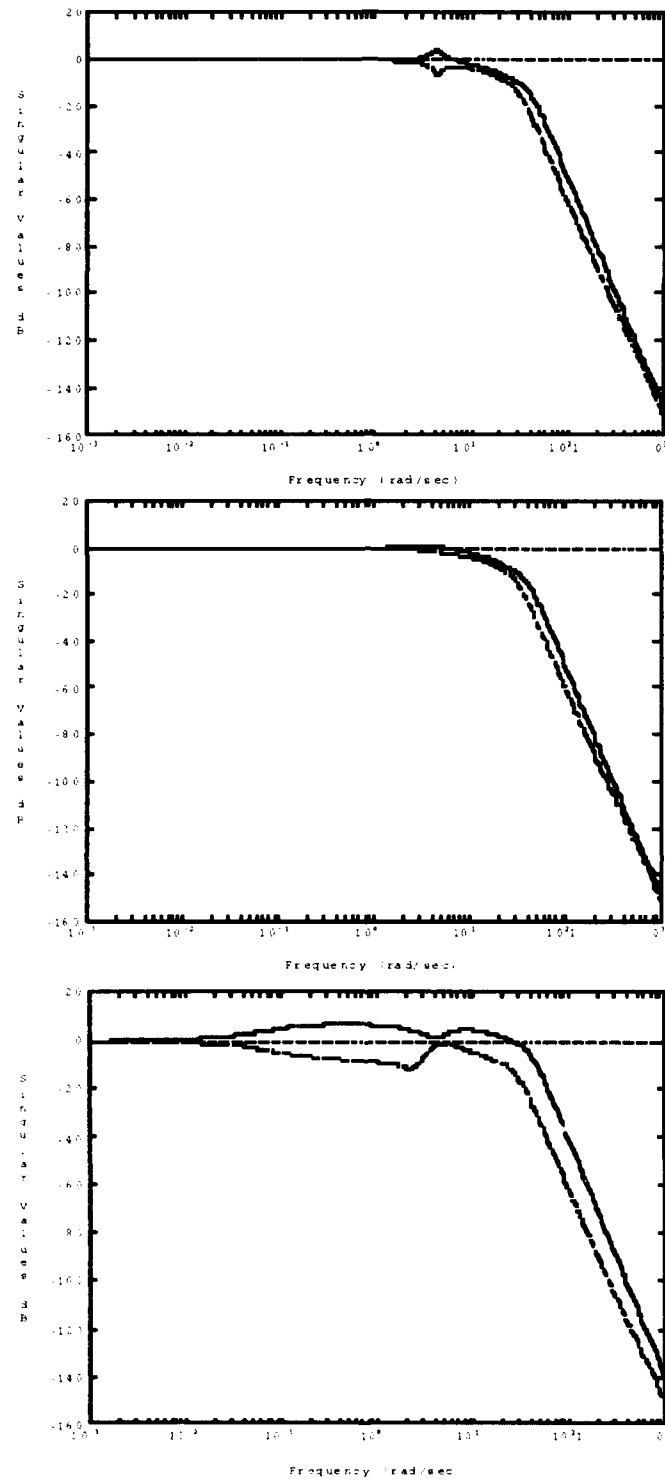


Figure 28 Perturbed Complementary Sensitivity Curves of Three Designs

3.5 Summary

In aircraft longitudinal control, normally the lightly damped, low frequency phugoid mode does not cause a problem in flying qualities. For conventional aircraft pitch angle to elevator response, with the phugoid poles and the two zeros $(S + 1/T_{\theta 1})$, $(S + 1/T_{\theta 2})$ on real axis, the LQG/LTR compensator will not invert the plant dynamics. Using SOF method cannot shift the phugoid poles far from their original location, and the LQG/LTR design for the SOF inner closed loop plant doesn't give too much improvement on overall closed loop system performance and stability robustness. If the nominal plant has undesired modes at moderate frequency, like lightly damped short period modes, an undesired plant inversion can be prevented by using SOF method before the LQG/LTR compensator design. The REA method offer more flexibility on assigning eigenvalues.

In the A-4 aircraft lateral-directional MIMO control design, the SOF method largely improved closed loop performance and stability robustness. The REA method showed a drawback for MIMO system target loop shaping in LQG/LTR compensator design, because once the Kalman filter or LQ Regulator state and control weighting matrices are determined by the results of using the REA method, the loop shapes are hard to adjust/. Thus, the REA method doesn't have frequency domain closed loop system design flexibility.

IV X-29 Aircraft System Design and Results Analysis

Accounting for a moderate frequency unstable pole and non-minimum phase zero problem, we introduce the X-29 experimental forward sweep wing aircraft at sea level, 0.9 Mach flight condition. The X-29 is a unconventional flight vehicle. It use canards and flaprons for pitch control instead of horizontal tail, so longitudinally it is a MIMO system. The open loop plant of this MIMO system has one unstable pole and a very low frequency, low damping complex pair phugoid mode. When inserting a time delay into the system, a non-minimum phase zero is introduced. Even though the X-29 aircraft reinforces the wing structure with a tailored composite wing skin of the forward swept wing, it is still susceptible to wing divergence, a wing tip vertical oscillatory motion relative to the wing root. It will be excited when aileron control is used for roll control, or when doing pitch control, lift is generated on the wings. This structural mode is rare to see in conventional aircraft in the normal flight envelope. Control system design definitely needs to take this structural mode into account. To avoid this mode, the closed loop system bandwidth must be kept below the wing bending mode frequency, or like Liebst and Garrad [16], an eigenstructure assignment technique can be used to suppress this mode. Thus, the X-29 is expected to represent the "worst" model for LQG/LTR design, so the results from LQG/LTR with and without static output feedback can be compared.

4.1 Plant. The X-29 experimental aircraft nominal condition is sea level, 0.9 Mach. The longitudinal control is a MIMO system with pitch controlled by canards and flaprons. The outputs are AOA and pitch angle. The MIMO state space A and B matrices are given in Appendix A. The states, controls and outputs are

$$x = \begin{bmatrix} \text{airspeed (u) - ft/sec} \\ \text{AOA } (\alpha) - \text{deg} \\ \text{pitch angle } (\theta) - \text{deg} \\ \text{pitch rate (q) - deg/sec} \\ \text{wig tip deflection - ft} \\ \text{wign tip rate - ft/sec} \end{bmatrix}, \quad u = \begin{bmatrix} \text{flapron deflection - deg} \\ \text{canard deflection - deg} \end{bmatrix}, \quad y = \begin{bmatrix} \text{AOA } (\alpha) \\ \text{pitch angle } (\theta) \end{bmatrix}$$

Table 13 X-29 Open Loop Plant Eigenvalues, Eigenvectors and Zeros

mode	short period		phugoid	wing bending
eigenvalue	-11.907	7.306	-.000041±.0491i	-9.87±59.27i
eigenvector	.1175 .0810 .9648 .0183 .2189 .0041	-.0918 -.1343 -.9812 .0126 .0926 -.0019	.0001±.00009i .0577±.0653i -.0032±.0028i .00017±.00015i .00006±.000008i .00002±.000002i	-.0014±.00092i -.00037±.00018i .0146±.02i -.0029±.174i .999±.013i .00002±.000002i
zeros	-.000148, -7.076±65.17i			

The open loop plant eigenvalues, eigenvectors and zeros are listed in Table 13. The plant has an unstable pole at 7.306 rad/sec, and is comparatively more unstable than any aircraft. The phugoid mode is very slow ($\omega_n = .049$ rad/sec) and very lightly damped ($\zeta_{phu} = .0008$). It has a relatively low frequency wing bending structural mode at 60 rad/sec. The plant is unstable and minimum phase. In order to make the plant more difficult and to be more realistic for LQG/LTR design, a channel of time delay (.05 sec) with Pade first order approximations are added to the plant, so that one zero and one pole both at 40 rad/sec are added. The combination of unstable and lightly damped poles, as well as non-minimum phase zero will introduce some difficulty for LQG/LTR design.

4.2 Nominal plant LQG/LTR compensator design. The same low and high frequency matching technique as the A-4 aircraft MIMO design is applied. The nominal plant TFL curves are plotted in Figure 29. There is a spiky resonant peak at the phugoid frequency, and the curves are flat at low frequency, due to the low frequency zero cancelled the integral action at low frequency, so it may not have enough gain for low frequency command tracking and disturbance rejection. The $\bar{\sigma}$ and $\underline{\sigma}$ curves are widely separated at crossover frequency which makes the bandwidth hard to predict and difficult to keep low.

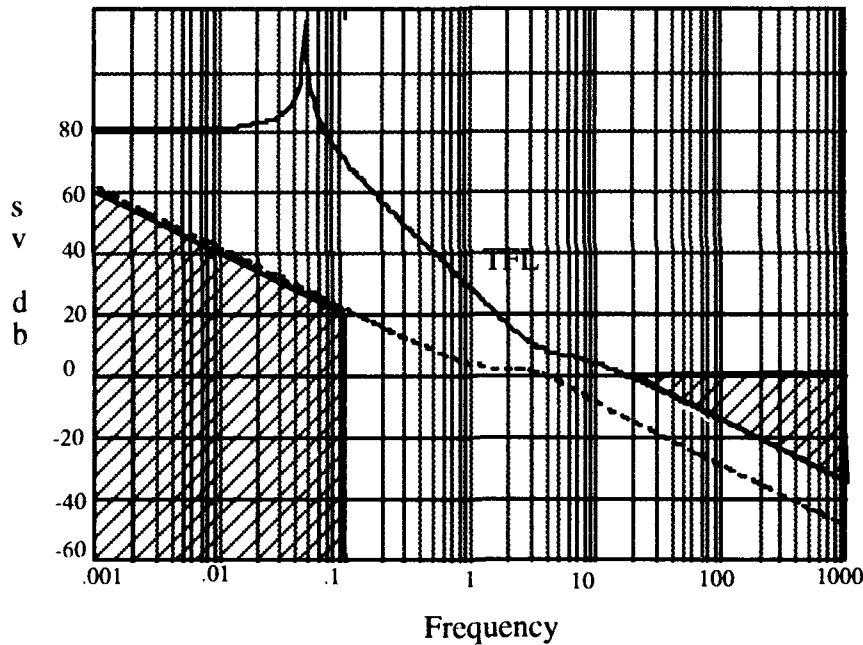


Figure 29 X-29 Nominal Plant TFL Singular Value Curve

In order to correct these problems, both control channels are augmented with integrators; the $\bar{\sigma}$ and $\underline{\sigma}$ curves matching technique is applied at 10 rad/sec frequency. The reshaped TFL curves are shown in Figure 30. Due to the unstable pole, the minimum bandwidth is limited to 7.306 rad/sec, and μ is selected to keep the bandwidth above this frequency, so that the crossover frequency can be high enough to

cover the unstable pole. Otherwise, the LQG/LTR compensator cannot "see" this unstable pole, and closed loop system performance may be affected. Another restriction on the selection of μ is the wing bending mode frequency. The crossover frequency needs to be kept lower than this frequency to avoid exciting the structural mode. A value of $\mu = 0.5$ is selected and with this value the high frequency robustness "barrier" is violated, but with $q = 300$ the high frequency robustness requirement can be met. The LTR singular value curves are also shown in Figure 30. The unsuccessful recovery of the target feedback loop shape for the non-minimum phase zero frequency is obvious; fortunately this is not within the system bandwidth, and should not affect the closed loop system, it also places a limit on the maximum allowable bandwidth.

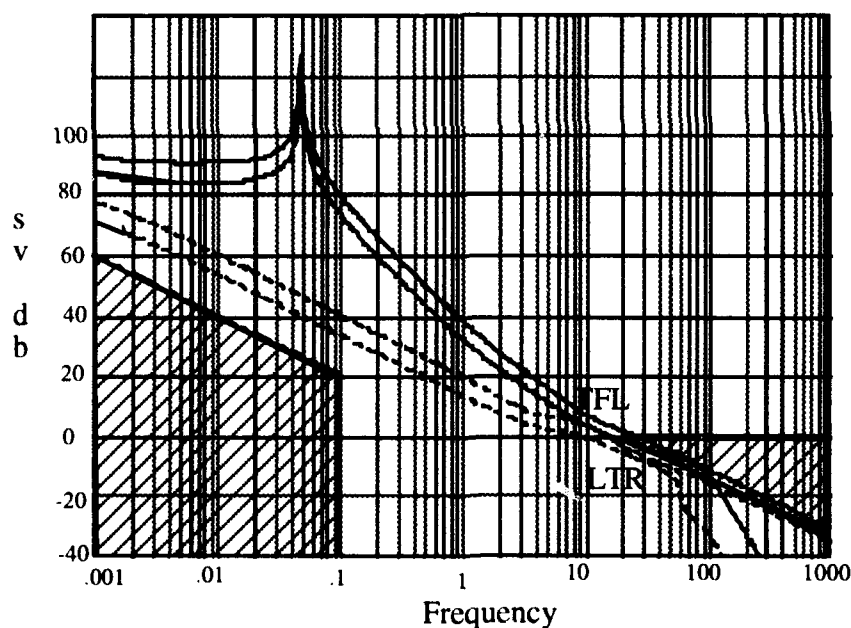


Figure 30 X-29 Nominal Plant Reshaped TFL and LTR Singular Value Curves

The LQG/LTR compensator and closed loop system poles and zeros are shown in Table 14. The compensator is stabilizing and the unstable short period pole went to the left-half-plane and became a complex pair of poles. It has decent damping and

natural frequency. The phugoid mode has disappeared, thus the compensator does not closely invert the plant. The wing bending mode damping is reduced slightly.

Table 14 X-29 Nominal Design Compensator and Closed Poles and Zeros

	poles	zeros
compensator	$-48.66 \pm 85.74i$ $-8.87 \pm 59.43i$ $-30.4 \pm 48.17i$ $-89.92 \pm 14.67i$ $-.0001487$	$-9.85 \pm 59.37i$ $-2.58 \pm 1.25i$ -40 -12.33 $-.0001488$
closed loop system	$-9.98 \pm 59.26i$ $-7.2 \pm 9.1i$ $-3.47 \pm 3.44i$ $-.000148$	

4.3 Static Output Feedback and LQG/LTR Compensator Design. In the nominal plant design, the unstable pole caused the minimum bandwidth limitation on loop shaping and the lightly damped phugoid mode gave the singular value curve a resonant peak. To avoid this problem, the unstable pole and lightly damped phugoid poles are shifted to stable and better damping locations. By viewing the corresponding eigenvector of the phugoid and unstable short period poles, airspeed, AOA, and pitch angle are selected as outputs. The unstable pole is assigned to a stable -2.1 rad/sec location, and the phugoid poles to $-.035 \pm .035i$. The achieved closed loop poles and the static gain matrix are:

$$\text{inner closed loop poles} = [-2.1, -.035 \pm .035i, -11.62 \pm 57.88i, -14.9 \pm 14.15i],$$

$$F = \begin{bmatrix} -.0416 & -1.3961 & -.0298 \\ -.0047 & -.104 & -.0033 \end{bmatrix}$$

With the SOF inner loop closed for the LQG/LTR compensator design, the $\bar{\sigma}$ and $\underline{\sigma}$ curves matching techniques is used close to crossover frequency. Since the unstable pole is gone, μ can be chosen to lower the system bandwidth to any desired frequency. A value of $q = 300$ was selected; the best TFL and LTR loop shapes obtained are shown in Figure 31. At very low frequency some part of the $\underline{\sigma}$ curve doesn't clear the low frequency "barrier", but the frequency is so low that it should not affect closed loop system performance.

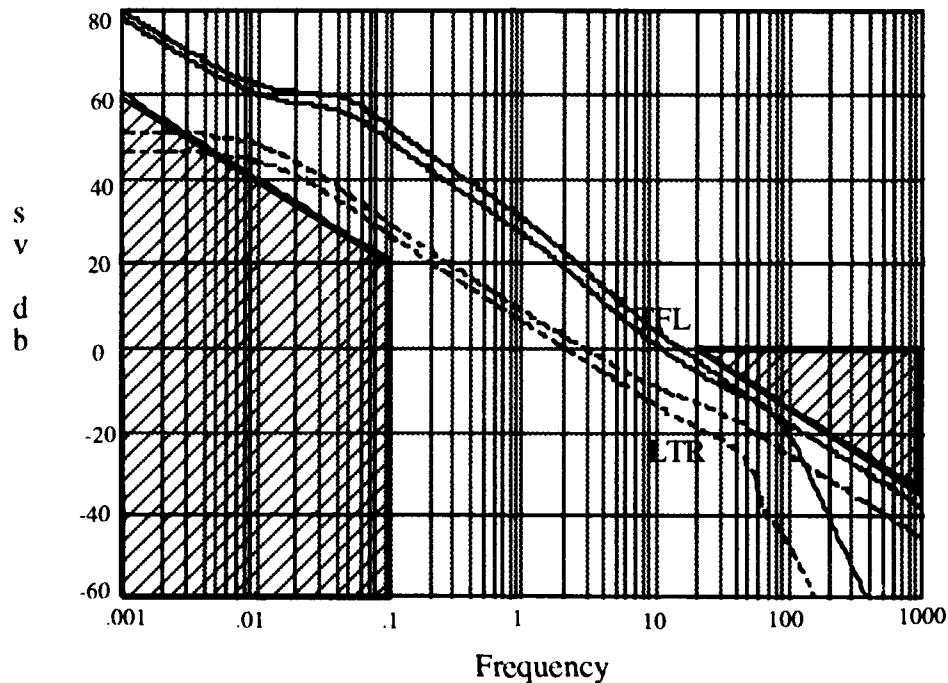


Figure 31 X-29 SOF Design TFL and LTR Singular Value Curves

The LQG/LTR compensator and closed loop system poles and zeros are shown in Table 15. The short period and wing bending modes have better damping than the nominal design.

Table 15 X-29 SOF Design Compensator and Closed Loop System Poles and Zeros

	poles	zeros
compensator	$-47.89 \pm 7.8i$ $-9.85 \pm 5.95i$ $-33.87 \pm 40.07i$ $-69.84 \pm 17.99i$ $-.000148$	$-11.54 \pm 57.56i$ $-12.42 \pm 14.08i$ -4.843 $-.0801$ $-.000149$
closed loop system	$-.00015$ $-.081$ -2.42 $-7.925 \pm 3.56i$ $-10.19 \pm 59.77i$	

4.4 Result comparisons. From the A-4 aircraft MIMO plant design, we know that the robust eigenstructure assignment method is good for eigenstructure assignment, but is not suitable for follow-on LQG/LTR loop shaping. Hence, we will not use the REA method for the X-29 aircraft MIMO system design.

The closed loop system poles of the nominal and SOF designs are not very different, because the compensators don't invert all the plant dynamics. However, by looking at the closed loop system response of step pitch angle input shown in Figure 32, the SOF method has better damping and less overshoot due to the system bandwidth being reduced. Non-minimum phase response (initial response direction opposite to the input direction) is not very apparent, because the non-minimum zero is located at relatively high frequency. The complementary sensitivity singular value curves are shown in Figure 33. The nominal design has a large peak close to wing bending mode frequency.

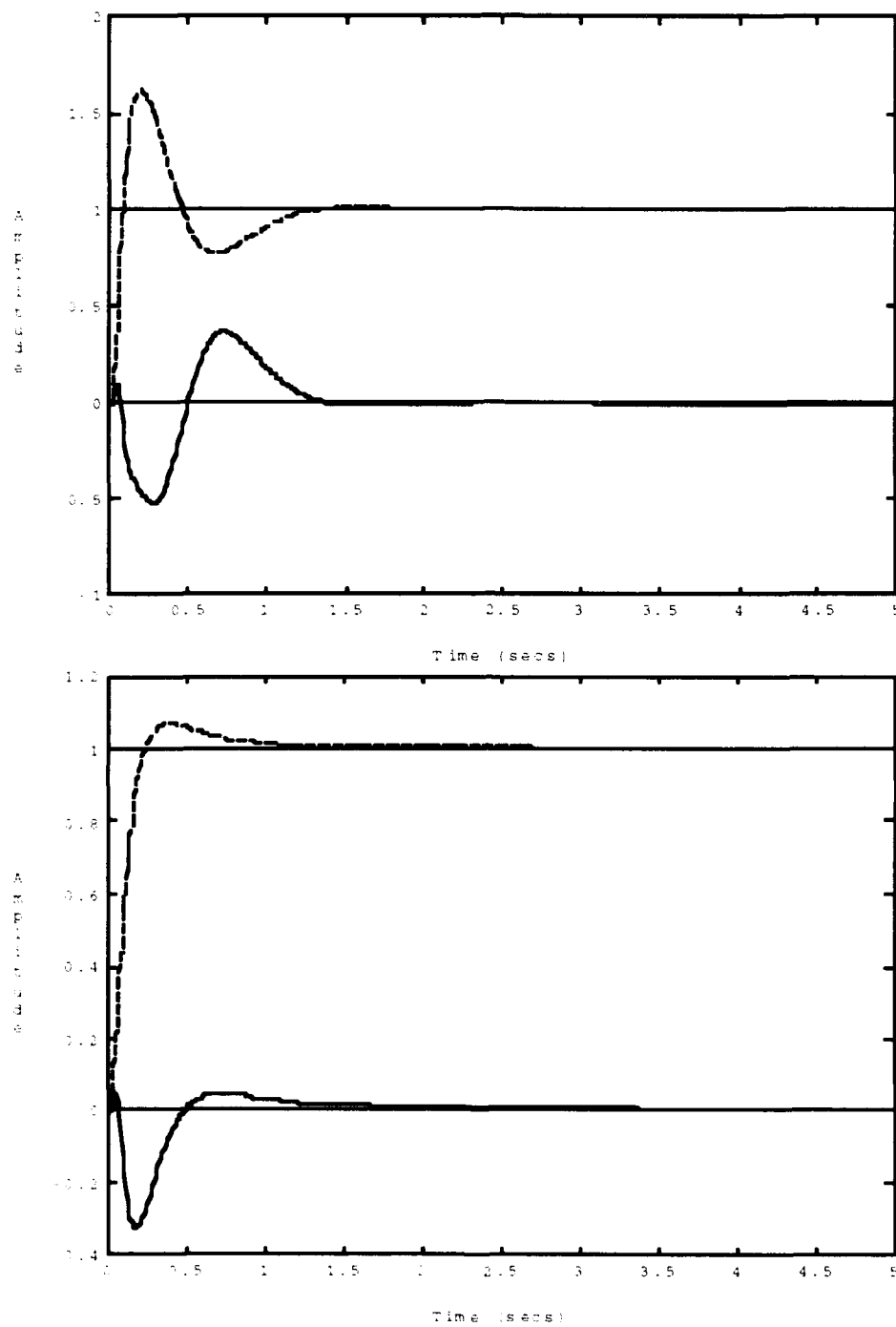


Figure 32 X29 θ Step Input Responses of Nominal and SOF designs (top down)

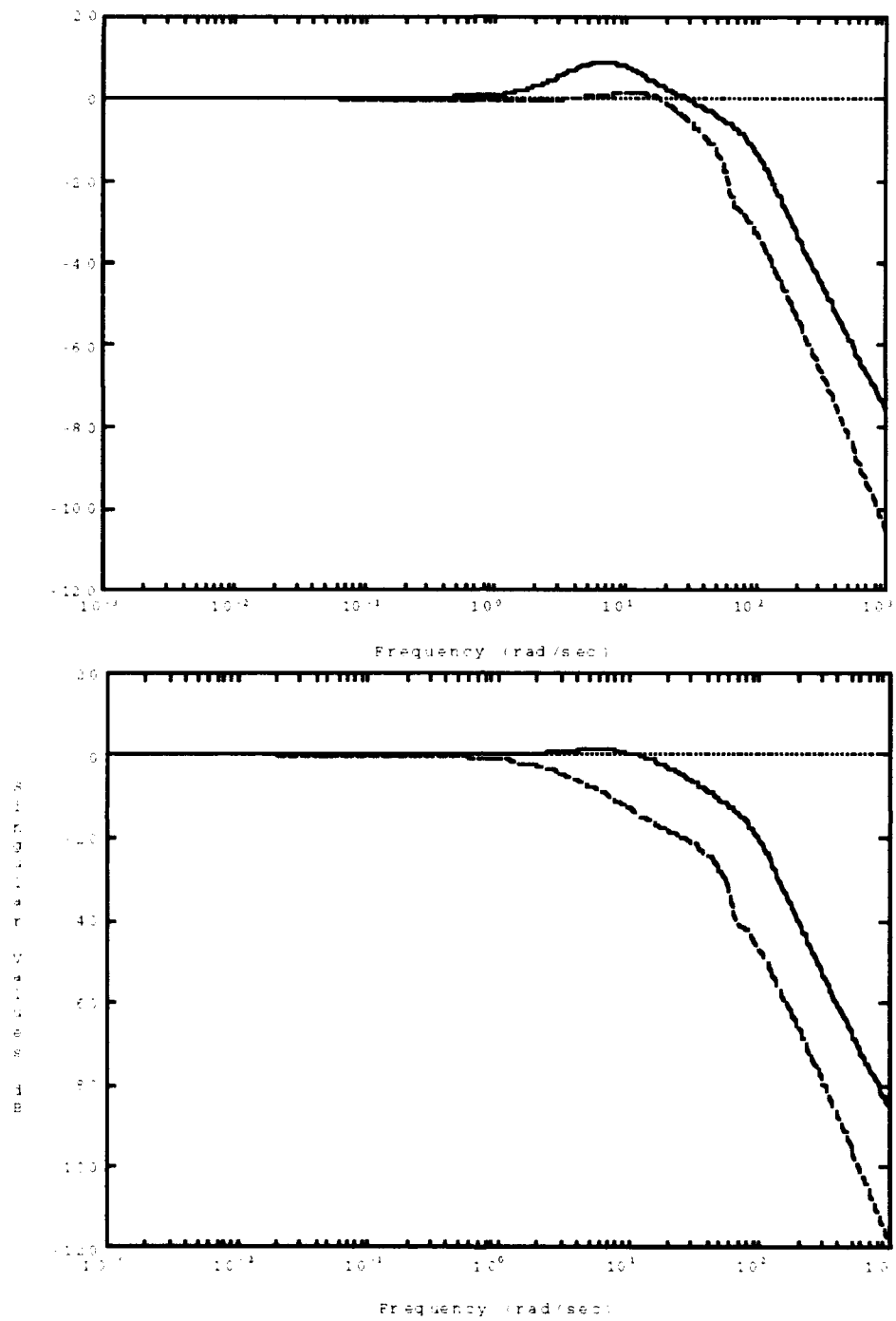


Figure 33 X29 Complementary Sensitivity Curves of Nominal and SOF Designs

Due to the higher closed loop system bandwidth, the nominal design has a higher maximum singular value, thus less robustness at high frequency. Figure 34 shows that both design have good noise rejection; this is due to the nominal design having low enough GK gain at high frequency. Figure 35 is the sensitivity singular value plots for both designs. Because the designed SOF target feedback loop shape has a lower minimum singular value, the sensitivity of the SOF design is higher than the nominal design, but this should not affect command tracking and disturbance rejecting capability. The nominal design has a peaked sensitivity which is higher than the SOF design. This affects the independent stability margins. Figure 36 shows that both designs have good disturbance rejection.

The independent gain and phase margins are given in Table 16. The SOF design has better stability margins; it is more robust.

Table 16 X-29 Stability Margins of Nominal and SOF Designs

design	nominal	SOF
independent gain margin (db)	[-5.3, 3.27]	[-16.36, 5.33]
independent phase margin (deg)	± 26.44	± 50.18

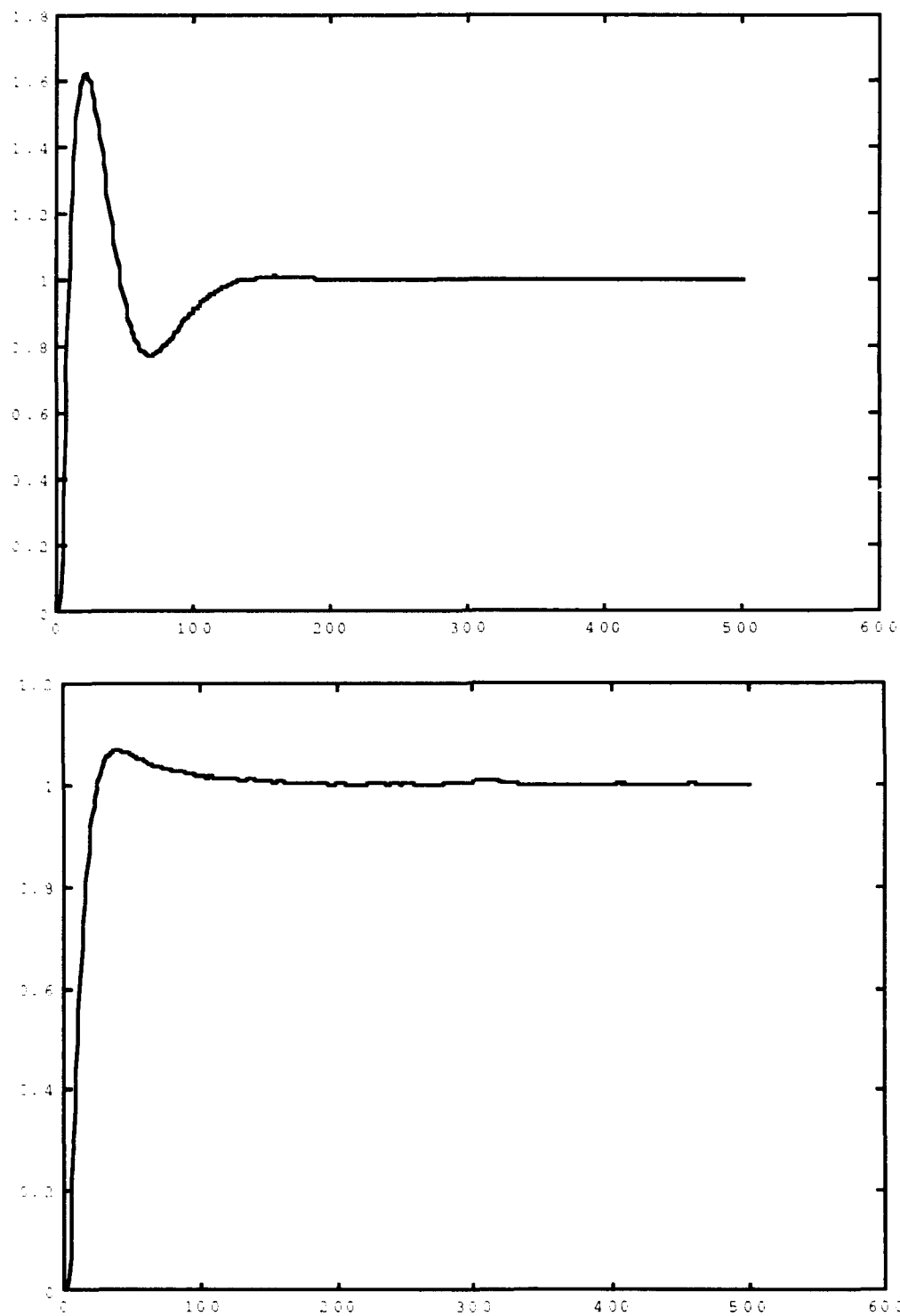


Figure 34 X29 Step Input with Noise Responses of Nominal and SOF Design

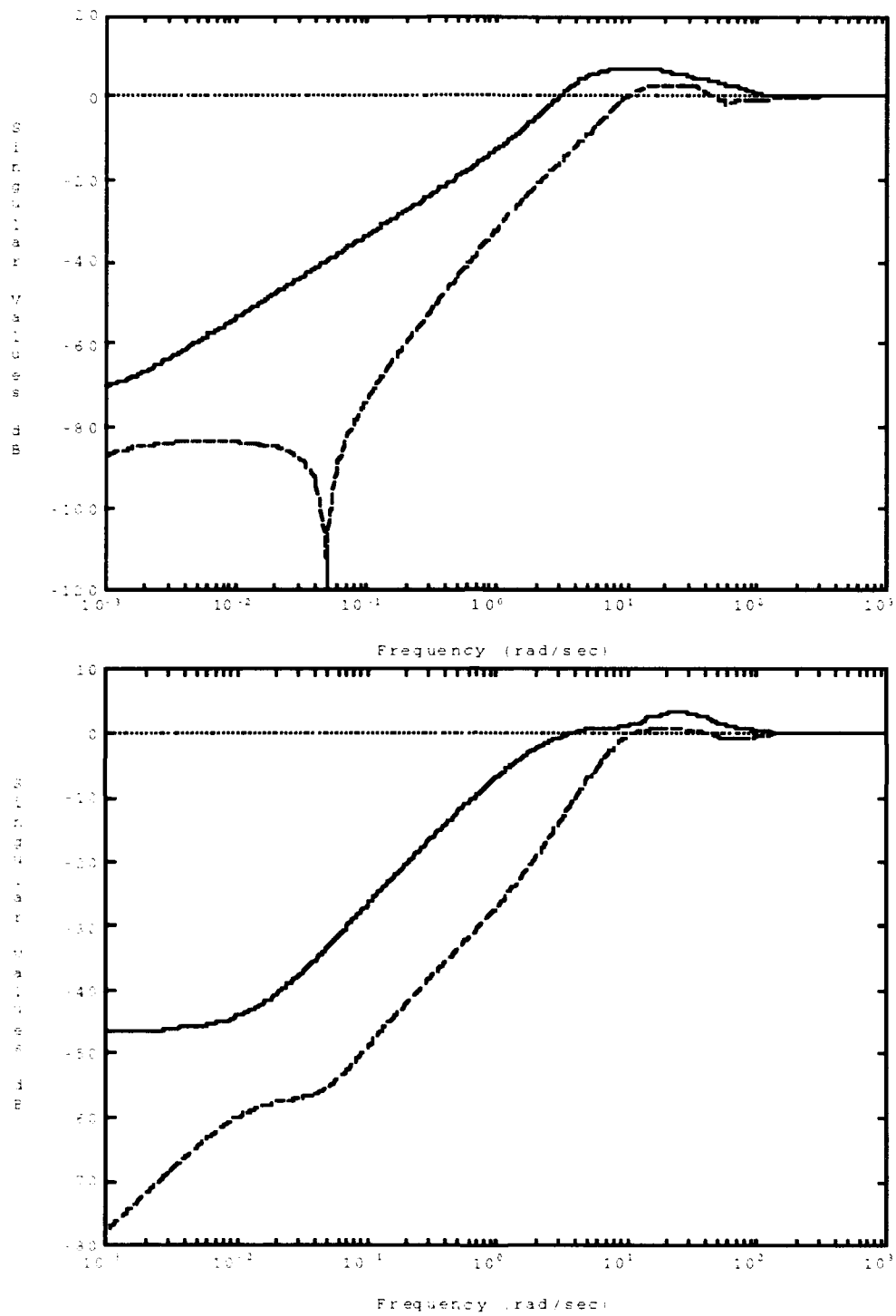


Figure 35 X29 Sensitivity Curves of Nominal and SOF Design

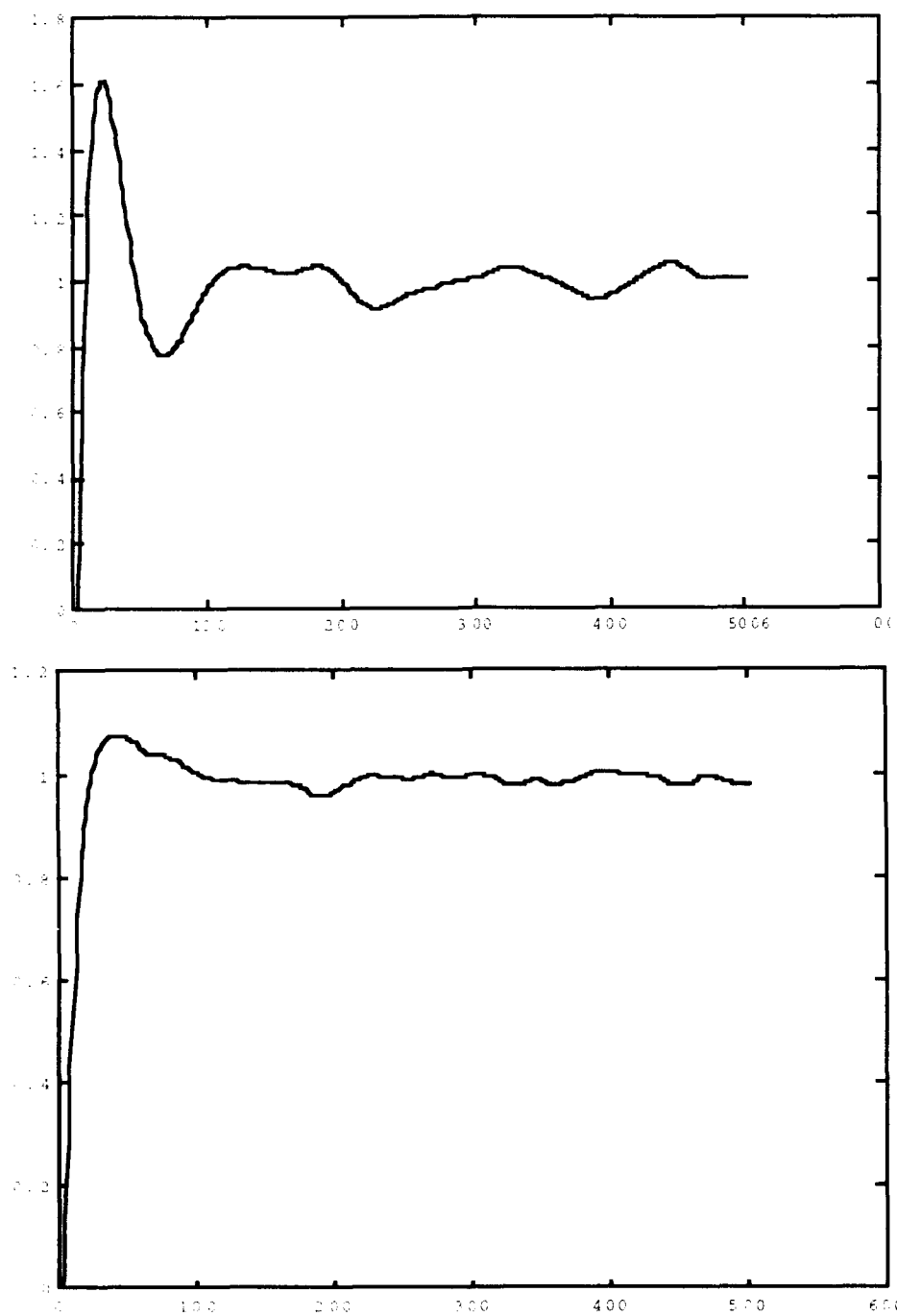


Figure 36 X29 Step Input with Disturbance Response of Nominal and SOF Design

4.5 *Summary*

Using the SOF method on the X-29 experimental aircraft, LQG/LTR compensator design with unstable, non-minimum phase plant and relatively low frequency structural wing bending mode. A pair of phugoid poles were assigned successfully to better damping locations. One unstable short period pole was assigned to left-half-plane. With this design, the minimum bandwidth limitation can be removed; the closed loop system is not too susceptible to wing bending. System robustness is improved, this is shown by reduced complementary sensitivity and increased independent gain and phase margins.

V Conclusion and Recommendation

This thesis showed that static output feedback (SOF) and robust eigenstructure assignment (REA) methods can be used to improve LQG/LTR design for aircraft flight control systems, when the plant has lightly damped, low frequency poles. In Chapter II, background information for Linear Quadratic Gaussian and Loop Transfer Recover (LQG/LTR) was developed. The procedure of using static output feedback to reassign system poles was also presented. The algorithms of LQG/LTR and use of static output feedback are written in MATLAB M-File and given in Appendix B. The robust eigenstructure assignment algorithm was developed by Huckabone [9: 78-103]; the LQREA program used by Huckabone for eigenstructure assignment was used here to assign the closed loop Kalman filter eigenvalues.

Three aircraft models were used for designing LQG/LTR compensators with the stated methods. An A-4 aircraft longitudinal control is used for a SISO model; it has a pair of lightly damped phugoid poles. A-4 lateral directional control model which has lightly damped Dutch roll mode, and X-29 experimental aircraft longitudinal control model which has lightly damped phugoid, unstable short period, wing bending structural modes and non-minimum phase zero, were used as MIMO system designs. The X-29 model only applied Static Output Feedback method, since the Robust Eigenstructure Assignment method has deficiencies (observed during the A-4 MIMO system loop shaping in LQG/LTR compensator design). From the results presented in Chapter III and IV, following conclusions are obtained :

Static Output Feedback method

In the A-4 MIMO system design, nominal plant with a low damping Dutch roll mode, the LQG/LTR designed closed loop system has a lightly damped Dutch roll mode. The undesired plant inversion made the closed loop time response bad. Under

the Static Output Feedback method, the Dutch roll poles can be exactly assigned to improve damping location as desired, but the assignable region of the desired poles is limited, if system stability is considered. The output must be selected correctly to assign the specific poles. This inner closed loop plant is then used for the LQG/LTR compensator design. The closed loop system has much better damping and the stability and robustness is also improved. In the X-29 aircraft model, the static output feedback method also successfully assigned better damping phugoid poles, and the system bandwidth can be reduced, making the aircraft less susceptible to the wing bending mode. After using the Static Output Feedback method to move the unstable pole to the left -half- plane, the closed loop system of LQG/LTR design improved robustness. This is shown by reduced high frequency complementary sensitivity and better independent gain and phase margins.

In SISO model design we didn't obtain much improvement by using Static Output Feedback method. This is due to the plant not having characteristics that allow large pole movement from the nominal plant, when using single loop constant gain feedback. If the plant has low damping short period poles instead of low damping, low frequency phugoid poles, and no transmission zero close to the undesired poles, then the undesired plant inversion can be avoided by using Static Output Feedback method.

The robustness of the gain and LQG/LTR compensator were checked by perturbing the plant with reduced damping poles. The perturbed closed system is still stable and performs reasonably well.

Robust Eigenstructure Assignment method

For both the SISO and MIMO A-4 aircraft models, the LQREA program was used to assign the closed loop Kalman filter achievable eigenvalues close to the

desired eigenvalues. In both designs, the eigenvalues can be moved closer to the vicinity of the desired poles than the SOF method. Kalman filter closed loop eigenvalues can be significantly changed from the nominal open loop plant. In the SISO problem, after using the REA method the LQG/LTR closed loop system has the best time response, but the gain margin was reduced, with the phase margin slightly improved. In the MIMO problem, after the closed loop Kalman filter poles were reassigned, the LQREA program returned the state weighting matrix Q_f and control weighting matrix R_f . With this fixed Q_f and R_f , we can not reshape the Kalman filter transfer function using the standard LQG/LTR loop shaping techniques; that is, the frequency domain loop shaping is not feasible if we use the Robust Eigenstructure Assignment algorithm. For most system, where full state feedback is not possible, combined LQ Regulator and estimator (LQG) is required for compensator design. If the Robust Eigenstructure Assignment method for LQG/LTR compensator design is used, the performance and stability robustness will be hard to design.

The Robust Eigenstructure Assignment algorithm was designed mainly for the usage of assign eigenstructure with the constraints of closed loop eigenstructure of LQR or Kalman filter, not for LQG/LTR compensator design. And the comparisons on performances and stability robustness with SOF design were based on the LQG/LTR design results. Thus the result of comparisons did not reflect either designing methodology is superior than the other.

Recommendation for further research

In LQG/LTR design, the closed loop poles are determined by the designed Kalman filter and the tuned LQ Regulator. From the results of this study, the compensator will invert the plant dynamics if there is no system transmission zeros close to system pole. If there is transmission zero on the real axis which close to any

of the poles, then the pole will not have compensator's zero close to it and the plant inversion will not happen. The closeness of a compensator zero to an open loop plant pole is also affected by the Γ matrix chosen for loop shaping. Compensator and plant pole-zero relations will affect the closed loop system characteristics. How the compensator characteristics are affected by transmission zeros and the choosing of the Γ matrix in LQG/LTR design is worth some study.

It has been shown that the Robust Eigenstructure Assignment algorithm is excellent for assigning eigenstructure with good robustness. The LQREA program used is the combination of several subroutines in different softwares; it is mainly for assigning the eigenstructure of a full state LQ Regulator or Kalman filter design. Expanding it for other robust compensator designs like LQG/LTR, or changing the form of the returned Q and R matrices, may improved the flexibility of using the output of the program.

Appendix A : Plant State Space Models

A-4 Aircraft Longitudinal Control State Space A, B matrices :

$$A = \begin{bmatrix} -0.0129 & -0.0651 & 0 & -0.5585 & 0 \\ -0.0091 & -0.8166 & 1.0000 & 0 & -0.0896 \\ -0.0201 & -12.3900 & -1.4200 & 0 & -19.4400 \\ 0 & 0 & 1.0000 & 0 & 0 \\ 0 & 0 & 0 & 0 & -20.0000 \end{bmatrix}, \quad B = \begin{bmatrix} 0 \\ 0 \\ 0 \\ 0 \\ 20 \end{bmatrix}$$

A-4 Aircraft Lateral Directional Control State Space A, B Matrices :

$$A = \begin{bmatrix} -0.228 & 0 & 0.05 & -1 & -0.074 & 0.79 \\ -34.9 & -1.516 & 0 & 0.875 & 426 & 199.2 \\ 0 & 1 & 0 & 0 & 0 & 0 \\ 18.73 & 0.0398 & 0 & -0.565 & 9.6 & -166 \\ 0 & 0 & 0 & 0 & -20 & 0 \\ 0 & 0 & 0 & 0 & 0 & -20 \end{bmatrix}, \quad B = \begin{bmatrix} 0 & 0 \\ 0 & 0 \\ 0 & 0 \\ 0 & 0 \\ 20 & 0 \\ 0 & 20 \end{bmatrix}$$

X-29 Longitudinal Control State Space A, B Matrices :

$$A = \begin{bmatrix} .000526 & .092764 & -.562 & -.2536 & -.1405 & .0015 \\ -.0036887 & -2.8810 & -.0004672 & 1.006 & 4.3699 & -.046879 \\ 0 & 0 & 0 & 1 & 0 & 0 \\ .000116 & 79.560 & .00001475 & -.831 & -60.447 & 1.0096 \\ 0 & 0 & 0 & 0 & 0 & 1 \\ -.439 & -543.84 & -.00000118 & 1.1589 & -3642 & -20.64 \end{bmatrix},$$

$$B = \begin{bmatrix} 1.2296 & .49255 \\ -5.5524 & -15.324 \\ 0 & 0 \\ -233.28 & 1839.9 \\ 0 & 0 \\ -1298.5 & 147.50 \\ 0 & 0 \end{bmatrix}$$

Appendix B : Static Output Feedback Eigenstructure Assignment

```
% Assign eigenvalues and eigenvectors:

%%do a loop to calculate different eigenvalues with increasing
damping.
%%calculate projection of desired eigenvector on achievable
eigenvector.

for imh=4.3:-.5:0
reh=((4.34)^2-(imh)^2)^.5;
eu1=-reh+i*imh
ls=inv(eu1*eye(6)-am)*bm;
va1=ls*inv(ls'*ls)*ls'*vdd;

eu2=-21;
ls=inv(eu2*eye(6)-am)*bm;
va2=ls*inv(ls'*ls)*ls'*vda1;

eu3=-21;
ls=inv(eu3*eye(6)-am)*bm;
va3=ls*inv(ls'*ls)*ls'*vda2;

% Achievable eigenvector matrix
va=[va1 va2 va3];

% model transformation

ti=[bm tp]
at=inv(ti)*am*ti;
ct=cm*ti;
vt=inv(ti)*va;

%Partition A matrix
a1=at(1:2,:);

%separate real and imaginary part of eigenvector
```



```

vt1=[real(vt(:,1)) imag(vt(:,1)) vt(:,2) vt(:,3) ];

%calculate Z matrix and separate real and imaginary parts
z=[eu1*vt(1:2,1) eu2*vt(1:2,2) eu3*vt(1:2,3) ];
z1=[real(z(1:2,1)) imag(z(1:2,1)) z(1:2,2) z(1:2,3) ];

%calculate output feedback gain matrix
f=(z1-a1*vt1)*inv(ct*vt1)

%plot the movement of assigned poles while desired pole select
differently

ac=am+bm*f*cs1;
[p,z]=pzmap(ac,bm,cm,dm1)
axis([-22,8,-10,10]);
pzmap(ac,bm,cs1,dm1)
%if eu2==-.5
if imh==4.32
hold
end
end

hold off

title('poles movement w/ S.O.F=(phi,r),const Wn, actuator ')

```

Bibliography

1. Andry, A.N. and others. "Eigenstructure Assignment for Linear System," *IEEE Transaction on Aerospace and Electronic Systems*, VOL. AES-19, NO.5: 711 - 729, (September 1983).
2. Athans, M. and Stein, G. "The LQG/LTR Procedure for Multivariable Feedback Control Design," *IEEE Transaction on Automatic Control*, AC-32, (February 1987).
3. Athans, M. "A Tutorial on the LQG/LTR Method," *Proceeding, of the American Control Conference*. Seattle, WA, June 1986 (1289 - 1296).
4. Athans, M. and others. "Linear Quadratic Gaussian with Loop Transfer Recovery Methodology for the F-100 Engine," *IEEE Journal of Guidance and Control*, Vol. 91, (January - February 1986).
5. Davison, E.J. and Wang, S.H. "On Pole Assignment in Linear Multivariable System Using Output Feedback," *IEEE Transaction on Automatic Control*, AC-20: 516-518, (August 1975).
6. Doyle, J.C. and Stein, G. "Multivariable Feedback Design : Concepts for a Classical / Modern Synthesis," *IEEE Transaction on Automatic Control*, AC-32: 105 - 114, (February 1987).
7. Doyle, J.C. and Stein, G. "Robustness with Observers," *IEEE Transaction on Automatic Control*, AC-24: 607 - 610, (August 1979).
8. Freudenberg, J.S. and Looze, D.P. "Right Half Plane Poles and Zeros and Design Tradeoffs in Feedback Systems," *IEEE Transaction on Automatic Control*, AC-30: 555- 565, (June 1985).
9. Franklin, Gene F. and Powell, David J. Emami-naeini, Abbas. *Feedback control of Dynamic Systems*. Massachusetts : Addison - Wesley Publishing Company, Inc., 1986.
10. Harvey, Charles. A. and Stein, G. "Quadratic Weights for Asymptotic Regulator Properties," *IEEE Transaction on Automatic Control*, AC-23: 378 - 387, (June 1978).
11. Huckabone, Capt Thomas C. *An Algorithm for Robust Eigenstructure Assignment Using the Linear Quadratic Regulator*. MS thesis, AFIT / GAE / ENY / 91D-7. School of Engineering, Air Force Institute of Technology (AU), Wright-Patterson AFB OH, December 1991.

12. Kazerooni, H. and Houpt, P.K. " On the Loop Transfer Recovery," *International Journal of Control*, 43-3 : 981 (March 1981).
13. Kazerooni, H. and others. "An Approach to Loop Transfer Recovery Using Eigenstructure Assignment," *In Proceedings of American Control Conference*, June 1985 (769 - 803), Boston.
14. Kimura, H. " Poles Assignment by Gain Output Feedback," *IEEE Transactions on Automatic Control*, AC-20 : 509 -516 (August 1975).
15. Kwakernaak, Huibert and Sivan, Raphael. *Linear Optimal Control Systems*. New York : John Wiley & Sons, Inc., 1972.
16. Liebst, B.S. and others. " Design of an Active Flutter Suppression System," *Journal of Guidance, Control, and Dynamics*, Vol. 9-1 (January - February 1986).
17. Maciejowski, J. M. *Multivariable Feedback Design*. Massachusetts : Addison - Wesley Publishing Company, Inc., 1989.
18. Moore, B.C. " On the Flexibility Offered by State Feedback in Multivariable Systems Beyond Closed Loop Eigenvalue Assignment," *IEEE Transaction on Automatic Control*, pp. 689 - 692 (October 1976).
19. Quinn, Wilma W. *Multivariable Control of a Forward Swept Wing Aircraft*. MS thesis, Massachusetts Institute of Technology, Laboratory of Information and Design Systems, Cambridge, Massachusetts.
20. Ridgely, D.Brett. and Banda Siva. *Introduction to Robust Multivariable Control*. AFWAL - TR - 85 - 3102, Control Dynamics Branch, Flight Dynamics Laboratory, Wright - Patterson AFB OH, February 1986 (AD - A165891).
21. Ridgely, D.Brett. and others. " Linear Quadratic Gaussian with Loop Transfer Recovery Methodology for an Unmanned Aircraft," *Journal of Guidance and Control*, Vol 10-1 : 82 - 89 (August 1989).
22. Robison, Lieutenant Jeffery D. *A Linear Quadratic Regulator Weight Selection Algorithm for Robust Pole Assignment*, MS thesis, AFIT / GAE / ENG / 90D - School of Engineering, Air Force Institute of Technology (AU), Wright-Patterson AFB OH, December 1990 (AD-A230598).
23. Sobel, K.M. and Shapiro, E.Y. " Eigenstructure Assignment for Design of Multimode Flight Control Systems," *IEEE Control System Magazine*, Vol 5 - 2, (May 1985).

24. Safonov, M.G. and Athans, M. "Gain and Phase Margin for Multiloop LQ Regulator," *IEEE Transactions on Automatic Control*, AC-22: 173 - 179, (April 1977).
25. Srinaathkumar, S. " Eigenvalue / Eigenvector Assignment Using Output Feedback," *IEEE Transactions on Automatic Control*, AC-29 : 79 - 81 (February 1978).
26. Zhang, Z.H. and Freudenberg, J.S. " Loop Transfer Recovery for Nonminimum Phase Plants," *IEEE Transactions on Automatic Control*, Vol. 35: 547 - 553, (May 1979).

Vita

An - Chi Ju was born on 4 January 1957 in Shinchu, Taiwan. He graduated from the Chinese Airforce Academy and received a Bachelor of Science in 1978. In 1977, he started flight training, receiving his wings after finishing training and served as fighter pilot in an operational squadron. During the operational pilot years, he flew the F-100A, F-104G aircraft, and was then selected to attend the Test Pilot School in Edwards AFB, California. In 1986 he completed TPS training, and was assigned to Indigenous Defense Fighter program in Aviation Industry Developing Center of Taiwan, as a flight test pilot. He did the first flight of the first twin seat IDF and many other flight test missions. In the summer of 1991, he was selected to attend the US Air Force Institute of Technology, School of Engineering until now.

Permanent address: 22-1 Lane 20 Chung-chen Rd.
Shalu, Taichung, Taiwan.

REPORT DOCUMENTATION PAGE

Form Approved
OMB No. 0704-0188

Public reporting burden for this collection of information is estimated to average 1 hour per response, including the time for reviewing instructions, searching existing data sources, gathering and maintaining the data needed, and completing and reviewing the collection of information. Send comments regarding this burden estimate or any other aspect of this collection of information, including suggestions for reducing this burden, to Washington Headquarters Services, Directorate for Information Operations and Reports, 1215 Jefferson Davis Highway, Suite 1204, Arlington, VA 22202-4302, and to the Office of Management and Budget, Paperwork Reduction Project (0704-0188), Washington, DC 20503.

1. AGENCY USE ONLY (Leave blank)		2. REPORT DATE December 1992	3. REPORT TYPE AND DATES COVERED Master's Thesis	
4. TITLE AND SUBTITLE IMPROVEMENTS TO LQG/LTR METHODOLOGY FOR PLANT WITH LIGHTLY DAMPED OR LOW FREQUENCY POLES			5. FUNDING NUMBERS	
6. AUTHOR(S) An-Chi Ju, Major, Taiwan, R.O.C				
7. PERFORMING ORGANIZATION NAME(S) AND ADDRESS(ES) Air Force Institute of Technology, WPAFB OH 45433-6583			8. PERFORMING ORGANIZATION REPORT NUMBER AFIT/GAE/ENY/92D-14	
9. SPONSORING / MONITORING AGENCY NAME(S) AND ADDRESS(ES)			10. SPONSORING / MONITORING AGENCY REPORT NUMBER	
11. SUPPLEMENTARY NOTES				
12a. DISTRIBUTION / AVAILABILITY STATEMENT Approved for public release; distribution unlimited			12b. DISTRIBUTION CODE	
13. ABSTRACT (Maximum 200 words) LQG/LTR design has a tendency to invert the plant's dynamics, which is undesirable if there are plant poles near the imaginary axis. In this study, Static Output Feedback (SOF) is applied to reassign plant poles before LQG/LTR is applied. Alternatively, Robust Eigenstructure Assignment (REA) was used to design the target loop transfer function with an ideal eigenstructure to avoid the undesirable cancellations. Both methods were applied to several aircraft design problems. Results showed that the methods can be effectively used so that the LQG/LTR design has improved stability and performance; however, it was found that each method had strengths and weaknesses.				
14. SUBJECT TERMS Linear Quadratic Gaussian / Loop Transfer Recovery; Static Output Feedback; Robust Eigenstructure Assignment; Optimal Control; Control Robustness			15. NUMBER OF PAGES 131	
			16. PRICE CODE	
17. SECURITY CLASSIFICATION OF REPORT Unclassified	18. SECURITY CLASSIFICATION OF THIS PAGE Unclassified	19. SECURITY CLASSIFICATION OF ABSTRACT Unclassified	20. LIMITATION OF ABSTRACT UL	